THE COLLIDER PHENOMENOLOGY OF SUPERSYMMETRIC MODELS

By

DAVID J. MULLER

Bachelor of Science

University of Illinois

Urbana-Champaign, Illinois

1992

Submitted to the Faculty of the
Graduate College of the
Oklahoma State University
in partial fulfillment of
the requirements for
the Degree of
DOCTOR OF PHILOSOPHY
December, 1998

THE COLLIDER PHENOMONOLOGY OF SUPERSYMMETRIC MODELS

Thesis Approved:

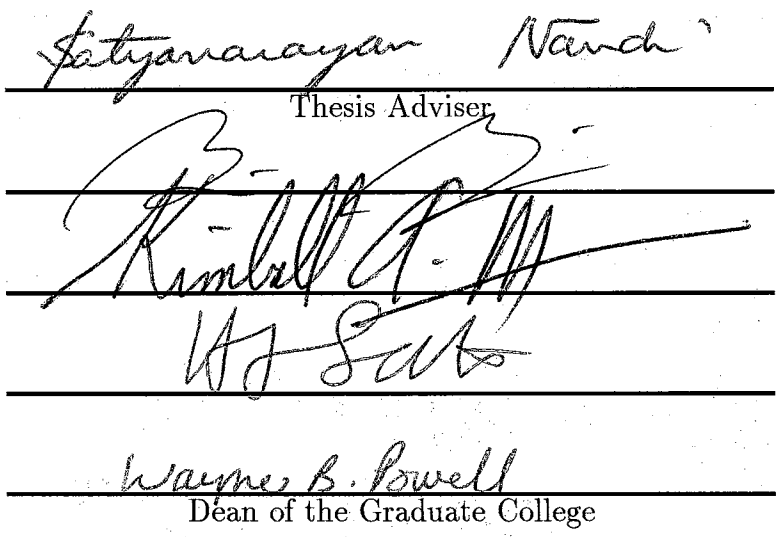

Thesis Adviser

Dean of the Graduate College

ACKNOWLEDGMENTS

I would like to express my appreciation to my advisor, Dr. Satyanarayan Nandi, for his guidance and support.

I wish to express my appreciation to Dr. Birne Binegar, Dr. Kimball A. Milton and Dr. Larry H. Scott for serving on my advisory committee.

This work reviews some of the research in which I participated during my years at Oklahoma State University. I am indebted to my collaborators: Dr. Bhaskar Dutta, Dr. Duane A. Dicus and Dr. Rabindra N. Mohapatra.

I thank the Department of Physics at Oklahoma State University for its support during my studies.

Finally, I wish to express my gratitude to my parents, Henry and Lois Muller, for their encouragement and support during my career in higher education.

TABLE OF CONTENTS

LIST OF TABLES

LIST OF FIGURES

CHAPTER I

INTRODUCTION

Supersymmetry

The Standard Model (SM) of particle interactions is highly successful at describing the interactions of elementary particles at low energy. Indeed, there have been no experimental results that unequivocally contradict the predictions of the SM: the SM is in excellent agreement with the LEP precision measurements. Moreover, no non-SM particles have yet been discovered. However, with the coming of the next generation of colliders such as the Large Hadron Collider (LHC) and possibly the Next Linear Collider (NLC), the question arises as to what form physics beyond the SM is likely to take.

Supersymmetry (SUSY) is considered by many theorists to be a promising candidate for such new physics. SUSY is a symmetry that relates bosonic and fermionic fields that differ by one half unit of spin [1]. There are a number of reasons why SUSY is considered an attractive extension of the SM. First, the SUSY algebra is the only nontrivial extension of the Poincaré algebra consistent with relativistic quantum field theory. SUSY evades the restriction of the Coleman-Mandula theorem that a group that nontrivially combines both the Lorentz group and a compact Lie group cannot have finite dimensional unitary representations [2]. Second, if SUSY is formulated as a local symmetry, gravity is automatically included into the theory. Third, SUSY is a requirement of superstring theories. Fourth, if SUSY is a symmetry of nature, then there exists a strong possibility that it will be detected at present or the next generation of colliders.

One of the most theoretically compelling reasons to believe that SUSY will be detected soon has to do with the Higgs sector of the SM. The SM gives masses

to the gauge bosons and fermions through the introduction of a single scalar $SU(2)_L$ doublet. When the neutral component of this doublet gets a vacuum expectation value (VEV), the electroweak (EW) symmetry is broken and the W and Z bosons obtain their masses. The fermions obtain their masses through Yukawa couplings to the Higgs boson. The degree of freedom that is not used up in giving masses to the gauge particles becomes the physical Higgs particle. By demanding unitarity at tree level in the scattering of the longitudinally polarized gauge bosons, $W_L^+W_L^- \to W_L^+W_L^-$, one can deduce that the mass of the light Higgs boson must satisfy $M_h < 860\,\text{GeV}$ [3].

There is a problem with having a light Higgs in that fermion loop corrections to the Higgs mass are quadratically divergent. There exists no symmetry in the SM to prevent such corrections. The presence of quadratic divergences to the Higgs mass tend to drive the Higgs' mass to the larger scale presumably representing some new physics (such as the Planck scale or the scale of some grand unified theory). This is a problem since we need the Higgs boson mass to be less than around one TeV. To obtain such a light Higgs boson, its mass must then be the difference between two very large numbers. Thus very precise fine-tuning in the parameters of the theory is required. This is known as the naturalness problem.

SUSY solves this problem through its introduction of scalar partners to the fermions. The couplings of these scalar partners are related to the coupling of the fermions in such a way that the quadratic scalar loop contributions cancel the quadratic fermion loop contributions if the mass differences between the fermions and the scalar partners are not too large (if SUSY were an exact symmetry, then the fermions would have the same mass as their scalar partners). Specifically, the masses of some of the scalar partners need to be below about one TeV. Thus, if SUSY is an actual symmetry of nature and is responsible for solving the naturalness problem, then we should see supersymmetric particles at the next generation of colliders.

The Minimal Supersymmetric Standard Model

The Minimal Supersymmetric Standard Model (MSSM) is the "simplest" supersymmetric model that can realistically describe low energy particle interactions.

Table I. The matter and Higgs superfields of the MSSM.

Superfield	$(SU(3)_C, SU(2)_L, U(1)_Y)$	Component Fields
$\hat{Q}$	$(3, 2, \frac{1}{3})$	$\begin{pmatrix} u_L \\ d_L \end{pmatrix}, \begin{pmatrix} \tilde{u}_L \\ \tilde{d}_L \end{pmatrix}$
$\hat{U}^c$	$(\bar{3}, 1, -\frac{4}{3})$	$u_L^c, \tilde{u}_L^c$
$\hat{D}^c$	$(\bar{3}, 1, \frac{2}{3})$	$d_L^c, \tilde{d}_L^c$
$\hat{L}$	$(1, 2, -1)$	$\begin{pmatrix} \nu_l \\ e_L \end{pmatrix}, \begin{pmatrix} \tilde{\nu}_L \\ \tilde{e}_L \end{pmatrix}$
$\hat{E}^c$	$(1, 1, 2)$	$e_L^c, \tilde{e}_L^c$
$\hat{H}_2$	$(1, 2, 1)$	$\begin{pmatrix} h_2^+ \\ h_2^0 \end{pmatrix}, \begin{pmatrix} \tilde{h}_2^+ \\ \tilde{h}_2^0 \end{pmatrix}$
$\hat{H}_1$	$(1, 2, -1)$	$\begin{pmatrix} h_1^0 \\ h_1^- \end{pmatrix}, \begin{pmatrix} \tilde{h}_1^0 \\ \tilde{h}_1^- \end{pmatrix}$

Its simple in the sense that it contains the minimum number of particles required to construct a realistic supersymmetric model of particle interactions. The MSSM uses the gauge group of the SM: $SU(3)_C \times SU(2)_L \times U(1)_Y$. In addition, the MSSM has the same three generations of quarks and leptons as the SM, but now the supersymmetric partners (frequently called the "superpartners") of these particles are introduced. The particle content of the theory is shown in Tables I and II.

Table I gives the matter fields of the theory. SUSY dictates that every SM fermion has a complex scalar associated with each of its chiral states. We denote the scalar superpartners by using the symbol for the superfield with a tilde over it. SUSY further dictates that these scalar fields have the same gauge quantum numbers as their corresponding fermion field. Collectively, these superpartners of the fermions are frequently referred to as sfermions. The scalar partners of the leptons are called sleptons, and the scalar partners of the quarks are called squarks.

In Table I, we have introduced two Higgs doublets. One Higgs doublet does not suffice for two reasons. First, the fermionic partners of the Higgs bosons, called

Table II. The gauge superfields of the MSSM.

Superfield	$(SU(3)_C, SU(2)_L, U(1)_Y)$	Component Fields	Superpartner Name
$\hat{G}_a$	(8, 1 , 0)	g_a^μ, $\tilde{g}_a$	gluino
$\hat{W}_i$	(1, 3, 0)	W_i^μ, $\widetilde{W}_i$	wino
$\hat{B}$	(1, 1, 0)	B^μ, $\tilde{B}$	bino

higgsinos, contribute to the triangle gauge anomalies [4]. Since the contributions of the SM fermions cancel among themselves, there would be nothing to cancel the Higgsino contributions if we introduce only one Higgs doublet. The simplest way to handle this is to introduce a second Higgs doublet with the opposite $U(1)_Y$ quantum number as the first Higgs doublet. The other reason is that separate Higgs doublets are required to give mass to the up and down type quarks since the superpotential is the product of superfields of the same chirality.

Table II gives the gauge fields of the theory. The superpartners of the gauge fields are generally called gauginos. In manner similar to that of the sfermions, gauginos are denoted using the same symbol as the gauge field with a tilde over it. The interactions between the chiral (matter) superfields and the gauge and gaugino fields are completely specified by the gauge symmetries and supersymmetry and they arise from the corresponding parts of the kinetic term in the Langrangian. There are no adjustable parameters here.

Aside from the new particles introduced into the theory, much of the new physics comes from the superpotential, W. The superpotential is a function of the chiral superfields, but not their complex conjugates. Renormalizability dictates that its terms contain products of no more than three chiral superfields. It is not allowed to contain derivative interactions. The most general superpotential that we can write with this particle content is

$$\begin{aligned} W &= \epsilon_{ij}(\lambda_U \hat{Q}^i \hat{H}_2^j \hat{U}^c + \lambda_D \hat{Q}^i \hat{H}_1^j \hat{D}^c + \lambda_L \hat{L}^i \hat{H}_1^j \hat{E}^c + \mu \hat{H}_1^i \hat{H}_2^j) \\ &\quad + W_{\text{non-MSSM}} \,. \end{aligned} \tag{1}$$

Here the first line is for one generation, but the extension to three is straightforward. The term $W_{\text{non-MSSM}}$ is given by

$$W_{\text{non-MSSM}} = \lambda_{ijk}\hat{L}^i\hat{L}^j\hat{E}^c + \lambda'_{ijk}\hat{L}_i\hat{Q}_j\hat{D}^c_k + \frac{1}{2}\lambda''_{ijk}\hat{U}^c_i\hat{D}^c_j\hat{D}^c_k + \kappa_i\hat{L}_i\hat{H}_2 \tag{2}$$

where i, j and k here are generational indices. From the superpotential and its complex conjugate, part of the scalar potential and the Yukawa interactions of the fermions with the scalars is obtained.

Unfortunately, the four terms in $W_{\text{non-MSSM}}$ each violate either baryon number or lepton number. The terms responsible for this can give unacceptable physics (*e.g.* rapid proton decay) [5]. One way to avoid this problem is to completely eliminate these terms altogether (however, this is not necessary to obtain acceptable physics [6]). In the MSSM, this is accomplished by adding a discrete symmetry to the theory called R-parity [7] which eliminates the baryon and lepton number violating terms. The R-parity of a state is related to its spin (S), baryon number (B) and lepton number (L) by

$$R_p = (-1)^{2S+3B+L} \tag{3}$$

so that the usual (known particles) have $R_p = 1$ (even R-parity) and their superpartners have $R_p = -1$ (odd R-parity). The dependence of R on B and L guarantees that R_p-conserving interactions conserve B and L. The baryon and lepton number violating terms in Eq. 2 are thereby eliminated.

The introduction of R-parity has important phenomenological implications. With R-parity conservation, the superpartners can only be pair produced and any of their decay products have to contain an odd number of SUSY particles. Furthermore, the lightest SUSY particle (LSP) then has to be stable since it has no R-parity conserving decay channels.

If SUSY were an exact symmetry, than all the particles in a supermultiplet would have the same mass. Since none of the superpartners of the known particles have ever been observed, SUSY must be a broken symmetry if it is an actual symmetry of nature. The mechanism for SUSY breaking is not known and more will be said about various models of SUSY breaking in the next section. In the MSSM, we

parametrize our ignorance by including terms that explicitly violate supersymmetry. These terms involve the scalar members of the chiral superfields and the gaugino members of the vector superfields. We do not include any terms that would reintroduce quadratic divergences into the theory and call these terms "soft" to indicate this: the presence of such SUSY breaking terms do not affect the relations among the various couplings present in the theory. The restriction that these terms be soft sets their dimension to be less than four. Thus the possible soft terms are mass terms, bilinear mixing terms and trilinear scalar mixing terms. The complete set (for one generation) of soft SUSY terms which respect the gauge symmetry and R-parity are [8]

$$\begin{aligned} -\mathcal{L}_{\text{soft}} &= m_1^2|H_1|^2 + m_2^2|H_2|^2 + B\mu\epsilon_{ij}(H_1^i H_2^j + \text{h.c.}) \\ &\quad + M_Q^2(\tilde{u}_L^* \tilde{u}_L + \tilde{d}_L^* \tilde{d}_L) + M_U^2 \tilde{u}_R^* \tilde{u}_R + M_D^2 \tilde{d}_R^* \tilde{d}_R \\ &\quad + M_L^2(\tilde{e}_L^* \tilde{e}_L + \tilde{\nu}_L^* \tilde{\nu}_L) + M_E^2 \tilde{e}_R^* \tilde{e}_R \\ &\quad + \frac{1}{2} M_1 \bar{\tilde{B}} \tilde{B} + \frac{1}{2} M_2 \bar{\tilde{W}}^i \tilde{W}^i + \frac{1}{2} M_3 \bar{\tilde{g}}^a \tilde{g}^a \\ &\quad + \epsilon_{ij}(\lambda_u A_u \tilde{Q}^i H_2^j \tilde{u}_R^* + \lambda_d A_d \tilde{Q}^i H_1^j \tilde{b}_R^* + \lambda_e A_e \tilde{L}^i H_1^j \tilde{e}_R^*) \ . \end{aligned} \tag{4}$$

Arbitrary masses for the scalars and gauginos have been introduced. These break the degeneracy between the particles and their superpartners. Trilinear (A) terms have also been introduced here. Non-zero A terms cause the scalar partners of the left and right handed fermions to mix when the Higgs bosons get vacuum expectation values. This is especially significant for the third generation fermions. A subscript 1 is typically used to denote the lighter of a sfermion pair, and a subscript 2 is typically used to denote the more massive one.

There is also significant mixing between the gauginos and Higgsinos. There are two charged Higgsinos, $\tilde{\text{h}}^{\pm}$. Each of these have the same conserved quantum numbers as the correspondingly charged wino. Since they have the same quantum numbers, they can mix to form mass eigenstates which are called charginos. They are denoted by $\chi_1^{\pm}$ and $\chi_2^{\pm}$ where $\chi_1^{\pm}$ is taken to be the less massive of the two. In the neutral fermion sector, the $\tilde{B}$ and the $\tilde{W}^3$ can mix with the neutral fermion partners

of the Higgs bosons, $\tilde{h}_1^0$ and $\tilde{h}_2^0$. The corresponding mass eigenstates are known as neutralinos and are denoted by χ_i^0 where i = 1, 2, 3, or 4 in order of increasing mass.

Communicating Supersymmetry Breaking

If supersymmetry were an exact symmetry, then all the supersymmetric particles would have the same masses as their supersymmetric partners. Since none of the supersymmetric partners of the known particles have ever been observed, SUSY must be a broken symmetry (if it is an actual symmetry of nature). It turns out that the phenomenology of SUSY theories depends to a great extent on the nature of the supersymmetry breaking. We would like to break SUSY spontaneously, but there is a potential problem with this. If the mechanism for SUSY breaking is coupled too closely to the SM spectrum, then that spectrum would have to obey the sum rule:

$$\mathrm{STr}\mathcal{M}^2 = 0 \tag{5}$$

where the supertrace, STr, is defined by

$$\mathrm{STr}\mathcal{M}^2 \equiv \sum_J (2J+1)(-1)^{2J}\mathcal{M}_J^2 \tag{6}$$

with the sum over the states in a given supermultiplet [9]. This implies that some of the superpartners must be lighter than their superpartners. Since none of the scalar partners of the SM fermions have been detected, this is a problem. There is a way out of this problem, however, in that $\mathrm{STr}\mathcal{M}^2 = 0$ holds only at tree level and only for renormalizable theories. So what could happen is that SUSY is broken dynamically, but in some sector which couples to SM particles and their superpartners via loops or non-renormalizable operators. These theories of SUSY breaking typically involve a "hidden sector" within which the SUSY breaking occurs. The sector that includes the SM particles and their superpartners is called the "visible sector". The fields that are responsible for communicating the SUSY breaking to the visible sector comprise the "messenger sector".

The question now arises as to what form the messenger sector takes. There are two commonly considered forms. The first is supergravity (SUGRA) where local

SUSY mixes the hidden and visible sectors through gravitational interactions. The mixing terms, being non-renormalizable, suppress the scale of SUSY breaking in the visible sector from the scale of SUSY breaking, $\sqrt{F}$, in the hidden sector:

$$\frac{F}{M_{\text{planck}}} \ll \sqrt{F} \, . \tag{7}$$

The sparticle spectrum is determined by five input parameters at the SUGRA or unification scale. Four of these are concerned with the soft terms: there is a common scalar mass m_0, a common gaugino mass $M_{1/2}$, a common A-term A_0, and B. The last parameter is μ from the superpotential.

The other commonly considered theories of communicating SUSY breaking are gauge mediated supersymmetry breaking (GMSB) theories. The defining characteristic of GMSB theories is that the SUSY breaking is communicated to the visible sector through gauge interactions. The messenger sector is composed of some set of superfields with SM couplings but which are not part of the MSSM spectrum. Since the fermionic components of the messenger fields must be heavy and not contribute to the SM anomalies, they are taken to be vectorlike with respect to the SM gauge interactions. Moreover, to keep the coupling constant unification for which the MSSM is famous, the messenger sector is frequently taken to be composed of complete multiplets of some GUT group.

Since the messenger fields are charged under the SM gauge groups, the gauginos and scalar fields of the MSSM obtain their soft masses through loops of the messenger fields. The visible sector gauginos receive masses at the one loop level and their masses at the messenger scale satisfy

$$\tilde{M}_i(M) \propto \alpha_i \Lambda \tag{8}$$

where Λ is the effective scale of SUSY breaking in the visible sector and $\alpha_i \equiv \frac{g_i^2}{4\pi}$ is the coupling constant for the appropriate gauge interaction. The scalar fields obtain their masses at two loops giving the following approximate proportionality:

$$\tilde{m}^2(M) \propto \alpha_i^2 \Lambda^2 \tag{9}$$

where α_i is the largest coupling that contributes to the mass. We note that since the gaugino masses arise at one loop and the squared scalar masses arise at two loops,

the gaugino and scalar masses scale in α_i. Thus there is a hierarchy in the sparticle masses with the gluinos and squarks being much more massive than the slepton and EW gauginos.

The phenomenology of a SUSY model depends to a great extent on which SUSY sparticles are lowest in mass. This is especially true if R-parity is conserved. In GMSB models, the lightest supersymmetric particle (LSP) is the gravitino (in SUGRA theories the LSP is usually the lightest neutralino). Given the hierarchy of sparticle masses, the next to lightest supersymmetric particle (NLSP) can be the lightest neutralino or the lighter stau ($\tilde{\tau}_1$). The collider signals for GMSB depend critically on which is the NLSP.

Scope of this Work

In this work we consider the phenomenology of various supersymmetric models. First, we consider the phenomenology of the Higgs sector of the MSSM. As discussed above, the MSSM has two Higgs doublets. Of the eight scalar degrees of freedom, three are absorbed to give mass to the gauge bosons. This leaves five physical Higgs bosons which includes a charged pair ($H^{\pm}$). If this charged Higgs boson is light enough, then it provides for a decay mode of the top quark beyond the usual SM decay $t \to W^+ b$. We study how this additional decay mode for the top quark affects the signatures for top quark production at the Fermilab Tevatron collider.

In the rest of this work, we then consider the phenomenology of models beyond the MSSM. In particular, we consider what the signatures could be for gauge mediated supersymmetry breaking models. In GMSB models, the lighter stau is frequently less massive than the lightest neutralino. When this is the case, the decay chains of the supersymmetric particles will typically involve the $\tilde{\tau}_1$. The decay of the $\tilde{\tau}_1$ then produces a τ lepton; thus τ lepton production could be an important part of the signal for SUSY production in the context of GMSB models. We study the feasibility of such signatures at Run II of the Tevatron.

The gauge group of the SM and the MSSM is rather ad-hoc. The possibility exists that the low energy weak interactions could be part of a larger gauge group. In

particular, this larger gauge group could be left-right symmetric, and the left-handed nature of the low energy weak interactions could be due to spontaneous symmetry breaking. We consider the phenomenology of such a supersymmetric left-right model in the context of GMSB. The Higgs sector of this model possesses doubly charged particles some of which could be light enough to be produced at the Tevatron. We will find that τ lepton production provides an even larger signal here than in GMSB models with minimal particle content. In addition, angular distributions between the highest E_T τ-jets can be used to distinguish this left-right model from other models with signatures involving τ leptons.

The analyses done in this work involve performing Monte Carlo simulations of the production and decays of particles at hadronic colliders (in particular, the Fermilab Tevatron collider). Some of the details of the code for the program that was used to perform the simulations can be found in the appendix. The CTEQ3M parton distributions were used [10].

CHAPTER II

CHARGED HIGGS BOSONS

Introduction

Extended Higgs sectors are a commonly considered extension of the SM. This is particularly true for supersymmetric theories where more than one Higgs multiplet is required for anomaly cancellation and to give masses to both up-type and down-type quarks. The MSSM takes the minimal Higgs structure of two Higgs doublets [11].

As mentioned in chapter I, the most general superpotential for this model which conserves baryon and lepton number is

$$W = \epsilon_{ij}[\mu \hat{H}_1^i \hat{H}_2^j + \lambda_U \hat{Q}^i \hat{H}_2^j \hat{U}^c + \lambda_D \hat{Q}^i \hat{H}_1^j \hat{D}^c + \lambda_L \hat{L}^i \hat{H}_1^j \hat{E}^c] \tag{10}$$

where the last three terms govern the interactions of the Higgs bosons with fermions. The scalar potential, V, is then formed from the "F" terms of this superpotential and the "D" terms of the gauge invariant kinetic energy terms in the action. Any dimension four terms in the scalar potential must respect the supersymmetry in order to prevent the reintroduction of quadratic divergences into the theory. Including all possible soft supersymmetry breaking terms, the scalar potential for the Higgs sector takes the form

$$\begin{aligned} V &= \frac{1}{8}g^2[4|H_1^{i*}H_2^i|^2 - 2(H_1^{i*}H_1^i)(H_2^{j*}H_2^j) + (H_1^{i*}H_1^i)^2 \\ &\quad +(H_2^{i*}H_2^i)^2] + \frac{1}{8}g'^2(H_2^{i*}H_2^i - H_1^{i*}H_1^i)^2 \\ &\quad +|\mu|^2(H_1^{i*}H_1^i + H_2^{i*}H_2^i) + V_{\text{soft}} \end{aligned} \tag{11}$$

where

$$V_{\text{soft}} = m_1^2(H_1^{i*}H_1^i) + m_2^2(H_2^{i*}H_2^i) + (B\mu\epsilon_{ij}H_1^iH_2^j + h.c.) \tag{12}$$

are soft breaking terms. Here $\epsilon_{12} = 1$. The parameters m_1, m_2 and B have dimensions of mass.

The Higgs doublet fields H_1 and H_2 acquire vacuum expectation values (vevs)

$$\langle H_1 \rangle = \begin{pmatrix} v_1 \\ 0 \end{pmatrix} \qquad \langle H_2 \rangle = \begin{pmatrix} 0 \\ v_2 \end{pmatrix} . \tag{13}$$

We may choose the phases for the Higgs doublet fields so that v_1 and v_2 are real and non-negative. We define $\tan\beta \equiv v_2/v_1$ with $0 \leq \beta \leq \pi/2$. The phenomenology of the Higgs sector depends to a great extent on the value of $\tan\beta$.

We are now in a position to explore the Higgs spectrum. Of the eight degrees of freedom of the complex Higgs doublets, three are absorbed to give masses to the W and Z bosons. This leaves five physical Higgs bosons: three neutral (h^0, H^0, and A^0) and a charged pair ($H^{\pm}$). If the charged Higgs boson is light enough, then it is possible that the top quark has a nonstandard decay mode into these bosons. If this is the case, then the signatures for top quark events at colliders such as the Fermilab Tevatron would differ from the SM expectation. Thus, the charged Higgs boson will either be detected through top quark decay or some bound will be placed on its mass through its nondetection. Note that in a simple nonsupersymmetric two Higgs doublet extension of the Standard Model, bounds on the $b \to s\gamma$ rate place limits on the charged Higgs mass above the top quark mass. In a supersymmetric version of the model, possible cancellations from graphs involving the multitude of SUSY particles relaxes this bound. Hence, this analysis is performed in the context of the MSSM.

It has been pointed out that not only are the $H^+ \to c\bar{s}$ and $H^+ \to \nu_\tau \bar{\tau}$ decays important, but the decay $H^+ \to W^+ b\bar{b}$ is also present and becomes important in the low $\tan\beta$ region for charged Higgs masses above 140 GeV [12]. This can significantly affect the signature for top quark production by producing an excess of b-jets.

In this chapter, we investigate the signature for top quark production at the Fermilab Tevatron collider for the case where the charged Higgs boson is light enough for the top quark to decay into it. We determine the branching ratios for the decays

into various numbers of jets and leptons as a function of $\tan\beta$ and the charged Higgs mass.

Bounds on $M_{H^\pm}$ and $\tan\beta$

Numerous limits have already been placed on the values that the mass of the charged Higgs boson and $\tan\beta$ can take. One such limit can be obtained from the following relation which holds at tree level

$$M_{H^\pm}^2 = M_{A^\circ}^2 + M_W^2 \tag{14}$$

where $M_{H^\pm}$ is the mass of the charged Higgs boson and M_{A° is the mass of the pseudoscalar Higgs. The current OPAL 95% C.L. limit of $M_{A^\circ} > 70\,\text{GeV}$ for $\tan\beta > 1$ [13] then implies that $M_{H^\pm} > 107\,\text{GeV}$. For such values of $\tan\beta$, the one-loop corrections tend to shift the charged Higgs mass down from its tree-level value by less than 10 GeV. The size of the total correction decreases with increasing $\tan\beta$ [14]. Moreover, limits from the nonobservance of direct pair production of charged Higgs bosons at LEP (including LEP2) set lower bounds on the charged Higgs mass. At the 95% confidence level, the DELPHI collaboration sets a lower bound of 56.5 GeV, ALEPH sets a lower bound of 52 GeV, OPAL sets a lower bound of 56 GeV, and L3 sets a lower bound of 57.5 GeV [15].

Bounds on the values for $M_{H^\pm}$ and $\tan\beta$ have also been obtained by considering the charged Higgs contribution to inclusive semi-tauonic B-decays [16]. Recently, the supersymmetric short-distance QCD corrections have been incorporated into the analysis. Using the current bounds on the sparticle masses, the bound

$$\tan\beta \lesssim 0.43(M_{H^\pm}/\text{GeV}) \tag{15}$$

at the 2σ level for $\mu < 0$ is obtained (the μ term in the superpotential is taken to be $-\mu H_1 H_2$). For $\mu > 0$ these decays could yield no bound at all [17].

The CDF collaboration at the Tevatron has searched for charged Higgs decays of the top quark [18]. Recently they have searched for evidence of such decays by considering hadronic decays of the tau lepton since the charged Higgs decays primarily

to the tau for $\tan\beta > 4$. Seven events meet their cuts with an expected background of 7.4 ± 2.0 events. A region in the $\tan\beta - M_{H^\pm}$ plane is thereby excluded. In particular, charged Higgs bosons with $M_{H^\pm} < 147(158)\,\mathrm{GeV}$ are excluded in the large $\tan\beta$ limit ($\tan\beta > 100$) for a top quark mass of 175 GeV and top production cross section $\sigma_{t\bar{t}} = 5.0(7.5)\,\mathrm{pb}$. Moreover, to maintain consistency with the then observed top quark cross section of $\sigma = 6.8^{+3.6}_{-2.4}\,\mathrm{pb}$, $\sigma_{t\bar{t}}$ must increase at higher $\tan\beta$ to compensate for the lower branching ratio into the SM mode $\mathrm{Br}(t\bar{t} \to WbW\bar{b})$. This excludes more of the parameter space [18].

Similarly, Guchait and Roy have used Tevatron top quark data in the lepton plus τ channel to obtain a significant limit on the $H^\pm$ mass in the large $\tan\beta$ region [19]. They consider the lepton plus multijet channel looking for deviations from the SM prediction due to the charged Higgs' preferential coupling to the tau lepton. They thereby obtain an exclusion area in the $\tan\beta - M_{H^\pm}$ plane. Quantitatively, they obtain a mass limit of 100 GeV for $\tan\beta \geq 40$ increasing to 120 GeV at $\tan\beta \geq 50$. Essentially the same analysis was performed by Guasch and Solà but with the MSSM quantum corrections included [20]. They demonstrated that these corrections have a substantial impact on the allowed parameter space. In particular, for $\mu > 0$, these corrections decrease the cross section for the τ signal and a light charged Higgs mass ($\sim 100\,\mathrm{GeV}$) would be permitted for essentially any (perturbative) value of $\tan\beta$.

Production and Decay of Charged Higgs Bosons

We now consider the effects of the charged Higgs boson on the signatures for top quark production at the Tevatron. If the charged Higgs boson is lighter than the top quark, then the allowed decay modes for the top quark in the MSSM are $t \to bW^+$ and $t \to bH^+$; there are no other decay modes ignoring intergenerational mixing. The interactions of the charged Higgs bosons with quarks are represented by the Lagrangian:

$$\mathcal{L} = \frac{g}{2\sqrt{2}M_W} H^+ \left[\cot\beta \overline{U} M_U D_L + \tan\beta \overline{U} M_D D_R\right] + h.c. \qquad (16)$$

where U represents the three generations of up-type quarks and D represents the three generations of down-type quarks. M_U and M_D are diagonal up and down quark mass matrices. We have set the CKM matrix to the identity matrix since we are neglecting the small intergenerational mixings for our analysis. The widths for the top quark's decays are then

$$\begin{aligned}\Gamma(t \to bW) &= \frac{g^2}{64\pi M_W^2 M_t}\lambda^{\frac{1}{2}}(1, \frac{M_b^2}{M_t^2}, \frac{M_W^2}{M_t^2}) \times \\ &\quad \left[M_W^2(M_t^2 + M_b^2) + (M_t^2 - M_b^2)^2 - 2M_W^4\right] \qquad (17) \\ \Gamma(t \to bH) &= \frac{g^2}{64\pi M_W^2 M_t}\lambda^{\frac{1}{2}}(1, \frac{M_b^2}{M_t^2}, \frac{M_H^2}{M_t^2}) \times \\ &\quad \left[(M_t^2 \cot^2\beta + M_b^2 \tan^2\beta)(M_t^2 + M_b^2 - M_H^2) + 4M_t^2 M_b^2\right] \qquad (18)\end{aligned}$$

where $\lambda(x,y,z) \equiv x^2+y^2+z^2-2xy-2xz-2yz$. The branching fraction for $t \to bH^+$ is large ($>10\%$) for $\tan\beta \leq 1$ and $\tan\beta > \frac{M_t}{M_b}$.

The charged Higgs decays, in turn, into the standard fermions. Its coupling to the fermions increases with their mass, so the primary decay modes to consider for the charged Higgs are $H^+ \to c\bar{s}$ and $H^+ \to \nu_\tau \bar{\tau}$. The widths for these decays are

$$\begin{aligned}\Gamma(H^+ \to c\bar{s}) &= \frac{3g^2}{32\pi M_H M_W^2}\lambda^{1/2}(1, \frac{M_c^2}{M_H^2}, \frac{M_s^2}{M_H^2}) \times \\ &\quad \left[(M_s^2 \tan^2\beta + M_c^2 \cot^2\beta)(M_H^2 - M_c^2 - M_s^2) - 4M_c^2 M_s^2\right] \qquad (19) \\ \Gamma(H^+ \to \nu_\tau \bar{\tau}) &= \frac{g^2}{32\pi M_H^3 M_W^2}(M_H^2 - M_\tau^2)^2 M_\tau^2 \tan^2\beta \; . \qquad (20)\end{aligned}$$

In addition to these two-body decay modes, the three-body decay $H^+ \to \bar{b}bW$ is also important when $\tan\beta \lesssim 1$ and $M_{H^\pm} \gtrsim 120\,\mathrm{GeV}$ [12]. This decay is mediated by an off-shell top quark and is important due to the large value of the top quark's mass. As Eq. (16) shows, the coupling of the top quark to the charged Higgs boson increases with decreasing $\tan\beta$. The coupling is large enough at $\tan\beta \sim 1$ to overcome the extra suppression factors due to the gauge coupling of the W as well as the three-body phase space. As the charged Higgs' mass increases above 130 GeV, the off-shell propagator suppression factor is overcome.

For $\tan\beta \lesssim 0.7$, the decay $H^+ \to c\bar{s}$ dominates for values of the charged Higgs mass below 130 GeV otherwise the 3-body decay mode dominates. On the other hand,

for large $\tan\beta$, the decay $H^+ \to \nu_\tau \bar{\tau}$ dominates. The branching ratio for $H^+ \to \nu_\tau \bar{\tau}$ is essentially unity for $\tan\beta > 3$.

Analysis and Results

In this analysis we study the possible Tevatron signatures for charged Higgs production through top quark decay in the context of the MSSM. In defining the cuts used, we have the following two angles: θ which is the polar angle with respect to the proton beam axis and ϕ which is the azimuthal angle measured in the plane transverse to this axis. The transverse momentum is then defined as $p_T \equiv p\sin\theta$ and the transverse energy is defined as $E_T \equiv E\sin\theta$. The cuts employed are that final state charged leptons (electrons and muons) must have a p_T greater than 20 GeV and a pseudorapidity, $\eta \equiv -\ln(\tan\frac{\theta}{2})$, of magnitude less than 1. Jets must have an $E_T > 15\,\text{GeV}$ and $|\eta| < 2$. In addition, hadronic final states within a cone size of $\Delta R \equiv \sqrt{(\Delta\phi)^2 + (\Delta\eta)^2} = 0.4$ are merged to a single jet. The signature here for the hadronic decay of the τ lepton is to a single thin jet and we assume this is always true. Leptons within this cone radius of a jet are discounted. Throughout this analysis, the mass of the top quark is taken to be 175 GeV in accordance with current CDF and D0 collaboration measurements [21]. The simulations are performed using Monte Carlo techniques.

There are several possible final states available for top pair production. With the two decay possibilities of $t \to W^+b$ and $t \to H^+b$, there can be up to two b-jets at high $\tan\beta$ ($\tan\beta > 5$) or up to six b-jets at low $\tan\beta$. For the W decay channel, which is the only decay channel available to the top quark in the SM, the W bosons can decay to as many as two jets each or they can each decay leptonically. Thus in the SM case, one can expect after implementing the cuts any number of jets up to six and any number of charged leptons up to two. Introducing the possibility of the top quark decaying via the charged Higgs boson changes the branching ratios for the various decay channels. As stated in the previous section, for $\tan\beta > 3$ the charged Higgs boson decays into the τ lepton with a branching ratio (BR) that is essentially unity. With the hadronic decay of the τ to a thin jet, there should be a depletion

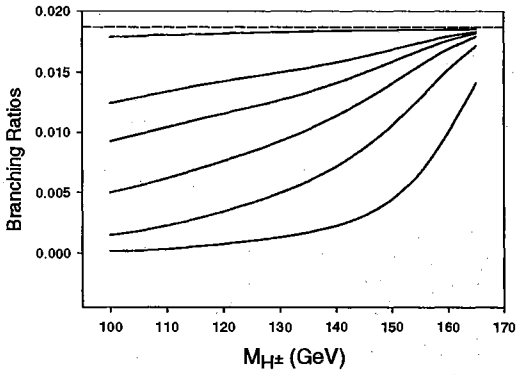

(a) From top to bottom, the curves are for $\tan\beta = 3$, 1, 0.8, 0.6, 0.4 and 0.2.

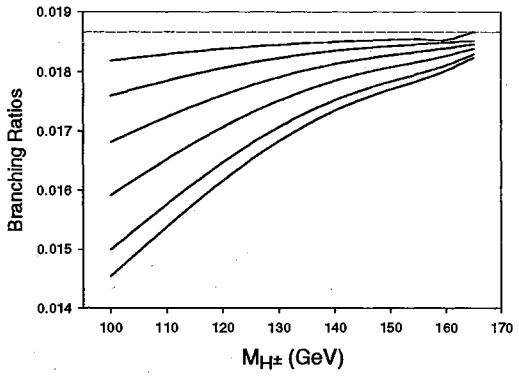

(b) From top to bottom, the curves are for $\tan\beta = 15$, 25, 35, 45, 55 and 60.

Figure 1. Branching ratios for the two jets and two leptons mode in top quark pair production at the Tevatron. The horizontal dashed lines give the SM expectation.

in the number of events with large numbers of jets. As $\tan\beta$ falls below five, on the other hand, the phenomenology depends to a great extent on the value of the charged Higgs mass and is very sensitive to the value of $\tan\beta$. With decreasing $\tan\beta$, $H^+ \to c\bar{s}$ becomes more and more important. As $\tan\beta$ gets to values around one, however, the three-body decay $H^+ \to \bar{b}bW$ dominates for $M_{H^\pm} > 130\,\mathrm{GeV}$.

Events that contain leptons are distinctive. This is particularly true for final states containing two or more leptons. While the production rates for these dilepton modes are rather small, their distinctive signature allows for a good separation from background. Thus the two jets and two leptons mode, which has the largest branching ratio of the dilepton modes, could be useful for charged Higgs detection after a long collider run. Fig. 1 gives the branching ratios versus charged Higgs mass for the two jets dilepton mode. Each curve represents a different value for $\tan\beta$. Fig. 1(a) gives the branching ratios for $\tan\beta < 3$, while Fig. 1(b) gives the BRs for $\tan\beta \geq 5$. As expected, the curves for the various allowed values of $\tan\beta$ all lie below the SM expectation. Thus if the decay $t \to H^+b$ is allowed, there will be a depletion of events for this mode which already has a small branching ratio for the SM case.

The two jets dilepton mode occurs when the decays of the $W^{\pm}$ or $H^{\pm}$ from each top quark leads directly or indirectly (from decays to τ leptons) to either an e or a μ. As $\tan\beta$ increases beyond approximately seven, the branching ratio for $t \to bH^+$ increases. For these values of $\tan\beta$, the predominant decay mode of the charged Higgs boson is $H^+ \to \bar{\tau}\nu_\tau$. There is less energy available for the electrons and muons from τ decays than in W decays since the electrons and muons from the subsequent τ decays occur further along the decay chain than those from direct W decay. So the electrons and muons from tau decays tend to be relatively soft and less likely to meet the p_T cuts. Thus as $\tan\beta$ increases (and so as the BR for $t \to H^+b$ increases), the branching ratio for the two jets dilepton decay mode gets smaller. The branching ratios for this mode increase to the SM value as $M_{H^\pm}$ increases towards 170 GeV and the phase space available for the charged Higgs decay of the top quark goes to zero.

The depletion in the number of dilepton events with two jets is considerable for low values of $\tan\beta$ as well. For $\tan\beta = 1$, Fig. 1(a) shows that the branching ratio for this mode decreases rapidly as the charged Higgs mass decreases. This is due to the fact that as $\tan\beta$ falls below approximately 6, the branching ratio for $t \to H^+b$ increases. Moreover, as $\tan\beta$ falls below three, the branching ratio for $H^+ \to \bar{\tau}\nu_\tau$ decreases and one of the hadronic decay modes can dominate. For values of $M_{H^\pm} \lesssim 130\,\text{GeV}$, $H^+ \to c\bar{s}$ is the dominant decay mode for the charged Higgs and the decrease in dilepton events is due to a general lack in the production of leptons. For $M_{H^\pm} > 130\,\text{GeV}$, on the other hand, $H^+ \to \bar{b}bW$ dominates. The electrons and muons from the subsequent W decays tend to be quite soft and are frequently eliminated by the p_T cuts.

The single lepton decay modes have the advantage that they are produced at a greater rate than the dilepton modes while retaining some of the distinctiveness that lepton modes offer. Some of these modes are not available in the Standard Model. These particular modes are shown in Fig. 2. Fig. 2(a) is for the six jets and one charged lepton case, while Fig. 2(b) is for the five jets and one charged lepton case. These modes occur due to the three-body decay $H^+ \to \bar{b}bW$ which has an appreciable decay width only for $\tan\beta \lesssim 1$. We see from the two figures that the branching ratios

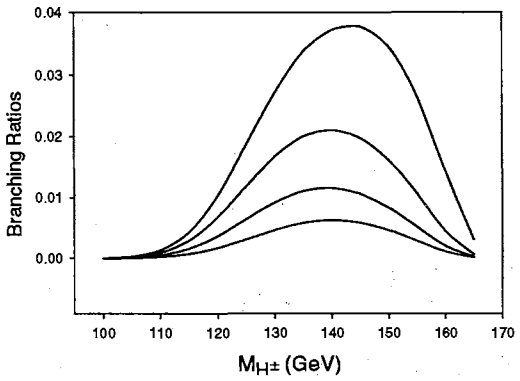

(a) Branching ratios for the 6 jets and 1 charged lepton case. From top to bottom, the curves are for $\tan\beta$ = 0.2, 0.4, 0.6 and 0.8.

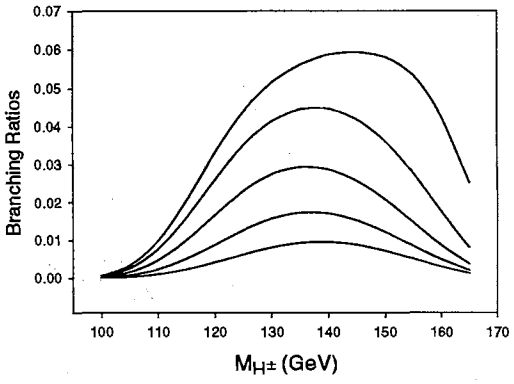

(b) Branching ratios fro the 5 jets and 1 charged lepton case. From top to bottom, the curves are for $\tan\beta$ = 0.2, 0.4, 0.6, 0.8 and 1.

Figure 2. Branching ratios for the 1 charged lepton modes with large numbers of jets that are not present in the Standard Model.

increase with increasing $M_{H^\pm}$ and reach a peak at $M_{H^\pm} \sim 140\,\text{GeV}$. This is due to the increase in the $H^+ \to \bar{b}bW$ branching ratio as the exchanged top quark gets closer to being on-shell and the propagator suppression decreases. As the charged Higgs mass increases further beyond 140 GeV, the branching ratios decrease sharply due to the decrease in the $t \to H^+b$ branching ratio as the phase space for this decay decreases.

Fig. 3 gives the branching ratios for the four jets and one lepton mode. Two of the jets in this mode are usually b-jets coming from the decay of the top quarks. This leaves two ways in which we can obtain a total of four jets and one charged lepton. The first way is for both of the top quarks to decay via W bosons with one W decaying hadronically and the other leptonically. The other way is for one of the top quarks to decay via the W which subsequently decays hadronically and the other decaying via the charged Higgs which decays indirectly to an electron or muon through the τ lepton. Other possibilities would involve the subsequent hadronic decays of the τ leptons from charged Higgs decays, but these cannot contribute to this mode as they typically lead to only one jet instead of the required two. Since only a subset of the possible top decays can give rise to the four jets and one charged lepton

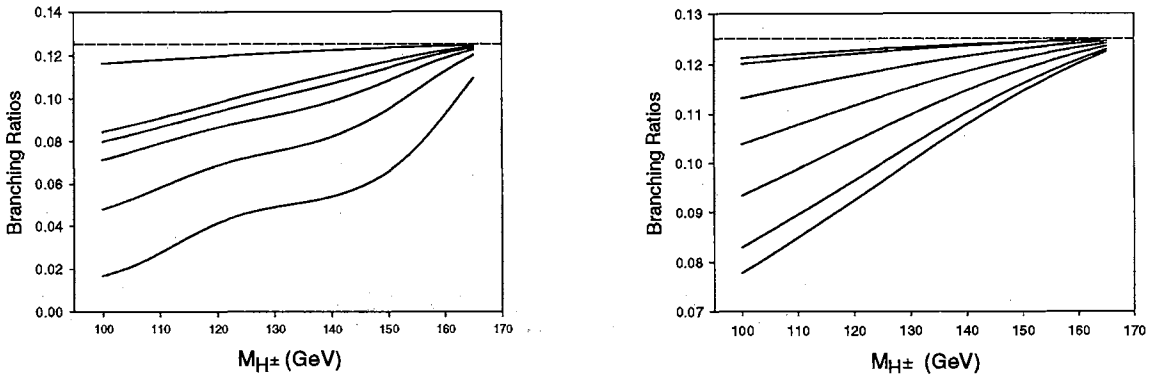

(a) From bottom to top, the curves are for $\tan\beta$ = 0.2, 0.4, 0.6, 0.8, 1 and 3.

(b) From top to bottom, the curves are for $\tan\beta$ = 5, 15, 25, 35, 45, 55 and 60.

Figure 3. Branching ratios for the 4 jets and 1 charged lepton mode. The horizontal dashed line gives the SM expectation.

mode, there will be a decrease in the number of events in this mode relative to the SM. This decrease is made more pronounced by the relative softness of the electrons and muons coming from the charged Higgs decay chain which tends to eliminate them when the p_T cuts are applied. As $\tan\beta$ increases beyond 5, the branching ratio for this mode decreases because of the increase in charged Higgs production. The minimum deviation from the SM occurs for $\tan\beta \sim 6-7$ as this is where the minimum in the branching ratio for $t \to H^+ b$ occurs.

We now consider the case for $\tan\beta < 5$. For $\tan\beta = 3$, charged Higgs production increases somewhat from $\tan\beta = 5$, but the branching ratio for $H^+ \to \bar{\tau}\nu_\tau$ remains close to one. As a result, we get slightly fewer events for this mode compared to the $\tan\beta = 5$ case. Fig. 3(a) shows that as $\tan\beta$ falls below 2, the branching ratios drop substantially below that of the SM. For $\tan\beta \lesssim 1$ and $M_{H^\pm} < 130\,\text{GeV}$, this is due to a depletion in leptonic events as the branching ratio for $H^+ \to c\bar{s}$ increases. For $\tan\beta \lesssim 1$ and $M_{H^\pm} > 130\,\text{GeV}$, on the other hand, events that have more than four jets are frequently produced due to the decay $H^+ \to \bar{b}bW$.

The three jets and single lepton mode, the branching ratios of which are given in Fig. 4, shows rather different behavior. In the $\tan\beta > 2$ region, the branching ratios for this mode are all above the SM expectation. These tend to increase with increasing

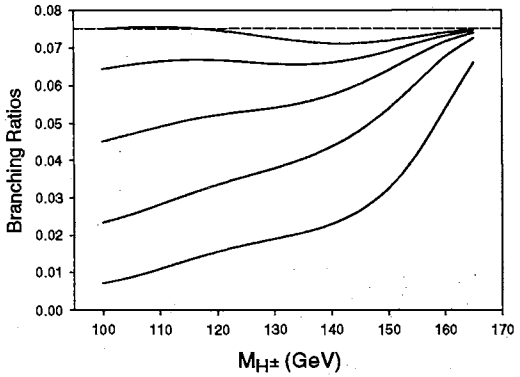

(a) From top to bottom, the curves are for $\tan\beta$ = 1, 0.8, 0.6, 0.4 and 0.2.

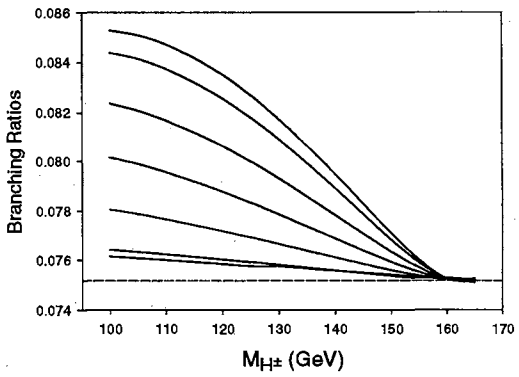

(b) From top to bottom, the curves are for $\tan\beta$ = 60, 55, 45, 35, 25, 15 and 5.

Figure 4. Branching ratios for the 3 jets and 1 lepton mode. The horizontal dashed line gives the Standard Model expectation.

$\tan\beta$. These features can be qualitatively understood as follows. Two of the jets are almost always b-jets coming from the decays of the top quarks. The remaining one jet and one lepton must come from the decays of the W and the charged Higgs boson. For $\tan\beta > 5$, the branching ratio before cuts for obtaining one jet (indirectly from τ decay) and one e or μ (directly or indirectly from τ decay) from WW, WH and HH are 0.18, 0.19 and 0.22, respectively. Thus, charged Higgs production naturally gives rise to branching ratios for the 3 jets and 1 charged lepton mode that are larger than the SM case. There are also other contributing factors for this increase. We have seen that the branching ratios for the four jets and one charged lepton case tend to be below the SM value. The events that would have had four jets but failed to meet the isolation cuts for two of the jets could be taken as a three jets with one charged lepton event. Finally, the branching ratios for the three jets with one charged lepton mode increase as $\tan\beta$ increases due to the corresponding increase in the branching ratio for the decay $t \to H^+ b$.

For the low $\tan\beta$ region ($\tan\beta \lesssim 1$), the branching ratios for the three jets with one charged lepton mode tend to fall below the SM expectation. This is due to the general decrease in events containing leptons as $\tan\beta$ falls below four and the branching ratios for $H^+ \to c\bar{s}$ and $H^+ \to \bar{b}bW$ increase. For example, for $\tan\beta \sim 6$

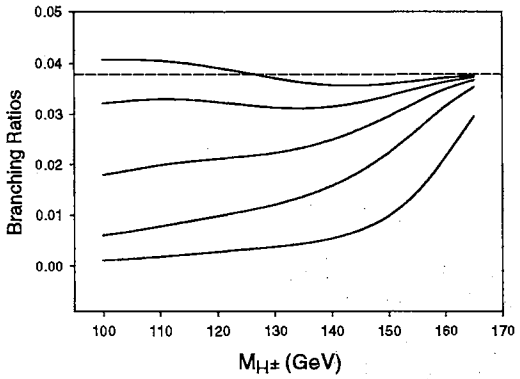

(a) From top to bottom, the curves are for $\tan\beta = 1$, 0.8, 0.6, 0.4 and 0.2.

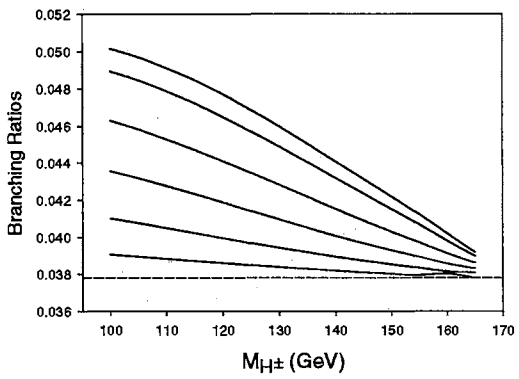

(b) From top to bottom, the curves are for $\tan\beta = 60$, 55, 45, 35, 25 and 15.

Figure 5. Branching ratios for the 2 jets and 1 charged lepton mode. The horizontal dashed line gives the Standard Model expectation.

and $M_{H^\pm} = 110\,\text{GeV}$, $H^+ \to c\bar{s}$ is the dominant decay mode with a BR of 69%, while for $\tan\beta \sim 6$ and $M_{H^\pm} = 140\,\text{GeV}$, $H^+ \to \bar{b}bW$ is the dominant decay mode with a BR of 73%.

The branching ratios for the two jets with one lepton mode are given in Fig. 5. Fig. 5(a) shows that the values of the branching ratios are larger than the SM case for $\tan\beta \gtrsim 3$ and increase with $\tan\beta$. In this mode, two of the jets are typically the b-jets coming from the decays of t and $\bar{t}$. The main process generating the two jets with one lepton events is then for both the W and charged Higgs bosons to decay leptonically with one of the charged leptons (typically from the charged Higgs) failing to meet the cuts. For $\tan\beta > 3$, the leptonic branching ratios for WW, WH and HH decays are 0.07, 0.18 and 0.12, respectively. Thus, charged Higgs production gives rise to branching ratios for this mode that are larger than the SM expectation. As $\tan\beta$ increases, the branching ratios increase due to the increasing branching ratio for $t \to H^+b$. For $\tan\beta = 3$, $H^\pm$ production increases slightly from $\tan\beta = 5$, but the branching ratio for $H^+ \to \bar{\tau}\nu_\tau$ is still close to one. As a result, the branching ratio for the two jets with one charged lepton mode is somewhat larger than for the $\tan\beta = 5$ case. The $\tan\beta \lesssim 1$ curve lies below the SM case due to a decrease in

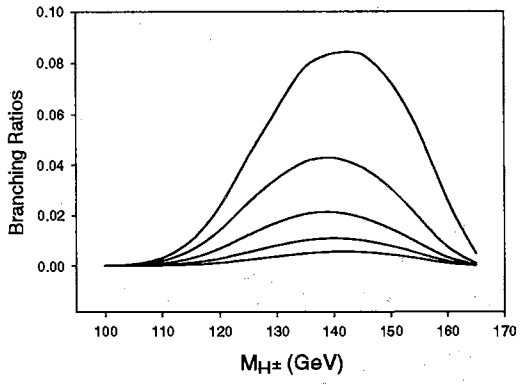

(a) The branching ratios for the 8 jets and 0 leptons mode. From top to bottom, the curves are for $\tan\beta = 0.2$, 0.4, 0.6, 0.8 and 1.

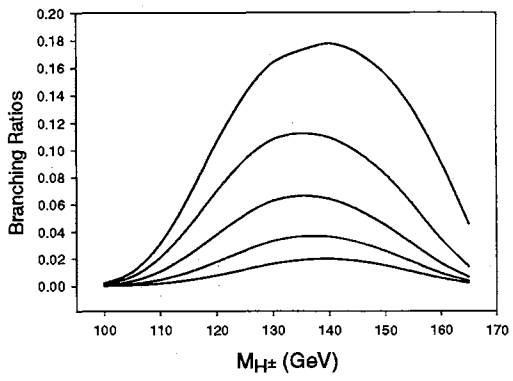

(b) The branching ratios for the 7 jets and 0 leptons mode. From top to bottom, the curves are for $\tan\beta = 0.2$, 0.4, 0.6, 0.8 and 1.

Figure 6. The branching ratios for the no charged lepton modes that are not present in the Standard Model.

leptonic events and an increase in the number of jets since $H^+ \to c\bar{s}$ and $H^+ \to \bar{b}bW$ are the dominant decay modes for the charged Higgs.

Events with purely hadronic final states are less useful due to the fact that they are harder to separate from the background at hadronic colliders. Nevertheless, these events can still be a source of interesting information on charged Higgs decays of the top quark. There are two modes here that are not present in the SM. These are the eight jets mode, the branching ratios for which are shown in Fig. 6(a), and the seven jets mode, the branching ratios for which are given in Fig. 6(b). These modes are due entirely to the $H^+ \to \bar{b}bW$ decay of the charged Higgs and are therefore only present for $\tan\beta \lesssim 1$. For these values of $\tan\beta$, the branching ratios for the eight and seven jets modes increase with increasing $M_{H^\pm}$ to reach a peak at $M_{H^\pm} \approx 140\,\text{GeV}$. For higher values of $M_{H^\pm}$, the branching ratio goes down because of a decrease in $\text{BR}(t \to H^+b)$ due to kinematic suppression. Fig. 7 shows the six jets case. For $\tan\beta \gtrsim 1$, the branching ratios tend to fall below the SM expectation and is due to the general decrease in jets from the τ decay of the charged Higgs. For lower values of $\tan\beta$, there is an increase in the number of jets due to the $H^+ \to \bar{b}bW$ decay. Fig. 8 gives the branching ratios for the five jets mode, Fig. 9 gives the branching ratios for

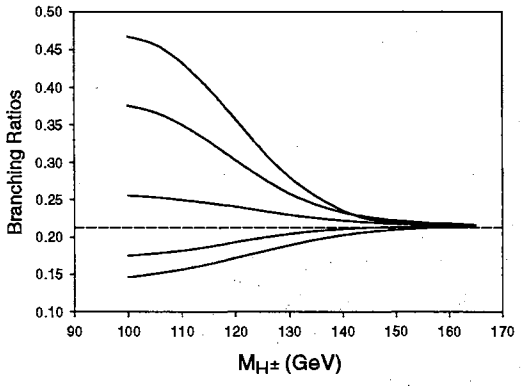

(a) From top to bottom, the curves are for $\tan\beta = 0.2$, 0.4, 0.6, 0.8 and 1.

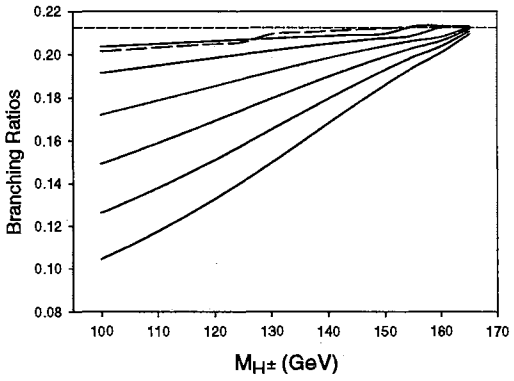

(b) From top to bottom, the solid curves are for $\tan\beta = 10$, 20, 30, 40, 50 and 60. The dashed curve is for $\tan\beta = 5$.

Figure 7. Branching ratios for the mode with 6 jets and no observed charged leptons. The horizontal dashed lines give the Standard Model expectation.

the four jets mode and Fig. 10 gives the branching ratios for the three jets mode. The branching ratios for the 2 jets mode are given in Fig. 11. For $\tan\beta \gtrsim 2$, the branching ratios are all above the SM case and increase with increasing $\tan\beta$ and increasing $M_{H^\pm}$. Thus, a significant enhancement in dijet production where both jets are high E_T b-tagged jets could be an interesting signal for charged Higgs production. For $\tan\beta < 0.8$, the branching ratios tend to fall below the SM value due to the increase in the number of jets due to the decay $H^+ \to \bar{b}bW$.

The CDF collaboration has performed a search for new particles ("X") decaying into $b\bar{b}$ produced in association with W bosons decaying into electrons or muons [22]. Specifically, they selected events that contain an electron or muon and two jets, at least one of which is b-tagged. Their main motivation was to look for W + SM Higgs events, but presumably the acceptances are roughly the same for the W + charged Higgs production. We can obtain events with this signature when one top quark decay to a W which then decays leptonically and the other top quark decays to a charged Higgs which then decays to a tau whose decay products fail to satisfy the cuts. This would leave us with two b-jets and a charged lepton. The branching ratios for such events are depicted in Fig. 12. As the graph demonstrates, the branching

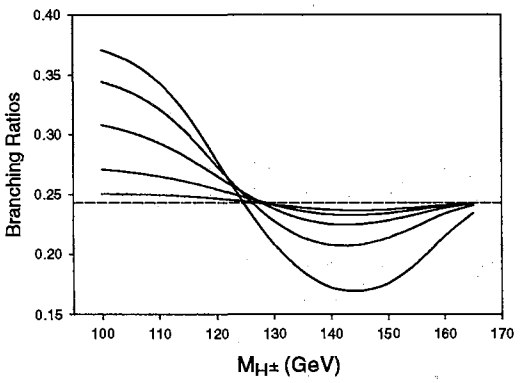

(a) From top to bottom on the left side, the curves are for $\tan\beta = 0.2$, 0.4, 0.6, 0.8 and 1.

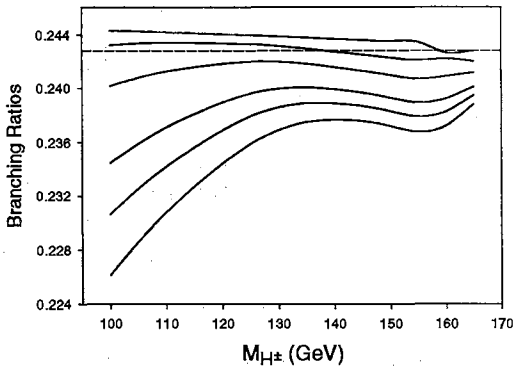

(b) From top to bottom, the curves are for $\tan\beta = 15$, 30, 40, 50, 55 and 60.

Figure 8. The branching ratios for the mode with 5 jets and no observed charged leptons. The horizontal dashed line gives the Standard Model expectation.

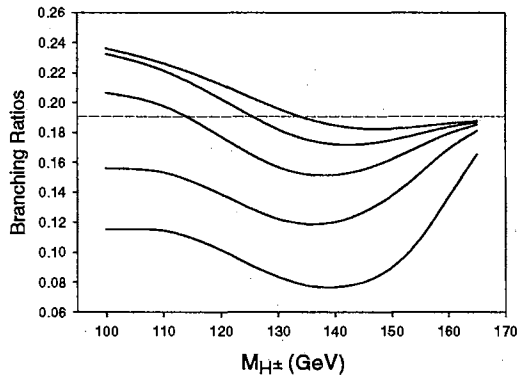

(a) From top to bottom, the curves are for $\tan\beta = 1$, 0.8, 0.6, 0.4 and 0.2.

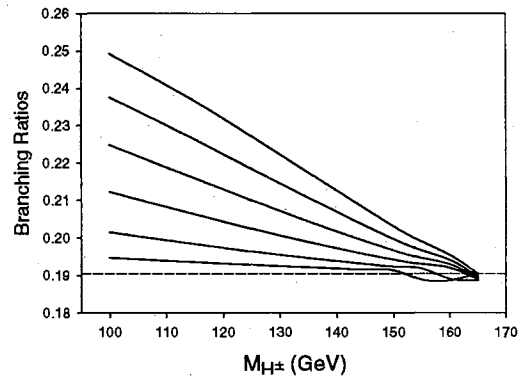

(b) From top to bottom, the curves are for $\tan\beta = 60$, 50, 40, 30, 20 and 10.

Figure 9. The branching ratios for the mode with four jets and no observed charged leptons. The horizontal dashed line gives the Standard Model expectation.

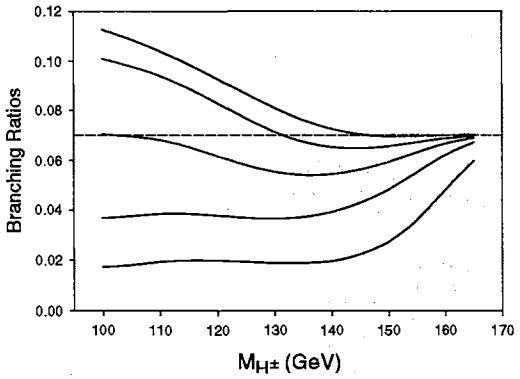

(a) From top to bottom, the curves are for $\tan\beta$ = 1, 0.8, 0.6, 0.4 and 0.2.

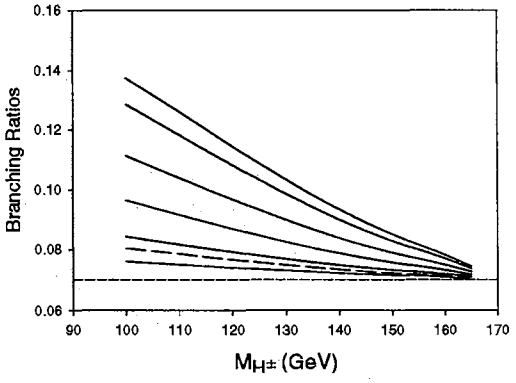

(b) From top to bottom, the solid curves are for $\tan\beta$ = 60, 55, 45, 35, 25 and 15. The dashed curve is for $\tan\beta = 3$.

Figure 10. The branching ratios for the mode with three jets and no observed charged leptons. The horizontal dashed line gives the Standard Model expectation.

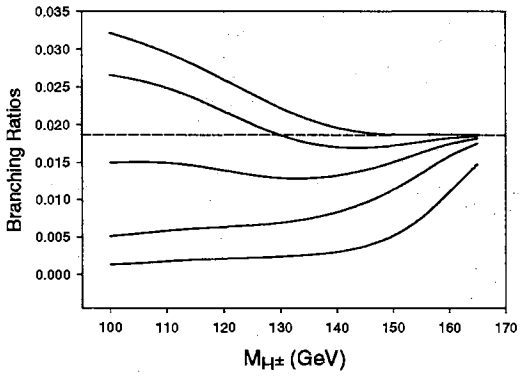

(a) From top to bottom, the curves are for $\tan\beta$ = 1, 0.8, 0.6, 0.4 and 0.2.

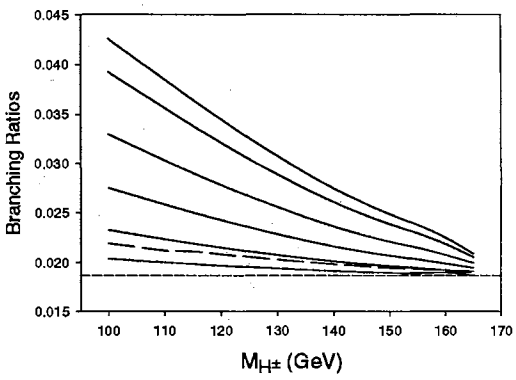

(b) From top to bottom, the curves are for $\tan\beta$ = 60, 55, 45, 35, 25 and 15. The dashed curve is for $\tan\beta = 3$.

Figure 11. The branching ratios for the mode with two jets and no observed charged leptons. The horizontal dashed line gives the Standard Model expectation.

ratio for this decay mode increases dramatically as $M_{H^\pm}$ decreases and the rate of top quark decay via the charged Higgs increases. For example, with $M_{H^\pm} = 110\,\text{GeV}$ and $\tan\beta = 55$, the branching ratio for this mode is 4.5%. The Standard Model expectation is about 3.7%, so we expect an excess cross section for this mode of about 0.06 pb assuming $\sigma_{t\bar{t}} = 7.5\,\text{pb}$. Using the mean value of the top quark pair production cross section reported by CDF, $\sigma_{t\bar{t}} = 7.5\,\text{pb}$, this means that the production cross section for this mode is about 0.34 pb. The CDF results set a 95% C.L. upper limit on $\sigma_{WX} \cdot B(X \to b\bar{b})$ of 20 pb for $M_X = 110\,\text{GeV}$. Factoring in the W decay rate to e's and μ's gives a 2 b-jets and 1 lepton cross section limit of about 5 pb. Thus the CDF results do not impose any real restriction on the charged Higgs decays of the top quark. As the total integrated luminosity increases for runs at the upgraded Tevatron, the charged Higgs signal may be observable in this mode. The absence of this signal will exclude some region of the $M_{H^\pm}$-$\tan\beta$ parameter space.

Conclusion

If the charged Higgs boson is light enough, it can provide an additional decay channel for the top quark. It can thereby potentially be detected at the Tevatron through top quark pair production. The presence of this charged Higgs production at the Tevatron would manifest itself through a change in the branching ratios for the various final states available to top quark pair production. Indeed, we have seen that the inclusion of the decay $t \to H^+ b$ leads to an overall decrease in the production of high p_T electrons and muons. In particular, the branching ratios for the two jets dilepton mode and the four jets with a charged lepton mode (both of which are important low background channels for investigating top quark production) are decreased. For values of $\tan\beta$ below about one, there are final states available to top quark pair production that are not available to the Standard Model. This is due to the three-body decay $H^+ \to \bar{b}bW$. Among the possible final states are the low background modes that contain a charged lepton with five or six jets (up to four of which can be b-tagged jets).

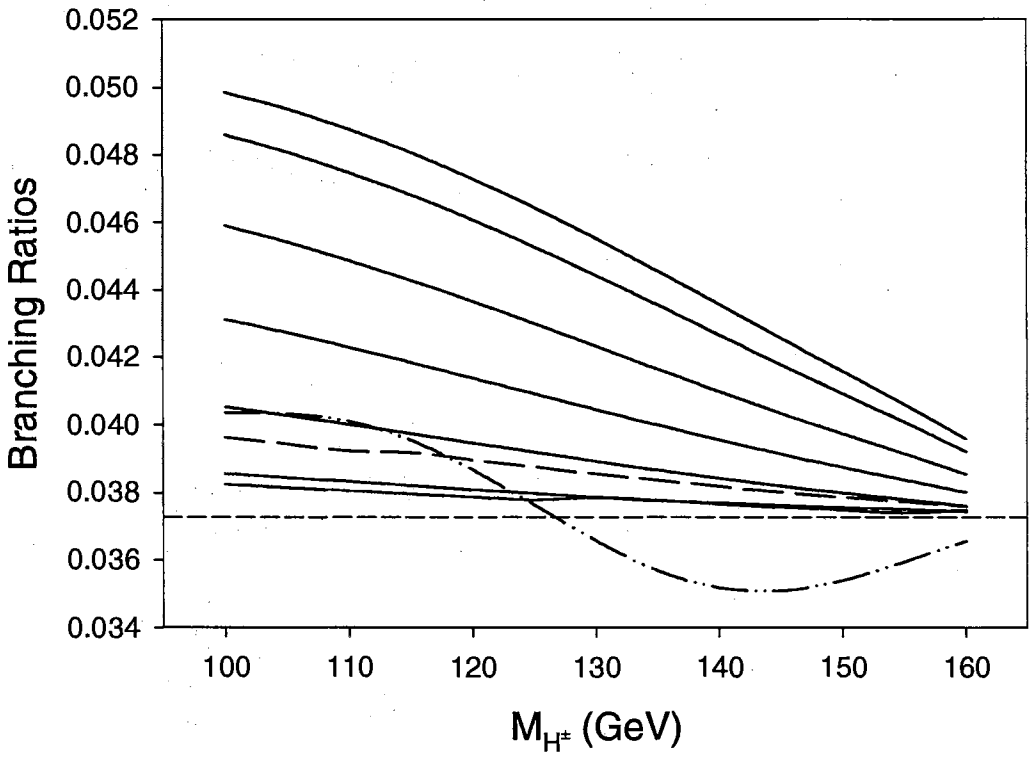

Figure 12. The branching ratios for the 2 jets and 1 charged lepton mode where at least one of the jets is b-tagged. From bottom to top, the solid curves are for $\tan\beta = 5$, 15, 25, 35, 45, 55 and 60. The upper dashed curve is for $\tan\beta = 3$, while the lower dashed curve is for $\tan\beta = 1$. The horizontal dashed line gives the SM expectation.

Current CDF data on the two b-jets and one charged lepton channel do not pose any real restriction on the charged Higgs decays of the top quark. On the other hand, data from an upgraded Tevatron could potentially detect the charged Higgs boson in this mode or rule out some significant portion of the $M_{H^\pm}$-$\tan\beta$ parameter space.

CHAPTER III

TAU SIGNALS FOR GAUGE MEDIATED SUSY BREAKING

Introduction

The expected phenomenology for SUSY production at colliders depends to a great extent on the assumed nature of supersymmetry breaking. Searches for SUSY have mostly been inspired by gravity mediated SUSY breaking theories, in particular by minimal supergravity. In these theories, the lightest neutralino is usually the lightest suspersymmetric particle. If R-parity is conserved, the LSP is stable and the decay chains of all other SUSY particles must eventually produce it. The LSP leaves the detector undetected thereby making large missing transverse energy ($\not\!\!E_T$) an important part of the signature for SUSY. In spite of extensive experimental searches, so far no experimental evidence for SUSY has been found at the Tevatron [23] or at LEP [24] except for one possible $e^+e^-\gamma\gamma$ plus $\not\!\!E_T$ event at the Tevatron [25].

Recently, gauge mediated SUSY breaking models have become very popular [26–28]. In GMSB theories, the gravitino ($\tilde{G}$) is the LSP and typically has a mass on the order of an eV. The coupling of the sparticles to the gravitino is rather weak. As a consequence, the decay chains of the sparticles will generally lead to the next to lightest supersymmetric particle which then decays to the gravitino. Thus the phenomenology of the model depends to a great extent on which particle is the NLSP. In minimal GMSB models, the NLSP is usually either the lightest neutralino or the lighter stau. Most phenomenological studies and experimental searches that have used GMSB as a framework have taken the next to lightest SUSY particle to be the lightest neutralino. When this is the case, the χ_1^0 decays to a photon and a gravitino. If this decay takes place within the detector, the signal involves high p_T

photons accompanied by large $\not\!\!E_T$ [29]. For much of the parameter space, however, the lighter of the two staus is the NLSP. In this case, the decays of SUSY particles produce the $\tilde{\tau}_1$ which subsequently decays to a τ lepton and a gravitino. If the $\tilde{\tau}_1$ decays occur within the detector, signatures for SUSY production will then generally include τ leptons from the $\tilde{\tau}_1$ decays and $\not\!\!E_T$ due to the stable gravitinos and neutrinos leaving the detector.

It was proposed [30] that GMSB models where the $\tilde{\tau}_1$ is the NLSP can lead to unusual and distinguishing signatures for gaugino production. The subsequent decays involve multiple high p_T τ leptons and possibly substantial $\not\!\!E_T$. The purpose of this chapter is to analyze in detail the signals for these decay modes at the Tevatron. In particular, we seek to determine the production rates for various distinguishing final states, the E_T spectrum of the τ jets and the $\not\!\!E_T$ distribution for the events.

Mass Spectrum and Production Mechanisms

Since the observed signal depends on the masses of the sparticles, we first begin by describing the model and the corresponding mass spectrum. In our model, the messenger sector consists of some number of multiplets that are $5 + \bar{5}$ representations of SU(5). They couple to a chiral superfield S in the hidden sector whose scalar component has a vacuum expectation value (VEV) $\langle s \rangle$ and whose auxiliary component has a VEV $\langle F_s \rangle$. By imposing the requirement that the electroweak symmetry is broken radiatively, the particle spectrum and the mixing angles depend on five parameters: M, Λ, n, $\tan\beta$ and the sign of μ. M is the messenger scale. Λ is equal to $\langle F_s \rangle / \langle s \rangle$ and is related to the SUSY breaking scale. The parameter n is dictated by the choice of the vector-like messenger sector and can take the values 1, 2, 3, or 4 to satisfy the perturbative unification constraint. The parameter $\tan\beta$ is the ratio of the Higgs doublet VEVs as defined in chapter II. The parameter μ is the coefficient in the bilinear term, $\mu H_u H_d$, in the superpotential. Constraints coming from $b \to s\gamma$ strongly favor negative values for μ [31] and, in the cases considered here, μ is taken to be negative. Demanding that the EW symmetry be broken radiatively fixes the

magnitude of μ and the parameter B (from the $B\mu H_u H_d$ term in the scalar potential) in terms of the other parameters of the theory.

The soft SUSY breaking gaugino and scalar masses at the messenger scale are given by [26,32]

$$\tilde{M}_i(M) = n\, g(\frac{\Lambda}{M})\, \frac{\alpha_i(M)}{4\pi}\, \Lambda \tag{21}$$

and

$$\tilde{m}^2(M) = 2\, n\, f(\frac{\Lambda}{M}) \sum_{i=1}^{3} k_i\, C_i \left(\frac{\alpha_i(M)}{4\pi}\right)^2 \Lambda^2 \tag{22}$$

where the α_i are the three SM gauge couplings and $k_i = 1$, 1 and 3/5 for SU(3), SU(2), and U(1), respectively. The C_i are zero for gauge singlets and are 4/3, 3/4 and $(Y/2)^2$ for the fundamental representations of SU(3), SU(2) and U(1), respectively (with Y given by $Q = I_3 + Y/2$). $g(x)$ and $f(x)$ are messenger scale threshold functions. We calculate the sparticle masses at the scale M using Eqs. (21) and (22) and run these to the electroweak scale using the appropriate renormalization group equations [33].

The decay chains and hence the signatures for the events depend on the particles initially produced as well as the hierarchy of the masses. Since SUSY breaking is communicated to the visible sector by gauge interactions, the mass differences between the superparticles depend on the their gauge interactions. This creates a hierarchy in mass between the electroweak and strongly interacting sparticles. Eq. (21) shows that the gluino is more massive than the EW charginos and neutralinos, while Eq. (22) shows that squarks are considerably more massive than sleptons. Given this hierarchy of sparticle masses and the current lower bounds on squark and gluino masses, the production of strongly interacting sparticles is probably not a viable search modes for SUSY at the Tevatron Run II. A more likely mechanism for producing SUSY particles is via EW gaugino production. At the Tevatron, chargino pair ($\chi_1^+\chi_1^-$) production takes place through s-channel Z and γ exchange and $\chi_2^0\chi_1^\pm$ production is through s-channel W exchange. Squark exchange via the t-channel also contributes to both processes, but the contributions are expected to be negligible since the squark masses are large in GMSB models. The production of $\chi_1^0\chi_1^\pm$ is suppressed due to the smallness of the coupling involved. In regions of the parameter space where the production of charginos and neutralinos is kinematically suppressed, the pair production of sleptons

($\bar{\tilde{\tau}}_1\tilde{\tau}_1$, $\bar{\tilde{\mu}}_1\tilde{\mu}_1$ and $\bar{\tilde{e}}_1\tilde{e}_1$) can be important. Their production occurs through s-channel Z and γ exchange.

Given the hierarchy of sparticle masses in GMSB models, there are roughly four possible cases to consider for SUSY production at the Tevatron:

$$\textbf{Case 1: } m_{\tilde{\nu}} > M_{\chi_2^0} \gtrsim M_{\chi_1^\pm} > m_{\tilde{e}_1,\tilde{\mu}_1} > M_{\chi_1^0} > m_{\tilde{\tau}_1}$$

$$\textbf{Case 2: } m_{\tilde{\nu}} > M_{\chi_2^0} \gtrsim M_{\chi_1^\pm} > M_{\chi_1^0} > m_{\tilde{e}_1,\tilde{\mu}_1} > m_{\tilde{\tau}_1}$$

$$\textbf{Case 3: } M_{\chi_2^0} \gtrsim M_{\chi_1^\pm} > m_{\tilde{\nu}} > M_{\chi_1^0} > m_{\tilde{e}_1,\tilde{\mu}_1} > m_{\tilde{\tau}_1}$$

$$\textbf{Case 4: } M_{\chi_2^0} \gtrsim M_{\chi_1^\pm} > m_{\tilde{\nu}} > m_{\tilde{e}_1,\tilde{\mu}_1} > M_{\chi_1^0} > m_{\tilde{\tau}_1}$$

The three sneutrino masses are nearly the same. The lighter of the selectrons and smuons are essentially right-handed and have the same mass. Also, for all the parameter points we considered, $\chi_1^\pm$ and χ_2^0 are nearly degenerate in mass.

The possible final state configurations at the Tevatron depend on the sparticle spectrum, but they will have certain aspects in common. Since the $\tilde{\tau}_1$ is the NLSP, the various possible decays modes will (usually) produce at least two τ leptons arising from the decays of the $\tilde{\tau}_1$'s. In addition, there can also be large $\not\!\!E_T$ due to the stable gravitinos and neutrinos escaping detection.

A special situation of cases 2 and 3 arise when the lighter selectron and the lighter smuon are nearly degenerate in mass to the lighter stau. When the mass difference between the slectron and the stau is less than twice the mass of the τ lepton, essentially the only decay mode for the selectron is $\tilde{e} \to e\tilde{G}$. The lighter smuon likewise decays via $\tilde{\mu} \to \mu\tilde{G}$. This situation is referred to as the "co-NLSP" case.

Analysis and Results

We now give a detailed analysis of the possible Tevatron signatures for SUSY production in the context of GMSB models where the lightest stau is the NLSP. This analysis is performed in the context of the Main Injector (MI) and TeV33 upgrades of the Tevatron collider. The center of mass energy is taken to be $\sqrt{s} = 2\,\text{TeV}$ and

the integrated luminosity is taken to be $2\,\mathrm{fb}^{-1}$ for the MI upgrade and $30\,\mathrm{fb}^{-1}$ for the TeV33 upgrade [34]. The simulations are performed using a computer program that utilizes Monte Carlo methods.

In performing this analysis, the cuts employed are that final state charged leptons must have $p_T > 10\,\mathrm{GeV}$ and $\eta < 1$. Jets must have $E_T > 10\,\mathrm{GeV}$ and $|\eta| < 2$. In addition, hadronic final states within a cone size of $\Delta R \equiv \sqrt{(\Delta\phi)^2 + (\Delta\eta)^2} = 0.4$ are merged to a single jet. Leptons within this cone radius of a jet are discounted. For a τ-jet to be counted as such, it must have $|\eta| < 1$. The most energetic τ-jet is required to have $E_T > 20\,\mathrm{GeV}$. In addition, a missing transverse energy cut of $\not\!\!E_T > 30\,\mathrm{GeV}$ is imposed.

We consider several examples with different input parameters. In our analysis, we restrict ourselves to those regions of the parameter space where the $\tilde{\tau}_1$ decays promptly to a τ and a gravitino. The parameter space is also restricted to those regions where $m_{\tilde{\tau}_1} \gtrsim 70$ GeV since LEP-2 results place the bound $m_{\tilde{\tau}_1} \geq 72$ GeV [35].

A Stau NLSP Case with $n = 2$

In this section we do the analysis for points along the line defined by the parameter values $M/\Lambda = 3$, $n = 2$ and $\tan\beta = 15$. We vary Λ from 35 TeV to 85 TeV. The masses for the sparticles that are of interest here are given in Fig. 13. Note that the sneutrino mass is always above that of the lightest chargino and the lightest two neutralinos. Thus the sneutrinos do not figure into the decay chains of the major SUSY production mechanisms. Note that the lightest neutralino is below the selectron/smuon mass at the lower end of the Λ scale ($\Lambda \lesssim 45\,\mathrm{TeV}$). Thus for $\Lambda \lesssim 45\,\mathrm{TeV}$ the mass spectrum is of type 1. For $\Lambda \gtrsim 45\,\mathrm{TeV}$, the mass spectrum is of type 2. In this region of Λ, there are more decay modes for the various particles due to the increasing masses of all the sparticles as well as the shift in the position of the lightest neutralino in the mass hierarchy.

The cross sections for these parameters are given in Fig. 14. From the figure, the cross sections for $\chi_1^+\chi_1^-$ and $\chi_2^0\chi_1^\pm$ production dominate for the region where Λ is below 65 TeV. As Λ increases, the masses of the gauginos increase significantly and

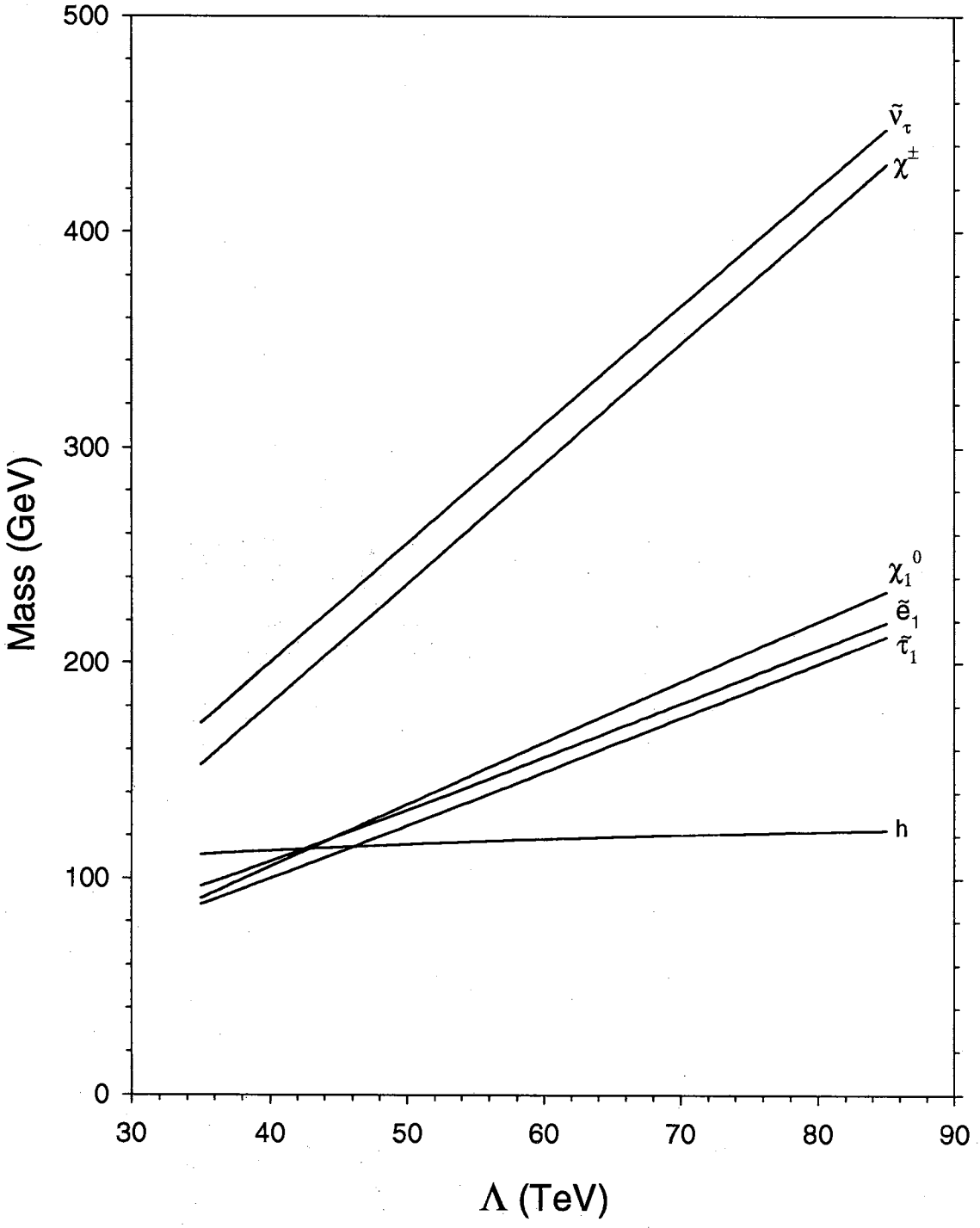

Figure 13. Masses for the sparticles of interest for the line defined by $n = 2$, $\tan\beta = 15$ and $M/\Lambda = 3$. $M_{\chi_2^0} \approx M_{\chi_1^\pm}$ and $M_{\tilde{\mu}_1} \approx M_{\tilde{e}_1}$.

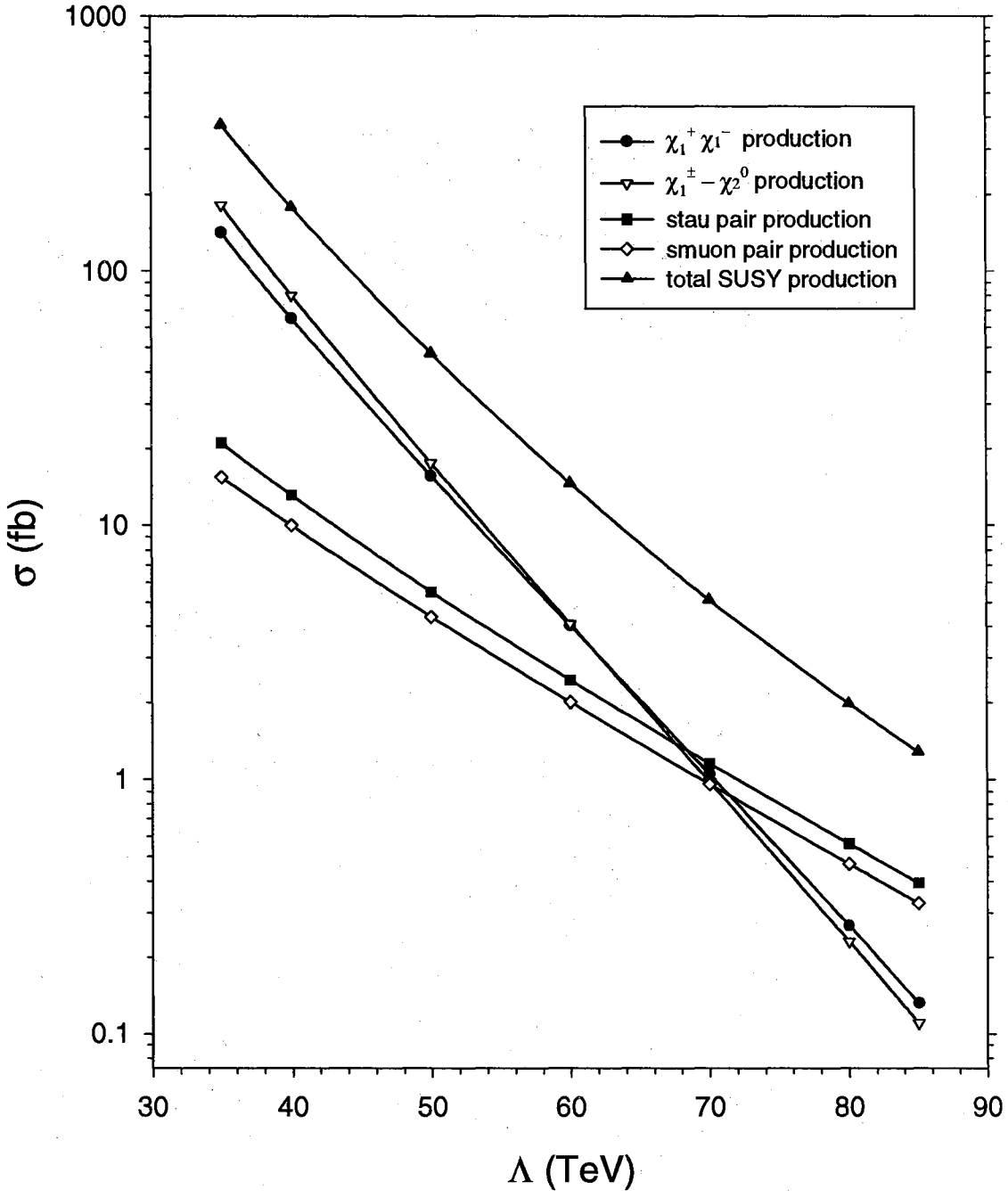

Figure 14. Cross section for the important SUSY production processes at the Tevatron for the line defined by $n = 2$, $\tan\beta = 15$ and $M/\Lambda = 3$. The $\chi_2^0\chi_1^\pm$ cross section includes production of both signs of the chargino.

hence the cross section falls off. For $\Lambda \gtrsim 70\,\mathrm{TeV}$, the production modes $\tilde{\tau}_1^+\tilde{\tau}_1^-$ and $\tilde{e}_1^+\tilde{e}_1^-$ are dominant, but the cross sections tend to be rather low.

The signatures for SUSY production depend on the allowed decay modes of the sparticles and their branching ratios. The branching ratios for the sparticles of interest are given in Table III. Since the $\tilde{\tau}_1$ is the NLSP, it decays via $\tilde{\tau}_1 \to \tau\,\tilde{G}$. The decays of the selectron and smuon depend strongly on the value of Λ. For Λ below $\sim 45\,\mathrm{TeV}$, the lightest neutralino has a mass below that of $\tilde{\mu}_1$ and $\tilde{e}_1$. As a consequence of this, the main decay mode of lighter smuon is $\tilde{\mu}_1 \to \chi_1^0\,\mu$, and the main decay mode of the lightest selectron is $\tilde{e}_1 \to \chi_1^0\,e$. For higher values of Λ, however, the lightest neutralino mass increases above that of $\tilde{e}_1$ and $\tilde{\mu}_1$. Then the only available two-body decay mode for the lighter smuon is $\tilde{\mu}_1 \to \mu\,\tilde{G}$, and the lighter selectron correspondingly decay via $\tilde{e}_1 \to e\,\tilde{G}$. Given the smallness of the coupling involved, though, the possibility exists that some three-body decays could be important. Indeed, the neutralino mediated decays $\tilde{\mu}_1^- \to e^-\tau^-\tilde{\tau}^+$ and $\tilde{\mu}_1^- \to e^-\tau^+\tilde{\tau}^-$ are the important decay modes for these higher values of Λ.

Since the lightest neutralino tends to be one of the least massive sparticles, its only decay modes are $\chi_1^0 \to \tilde{\tau}_1\tau$ and the decays to $\tilde{\mu}_1$ and $\tilde{e}_1$ if χ_1^0 is greater in mass than those sparticles. Since the lightest neutralino is less massive than the selectrons and smuons for Λ, the only decay mode is $\chi_1^0 \to \tilde{\tau}_1\tau$. As Λ increases above $45\,\mathrm{TeV}$, $\tilde{\mu}_1$ and $\tilde{e}_1$ become increasingly important, although $\chi_1^0 \to \tilde{\tau}_1\tau$ remains the dominant decay mode.

Since the lightest chargino is mostly wino, it couples mainly to "left-handed" sfermions. Thus the decay mode $\chi_1^\pm \to \tilde{\tau}_1\nu_\tau$ is typically important due to the significant mixing of the left and right handed staus and the lower mass of the $\tilde{\tau}_1$. This decay mode is, in fact, essentially the only decay mode for low values of Λ for the parameters considered here. Thus with the subsequent decay $\tilde{\tau}_1 \to \tau\,\tilde{G}$, there are typically two τ leptons produced in $\chi_1^+\chi_1^-$ production at these values of Λ. As Λ increases, however, the decay mode $\chi_1^\pm \to \chi_1^0 W$ becomes available and becomes the dominant decay mode as Λ increases above $60\,\mathrm{TeV}$. With the two τ leptons that

Table III. Branching ratios of the sparticles of interest for the parameters $n = 2$, $\tan\beta = 15$ and $M/\Lambda = 3$. The decays of the $\tilde{\mu}_1$ are obtained by replacing the e with a μ in the $\tilde{e}_1$ decays.

	Λ (TeV)						
Decay Mode	35	40	50	60	70	80	85
$\chi_1^\pm \to \tilde{\tau}_1 \nu_\tau$	1	1	0.6787	0.5192	0.4440	0.3996	0.3833
$\chi_1^\pm \to \chi_1^0 W$	-	-	0.3213	0.4808	0.5560	0.6004	0.6167
$\chi_2^0 \to \tilde{\tau}_1 \tau$	0.5677	0.5965	0.6235	0.3075	0.2137	0.1719	0.1578
$\chi_2^0 \to \tilde{\mu}_1 \mu$	0.2162	0.2017	0.1660	0.0659	0.0378	0.0256	0.0217
$\chi_2^0 \to \tilde{e}_1 e$	0.2162	0.2017	0.1660	0.0659	0.0378	0.0256	0.0217
$\chi_2^0 \to \chi_1^0 Z$	-	-	0.0446	0.0318	0.0251	0.0219	0.0207
$\chi_2^0 \to \chi_1^0 \mathrm{h}$	-	-	-	0.5289	0.6856	0.7550	0.7780
$\chi_1^0 \to \tilde{\tau}_1 \tau$	1	1	0.8577	0.6542	0.5659	0.5215	0.5072
$\chi_1^0 \to \tilde{\mu}_1 \mu$	-	-	0.0711	0.1729	0.2170	0.2392	0.2464
$\chi_1^0 \to \tilde{e}_1 e$	-	-	0.0711	0.1729	0.2170	0.2392	0.2464
$\tilde{e}_1 \to \chi_1^0 e$	1	1	-	-	-	-	-
$\tilde{e}_1^- \to e^- \tau^- \tilde{\tau}^+$	-	-	0.5205	0.5287	0.5315	0.5310	0.5298
$\tilde{e}_1^- \to e^- \tau^+ \tilde{\tau}^-$	-	-	0.4795	0.4697	0.4634	0.4580	0.4554
$\tilde{e}_1 \to e \tilde{G}$	-	-	-	0.0016	0.0050	0.0110	0.0148

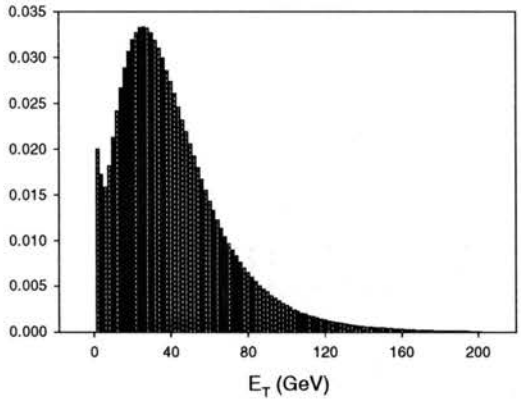

(a) The E_T distribution without cuts.

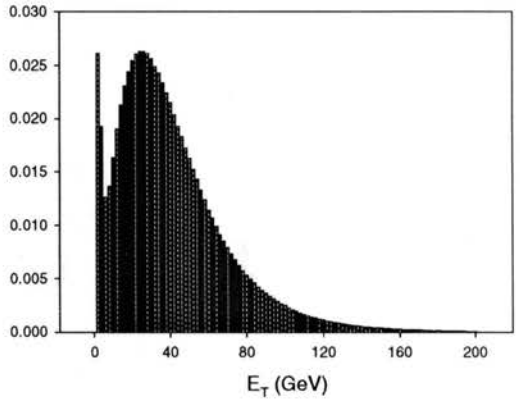

(b) The E_T distribution with the pseudorapidity cut $|\eta| < 1$ on τ-jets.

Figure 15. The E_T distributions of the leading τ jet for the parameters $n = 2$, $\tan\beta = 15$, $M/\Lambda = 3$ and $\Lambda = 35\,\text{TeV}$.

can be expected from the lightest neutralino decay and the $W \to \tau\nu_\tau$ decay, we can expect up to six τ leptons from $\chi_1^+\chi_1^-$ production at these larger values of Λ.

There are many decay modes for the second lightest neutralino as Table III shows. For low values of Λ, the dominant decay mode is $\chi_2^0 \to \tilde{\tau}_1\tau$ at 50 - 60%. The decays to the other sleptons are also important at 15 - 20%. Thus $\chi_1^\pm\chi_2^0$ production produces three τ leptons: two from the slepton decays of the neutralino and one from the decay $\chi_1^\pm \to \tilde{\tau}_1\,\nu_\tau$ followed by $\tilde{\tau}_1 \to \tau\,\tilde{G}$. As Λ increases above 55 TeV, The decay $\chi_2^0 \to \chi_1^0\,\text{h}$, where h is the Higgs boson, rapidly becomes the dominant decay mode. The decay $\chi_2^0 \to \chi_1^0 Z$ is also present, but of relatively little importance.

Given the cuts that we place on the τ-jets, the question arises as to how high we can expect the E_T of the τ-jets to be. Fig. 15 gives the E_T distribution of the highest E_T τ-jet for $\Lambda = 35\,\text{TeV}$. The pseudorapidity cut of $|\eta| < 1$ on τ-jets has been imposed in Fig. 15(b). The peak in the distribution occurs at about 25 GeV with a broad tail that reaches out beyond 120 GeV. Thus the leading τ-jets are relatively hard and many will pass the transverse energy cut of $E_T > 20\,\text{GeV}$. The next to highest E_T τ-jet is significantly different as Fig. 16 shows. Here the distribution peaks at a lower value of about 15 GeV and hardly extends at all beyond 80 GeV. Due to the softness of the secondary τ-jets, many of the τ-jets will tend to be eliminated by the cuts.

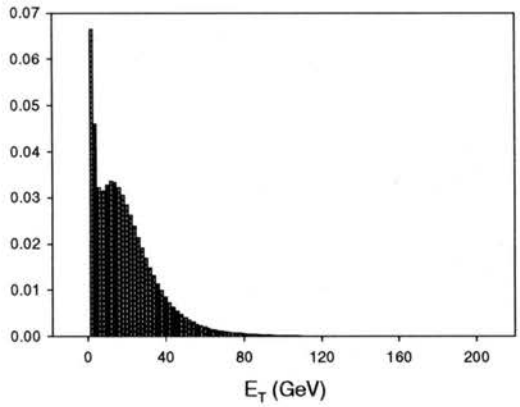

(a) The E_T distribution without cuts.

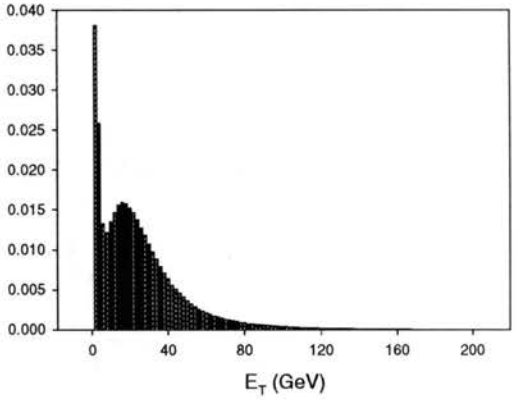

(b) The E_T distribution with the pseudorapidity cut $|\eta| < 1$ on τ-jets.

Figure 16. The E_T distributions of the secondary τ jet for the parameters $n = 2$, $\tan\beta = 15$, $M/\Lambda = 3$ and $\Lambda = 35\,\text{TeV}$.

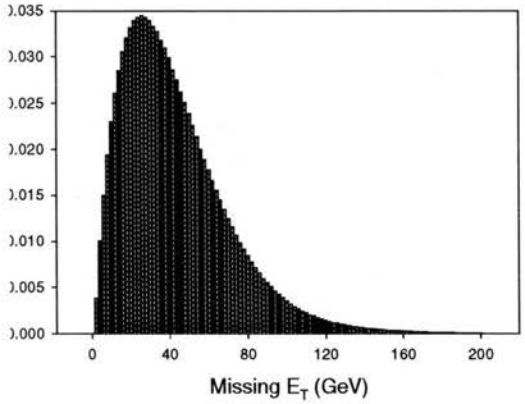

(a) The $\not{E}_T$ distribution without cuts.

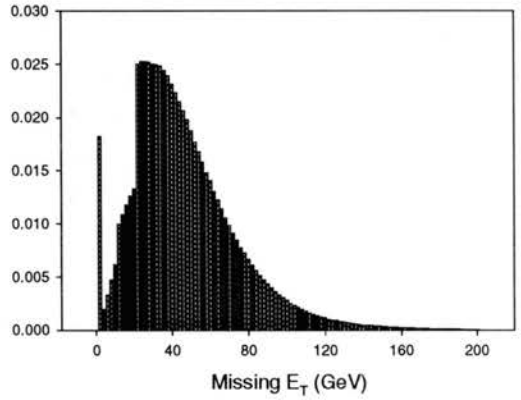

(b) The $\not{E}_T$ distribution with the E_T/p_T and pseudorapidity cuts on the jets and charged leptons.

Figure 17. $\not{E}_T$ distribution of the secondary τ jet for the parameters $n = 2$, $\tan\beta = 15$, $M/\Lambda = 3$ and $\Lambda = 35\,\text{TeV}$.

Table IV. Inclusive tau-jet branching ratios for the dominant production mechanisms for the parameters $n = 2$, $\tan\beta = 15$, $\Lambda = 35\,\mathrm{TeV}$ and $M = 105\,\mathrm{TeV}$.

Production Mode	1 τ-jet	2 τ-jets	3 τ-jets	4 τ-jets
$\chi_1^+\chi_1^-$: no cuts	0.4562	0.4200	-	-
with cuts	0.2577	0.1084	-	-
$\chi_1^\pm\chi_2^0$: no cuts	0.2408	0.4434	0.2723	-
with cuts	0.2558	0.1567	0.0259	-
$\tilde{\tau}_1^+\tilde{\tau}_1^-$: no cuts	0.4560	0.4203	-	-
with cuts	0.2523	0.0939	-	-
$\tilde{e}_1^+\tilde{e}_1^-$: no cuts	0.1128	0.3118	0.3834	0.1766
with cuts	0.2383	0.0778	0.0003	*negl.*

Also of interest is the $\not{E}_T$ distribution. With energetic and stable gravitinos and neutrinos produced in the decays, it is expected that large missing transverse energy could be an important part of the signal. Since the missing transverse energy is calculated from what is observed, however, the question arises as to whether significant cancellation occurs due to the many decay products. Fig. 17 gives the $\not{E}_T$ distribution for the case where $\Lambda = 35\,\mathrm{TeV}$. The figure demonstrates that the $\not{E}_T$ distribution is indeed broad with a tail reaching out beyond 120 GeV. The peak before cuts occurs at about 35 GeV and the peak still occurs at about 35 GeV when E_T/p_T and pseudorapidity cuts are applied to the various particles. Thus a 30 GeV cut should not be too restrictive. As Λ is increased, the $\not{E}_T$ distribution gets harder since the gaugino masses get larger as Λ is increased.

We now consider the specifics of the various final state possibilities. Table IV gives the inclusive branching ratios for different number of τ-jets for $\Lambda = 35\,\mathrm{TeV}$. As indicated above, this example always produces two τ leptons in chargino pair production. Before cuts the inclusive branching ratio for the two τ-jets mode in chargino pair production is 42%, while the one τ-jet mode in chargino pair production is 45.6%. After the cuts specified above, the branching ratios are cut down rather

Table V. Inclusive tau-jet branching ratios for the dominant production mechanisms for the parameters $n = 2$, $\tan\beta = 15$, $\Lambda = 50\,\text{TeV}$ and $M = 150\,\text{TeV}$.

Production Mode	1 τ-jet	2 τ-jets	3 τ-jets	4 τ-jets	5 τ-jets
$\chi_1^+\chi_1^-$: no cuts	0.3194	0.4099	0.1627	0.0291	0.0027
with cuts	0.3355	0.1610	0.0100	0.0004	*negl.*
$\chi_1^\pm\chi_2^0$: no cuts	0.1969	0.3961	0.3060	0.0626	0.0044
with cuts	0.3234	0.2238	0.0472	0.0014	*negl.*
$\tilde{\tau}_1^+\tilde{\tau}_1^-$: no cuts	0.4561	0.4201	-	-	-
with cuts	0.3345	0.1370	-	-	-
$\tilde{e}_1^+\tilde{e}_1^-$: no cuts	0.1130	0.3119	0.3833	0.1765	-
with cuts	0.3199	0.1207	0.0023	*negl.*	-

Table VI. Inclusive tau-jet branching ratios for the dominant production mechanisms for the parameters $n = 2$, $\tan\beta = 15$, $\Lambda = 70\,\text{TeV}$ and $M = 210\,\text{TeV}$.

Production Mode	1 τ-jet	2 τ-jets	3 τ-jets	4 τ-jets	5 τ-jets
$\chi_1^+\chi_1^-$: no cuts	0.2333	0.3821	0.2549	0.0728	0.0078
with cuts	0.3647	0.2119	0.0322	0.0023	*negl.*
$\chi_1^\pm\chi_2^0$: no cuts	0.1574	0.3455	0.3259	0.1210	0.0202
with cuts	0.3419	0.2334	0.0569	0.0071	0.0008
$\tilde{\tau}_1^+\tilde{\tau}_1^-$: no cuts	0.4561	0.4201	-	-	-
with cuts	0.3988	0.1711	-	-	-
$\tilde{e}_1^+\tilde{e}_1^-$: no cuts	0.1165	0.3133	0.3795	0.1743	-
with cuts	0.3901	0.1495	0.0013	*negl.*	-

substantially. The one τ-jet BR becomes 25.8% and the two τ-jet BR is 10.8%. The situation changes as Λ increases. This is demonstrated in Tables V and VI which are for $\Lambda = 50$ and 70 TeV, respectively. We see that there is now the possibility for many more τ-jets. This is due to the appearance of the decay mode $\chi_1^\pm \to \chi_1^0 W$. With the decay $\chi_1^0 \to \tilde{\tau}_1 \tau$ followed by $\tilde{\tau}_1 \to \tau \tilde{G}$ along with the decay $W \to \tau \nu_\tau$, there is now the possibility for producing up to six τ-jets. At $\Lambda = 50$ TeV, the BR for three τ-jets is 16.3%. This is cut down substantially after cuts, however, and the BR becomes only about 1%. $\Lambda = 70$ TeV gives similar results, although at this point the cross section for $\chi_1^+ \chi_1^-$ production is low.

Considering $\chi_2^0 \chi_1^\pm$ production, we recall that at $\Lambda \lesssim 45$ TeV, the decay modes of χ_2^0 are $\chi_2^0 \to \tilde{\tau}_1 \tau$, $\chi_2^0 \to \tilde{\mu}_1 \mu$ and $\chi_2^0 \to \tilde{e}_1 e$. With the subsequent decays $\tilde{\tau}_1 \to \tau \tilde{G}$ and $\tilde{\mu}_1 \to \mu \tau \tilde{\tau}_1$ along with the corresponding decay of the selectron, the number of τ leptons from χ_2^0 decay is two. With the one τ lepton from the chargino, we have up to three τ leptons from $\chi_2^0 \chi_1^\pm$ production at these values of Λ. We see from Table IV that for $\Lambda = 35$ TeV, the branching ratios for inclusive production of three τ-jets is 27.2% before cuts, while for one and two τ-jets the branching ratios are 24% and 44%, respectively. These branching ratios are cut back considerably once the cuts are included. In particular, the three τ-jets BR is reduced to only 2.6%. As Λ increases, the potential exists to create more than three τ-jets due to the new decay modes for $\chi_1^\pm$ and χ_2^0. The branching ratios for more than three τ-jets tend to be small after cuts, however, as Tables V and VI demonstrate.

Slepton production tends to be rather simple since there are relatively few decay modes available to the sleptons. This is especially true for production of the lightest stau as its only significant decay mode is $\tilde{\tau}_1 \to \tau \tilde{G}$. Thus for $\tilde{\tau}_1^+ \tilde{\tau}_1^-$ production up to two τ-jets are possible. As shown in Tables IV, V and VI, the branching ratios before cuts for the one and two τ-jets modes are 45.6% and 42%, respectively. After cuts, these drop down to 25 – 40% and 10 – 17%, respectively. The three-body decay modes of the lightest selectron and smuon mean that up to four τ-jets are possible in $\tilde{\mu}_1^+ \tilde{\mu}_1^-$ production and $\tilde{e}_1^+ \tilde{e}_1^-$ production. The branching ratios for three and four τ-jets in $\tilde{e}_1^+ \tilde{e}_1^-$ and $\tilde{\mu}_1^+ \tilde{\mu}_1^-$ production are greatly diminished after cuts.

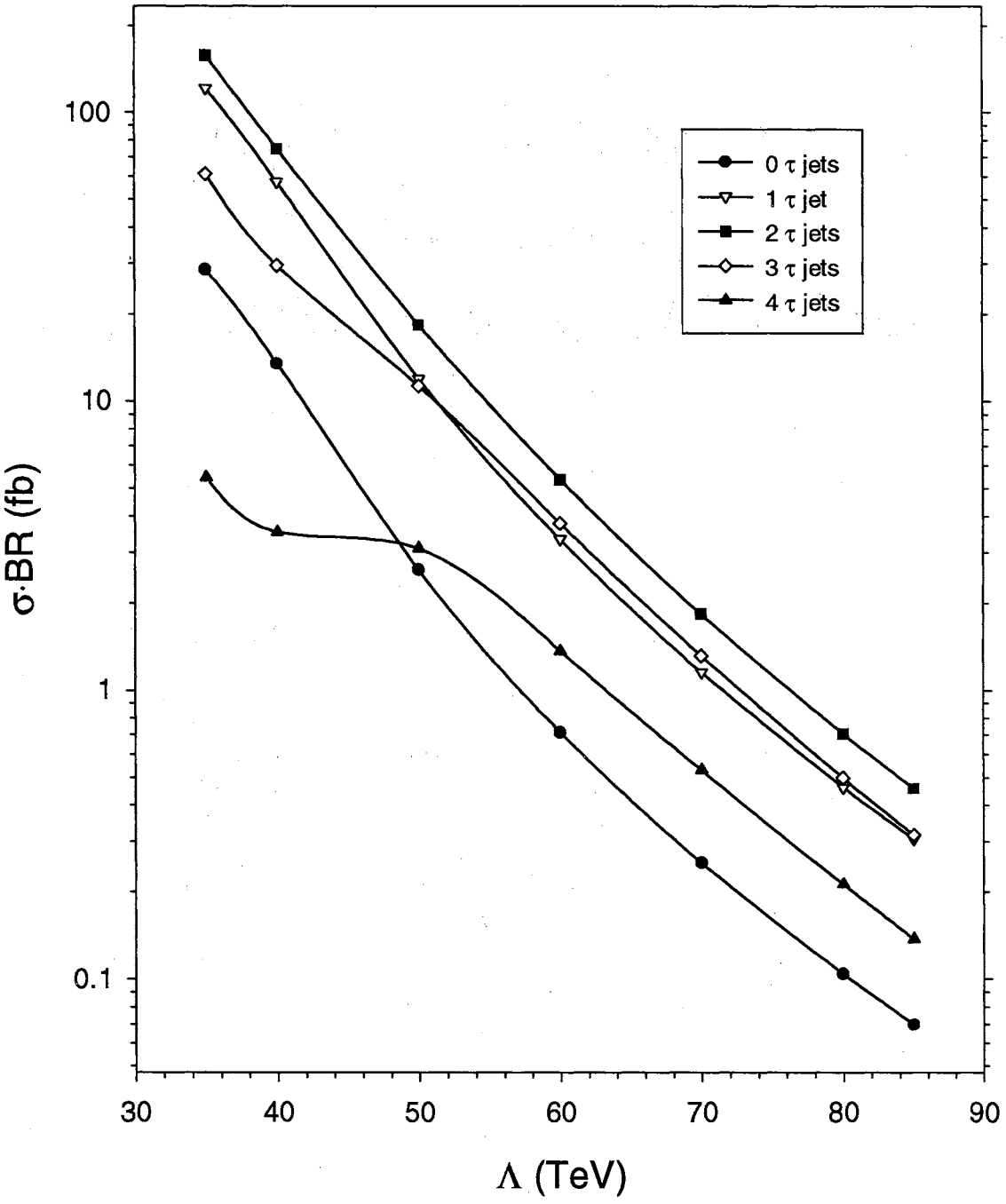

Figure 18. $\sigma \cdot BR$ before cuts for the inclusive τ-jets modes for the parameters $n = 2$, $\tan\beta = 15$ and $M/\Lambda = 3$.

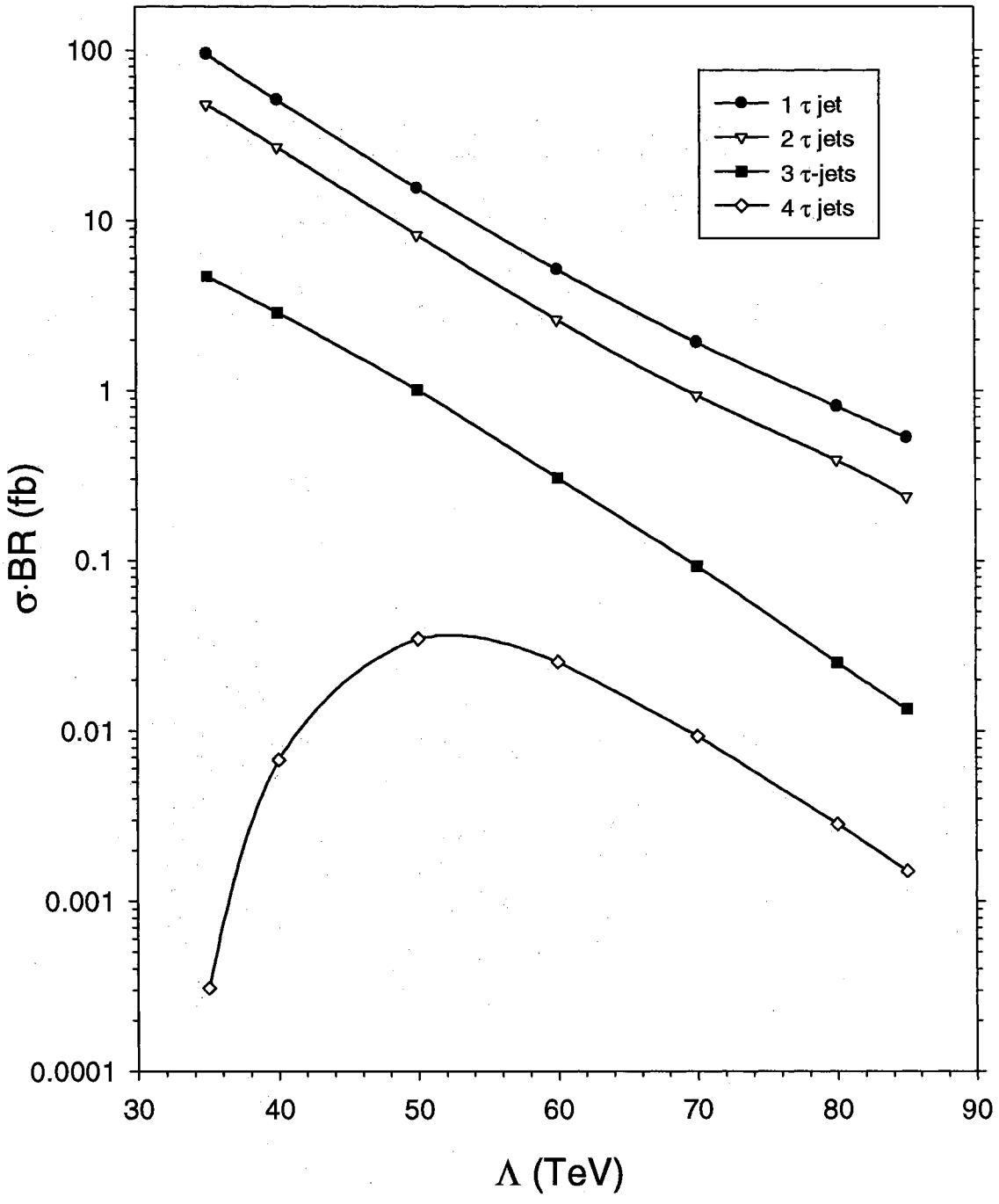

Figure 19. $\sigma \cdot BR$ after cuts for the inclusive τ-jets modes for the parameters $n = 2$, $\tan\beta = 15$ and $M/\Lambda = 3$.

The question now arises as to the observability of these modes at the Tevatron's Run II. The cross sections for inclusive τ-jet production before cuts are given in Fig. 18. All the SUSY production modes considered in this analysis are included. Events with more than four τ-jets are not included in the figure due to their extremely low branching ratios. The dominant decay mode is by far the two τ-jets mode. The one τ-jet and three τ-jets modes are also quite large.

Of course, the real issue is what the production cross sections are after the cuts have been imposed. These are given in Fig. 19. The graph shows that after cuts, the one τ-jet mode is dominant. The two τ-jets mode is of the same order of magnitude and the three τ-jets mode is not unappreciable. For $\Lambda = 35\,\text{TeV}$, the three τ-jets rate is 4.7 fb. For an integrated luminosity of $2\,\text{fb}^{-1}$ (approximately what is expected initially during Run II), this corresponds to ~ 9 observable events. For $30\,\text{fb}^{-1}$, the number of observable events is 141. The 2 τ-jets cross sections of 48.1 fb gives ~ 96 events for $2\,\text{fb}^{-1}$ of data and ~ 1440 for $30\,\text{fb}^{-1}$ of data. As Λ increases, the numbers are smaller due to the smaller SUSY production rate. For $\Lambda = 50\,\text{TeV}$, the expected number of events for three τ-jets is about 2 for $2\,\text{fb}^{-1}$ of data and 30 for $30\,\text{fb}^{-1}$ of data. The expected number of 2 τ-jets events is 16 and 248 for $2\,\text{fb}^{-1}$ and $30\,\text{fb}^{-1}$ of data, respectively. For $\Lambda = 70\,\text{TeV}$, the expected number of events for two τ-jets is 2 and 28 for $2\,\text{fb}^{-1}$ and $30\,\text{fb}^{-1}$, respectively.

The branching ratios for some of the more interesting individual modes in combined SUSY production are given in Table VII. The electrons and muons are typically too soft to pass the cuts. Thus requiring an e or μ to enhance the signal over background probably will be of little help.

A Stau NLSP Case with $n = 3$

We now consider a case where the ordering of the sparticles masses is quite different from the previous case. The parameters taken here are $n = 3$, $\tan\beta = 15$ and $M/\Lambda = 20$. We vary Λ from 25 to 55 TeV. The masses for these parameters are given in Fig. 20. We see that the ordering of the masses is of type 3: $M_{\chi_2^0} \gtrsim M_{\chi_1^\pm} > m_{\tilde{\nu}} > M_{\chi_1^0} > m_{\tilde{e}_1,\tilde{\mu}_1} > M_{\tilde{\tau}_1}$. This case is more complicated than the previous one due

Table VII. Production rates in fb for some of the more interesting final state configurations with and without cuts for the parameters $n = 2$, $\tan\beta = 15$ and $M/\Lambda = 3$.

	$\Lambda = 35\,\text{TeV}$		$\Lambda = 50\,\text{TeV}$	
	no cuts	cuts	no cuts	cuts
1 τ-jet	-	51.17	-	3.71
e/μ + 1 τ-jet	85.44	11.91	4.98	1.59
1 jet + 1 τ-jet	-	21.58	-	2.36
2 jets + 1 τ-jet	-	-	-	2.35
e/μ+ 2 jets + 1 τ-jet	-	-	-	0.69
2 τ-jets	157.3	40.64	9.18	3.91

to the shifting of the sneutrino masses below that of $\chi_1^\pm$ and χ_2^0. As a consequence, there are many decay modes for $\chi_1^\pm$ and χ_2^0 over the parameter space considered here. Moreover, the lightest selectron and smuon masses are always below that of the lightest neutralino. The result of all this is that the decay chains will generally be quite involved with many steps for the values of Λ considered here.

The branching ratios for the sparticles are given in Table VIII. Since the masses of the lighter selectron and the lighter smuon are always below that of the lightest neutralino, there are three decay modes available for the values of Λ considered: $\chi_1^0 \to \tilde{\tau}_1\tau$, $\chi_1^0 \to \tilde{\mu}_1\mu$ and $\chi_1^0 \to \tilde{e}_1 e$. The decay to the stau is the dominant decay mode especially at low values of Λ.

There are many potential decay modes for the chargino with these values of the parameters. Since the sneutrinos are now less massive than the chargino, these provide three decay modes that were not present in the example of the previous section: $\chi_1^\pm \to \tilde{\nu}_\tau\tau$, $\chi_1^\pm \to \tilde{\nu}_\mu\mu$ and $\chi_1^\pm \to \tilde{\nu}_e e$. For the entire range of parameters considered, these decays to the sneutrinos are always present as well as the decay $\chi_1^\pm \to \tilde{\tau}_1\nu_\tau$ which is the dominant decay mode for Λ less than about 50 TeV. As Λ increases, the mass difference between the lightest chargino and the lightest neutralino increases, and the decay $\chi_1^\pm \to \chi_1^0 W$ becomes kinematically allowed. At $\Lambda = 55\,\text{TeV}$,

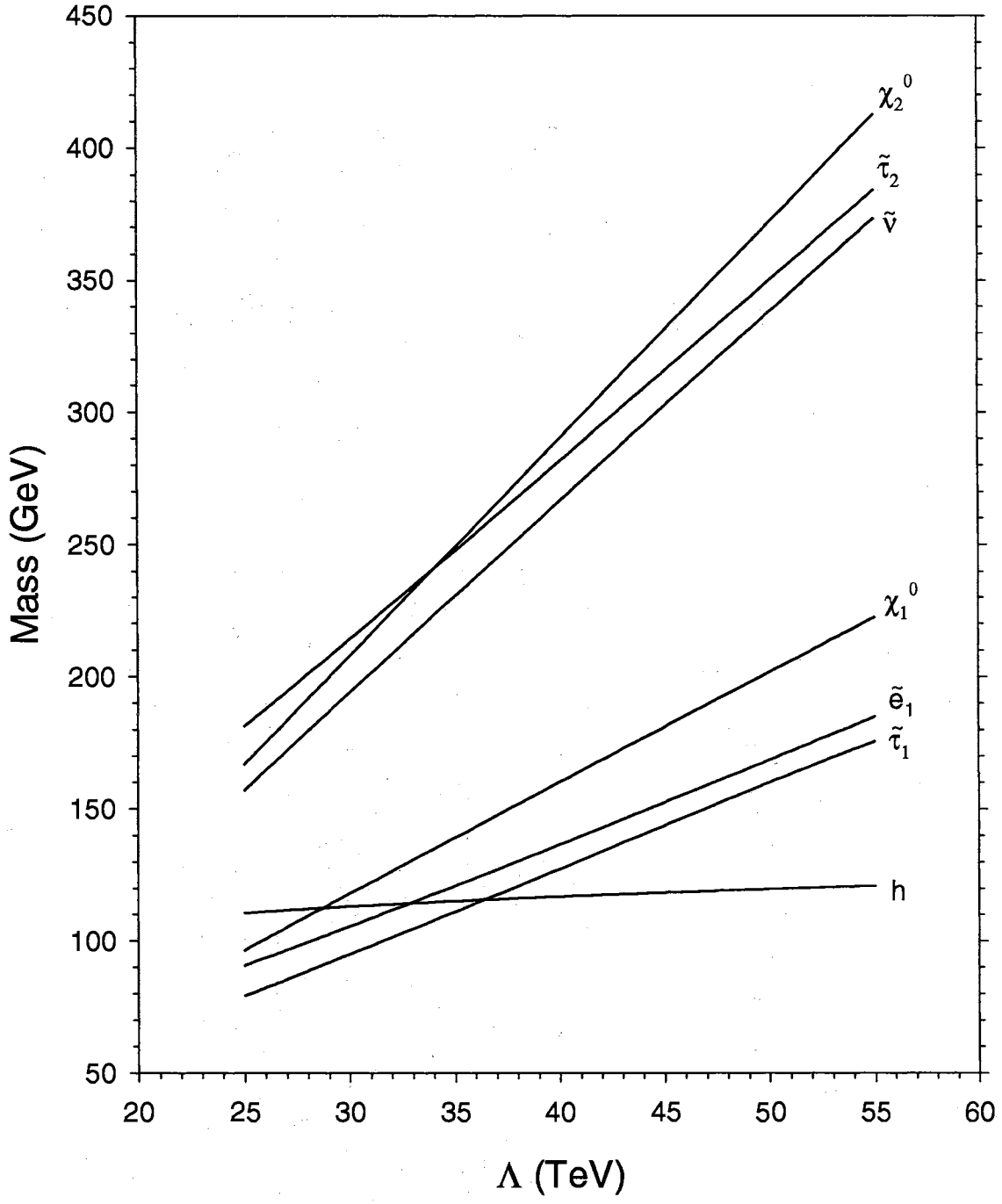

Figure 20. Masses for the sparticles of interest for the line defined by $n = 3$, $\tan\beta = 15$ and $M/\Lambda = 20$. χ_2^0 and $\chi_1^\pm$ are close in mass, and $\tilde{\mu}_1$ and $\tilde{e}_1$ are nearly degenerate in mass.

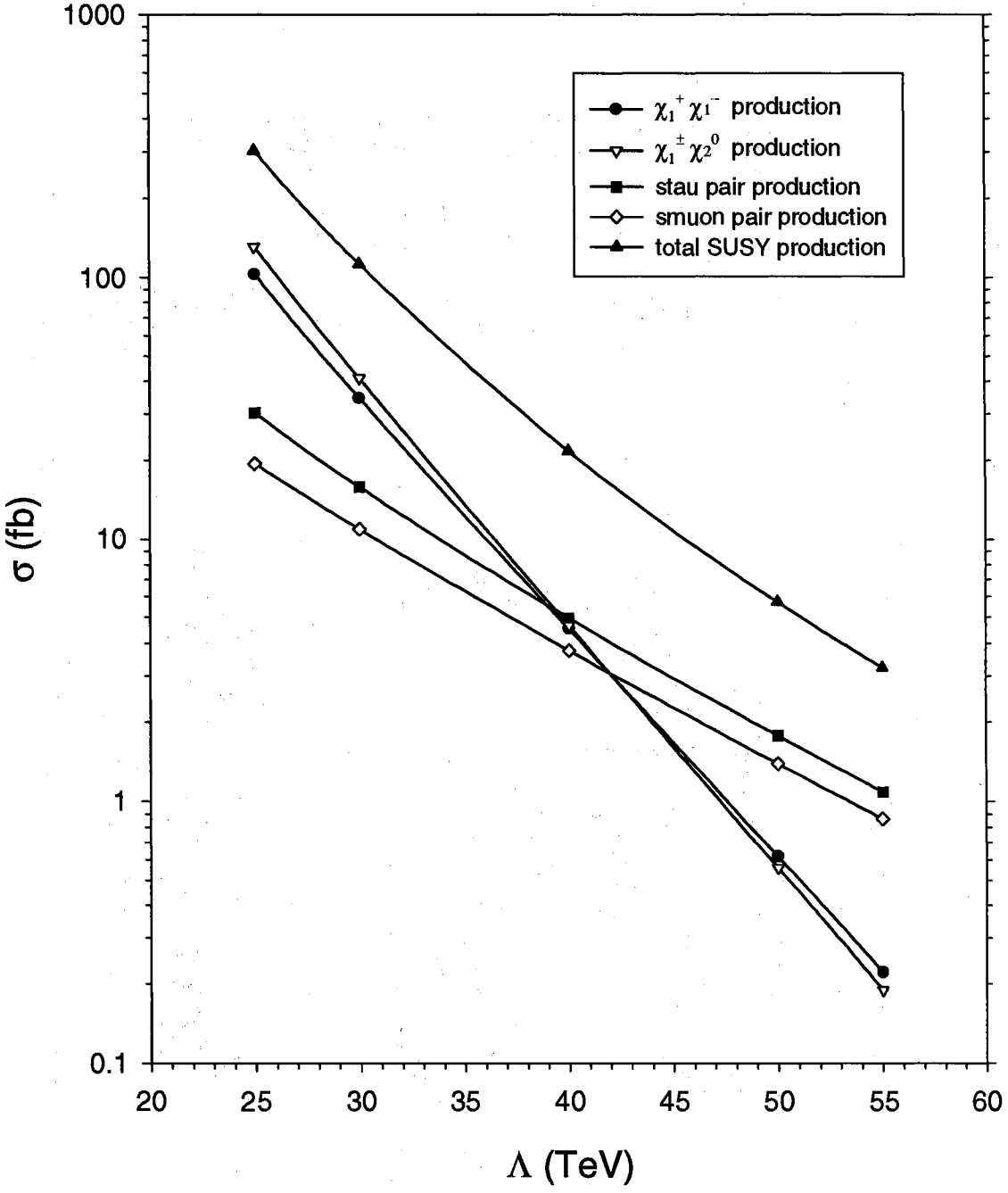

Figure 21. Cross sections for the important SUSY production processes at the Tevatron for the parameters $n = 3$, $\tan\beta = 15$ and $M/\Lambda = 20$. The $\chi_2^0\chi_1^\pm$ cross section includes production of both signs of the chargino.

Table VIII. Branching ratios of some of the sparticles of interest for the parameter set with $n = 3$, $\tan\beta = 15$ and $M/\Lambda = 20$.

	Λ (TeV)				
Decay Mode	25	30	40	50	55
$\chi_1^\pm \to \tilde{\tau}_1 \nu_\tau$	0.8062	0.6330	0.3514	0.2211	0.1839
$\chi_1^\pm \to \tilde{\tau}_2 \nu_\tau$	-	-	0.0118	0.0493	0.0643
$\chi_1^\pm \to \tilde{e}_2 \nu_e$	-	-	0.023	0.061	0.074
$\chi_1^\pm \to \tilde{\nu}_\tau \tau$	0.0729	0.1097	0.1379	0.1450	0.1467
$\chi_1^\pm \to \tilde{\nu}_e e$	0.0604	0.0954	0.1253	0.1342	0.1365
$\chi_1^\pm \to \chi_1^0 W$	-	0.0666	0.2022	0.1943	0.1832
$\chi_2^0 \to \tilde{\tau}_1 \tau$	0.5760	0.5653	0.2894	0.1678	0.1385
$\chi_2^0 \to \tilde{\tau}_2 \tau$	-	-	0.0142	0.0432	0.0542
$\chi_2^0 \to \tilde{e}_1 e$	0.1667	0.1335	0.0478	0.0207	0.0151
$\chi_2^0 \to \tilde{e}_2 e$	-	-	0.0240	0.0507	0.0602
$\chi_2^0 \to \tilde{\nu}_\tau \nu_\tau$	0.0317	0.0583	0.0760	0.0811	0.0845
$\chi_2^0 \to \tilde{\nu}_e \nu_e$	0.0294	0.0547	0.0722	0.07764	0.0810
$\chi_2^0 \to \chi_1^0 Z$	-	-	0.0196	0.0136	0.0119
$\chi_2^0 \to \chi_1^0 \mathrm{h}$	-	-	0.3127	0.3961	0.3983
$\chi_1^0 \to \tilde{\tau}_1 \tau$	0.7955	0.6011	0.4707	0.4268	0.4150
$\chi_1^0 \to \tilde{e}_1 e$	0.1023	0.1994	0.2646	0.2866	0.2925
$\tilde{e}^- \to e^- \tau^- \tilde{\tau}^+$	0.5563	0.5746	0.5898	0.5960	0.5977
$\tilde{e}^- \to e^- \tau^+ \tilde{\tau}^-$	0.4437	0.4254	0.4102	0.4040	0.4023

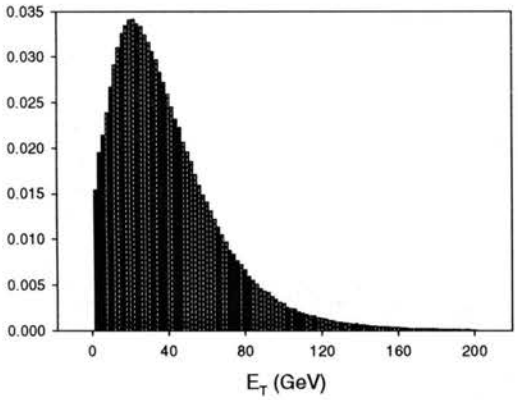

(a) The E_T distribution without cuts.

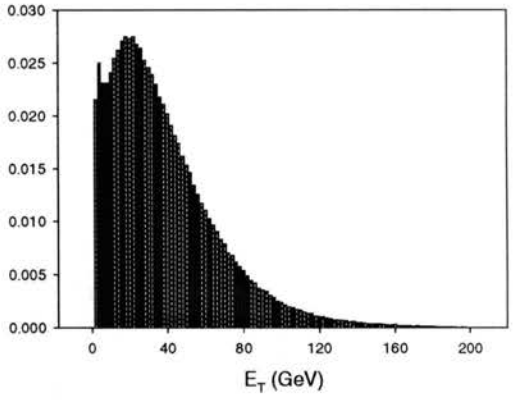

(b) The E_T distribution with the pseudorapidity cut $|\eta| < 1$ on τ-jets.

Figure 22. The E_T distributions of the highest E_T τ-jet for the parameters $n = 3$, $\tan\beta = 15$, $M/\Lambda = 20$ and $\Lambda = 25\,\text{TeV}$.

it is as important a decay mode as $\chi_1^\pm \to \tilde{\tau}_1\nu_\tau$. One other distinguishing characteristic of this case from the last one is that the heavier selectron and smuon have masses below that of $\chi_1^\pm$ and χ_2^0. Thus the decays $\chi_1^\pm \to \tilde{\tau}_2\nu_\tau$, $\chi_1^\pm \to \tilde{\mu}_2\nu_\mu$ and $\chi_1^\pm \to \tilde{e}_2\nu_e$ are available and their branching ratios are small, but not unimportant at large Λ.

For the second lightest neutralino, there are up to eleven main decay modes. For low values of Λ, the dominant decay mode is $\chi_2^0 \to \tilde{\tau}_1\tau$. The other slepton decay modes $\chi_2^0 \to \tilde{e}_1 e$ and $\chi_2^0 \to \tilde{\mu}_1\mu$ are also important. As Λ increases, the decay $\chi_2^0 \to \chi_1^0\,\text{h}$ becomes kinematically allowed and rapidly becomes the dominant decay. The decay modes to the sneutrinos also become more important.

The E_T distribution of the highest E_T τ-jet for $\Lambda = 25\,\text{TeV}$ is given in Fig. 22 and the E_T distribution of the secondary τ-jet is given in Fig. 23. The distribution for the leading τ-jet is quite similar to the previous case, but the secondary τ-jet spectrum is softer due to more of the τ leptons coming from further down the decay chain. The $\not{E}_T$ distribution is given in Fig. 24.

We now consider the details of the various final state possibilities. Table IX gives the inclusive branching ratios for different numbers of τ-jets for $\Lambda = 25\,\text{TeV}$. In principle, up to six τ leptons can be produced in $\chi_1^+\chi_1^-$ production, but the five and six τ lepton branching ratios are small. The most important mode before cuts is the

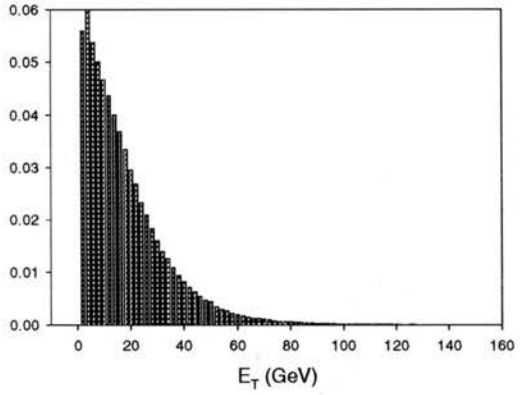

(a) The E_T distribution without cuts.

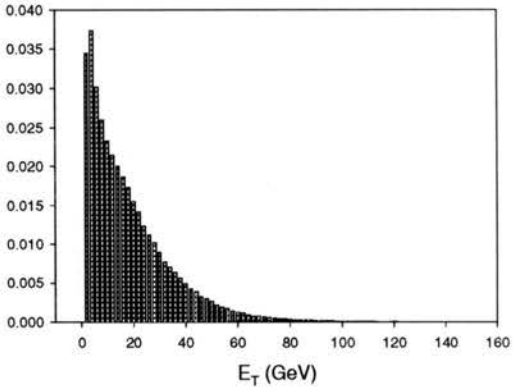

(b) The E_T distribution with the pseudorapidity cut $|\eta| < 1$ on τ-jets.

Figure 23. The E_T distributions of the second highest E_T τ-jet for the parameters $n = 3$, $\tan\beta = 15$, $M/\Lambda = 20$ and $\Lambda = 20\,\text{TeV}$.

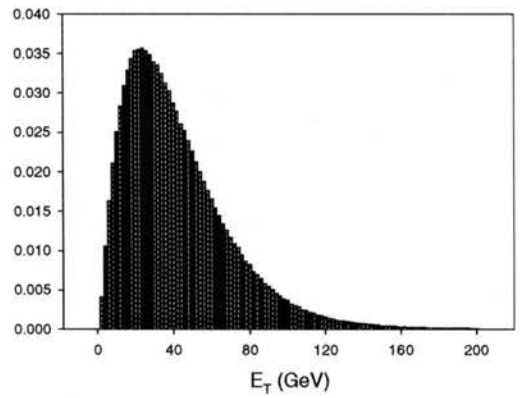

(a) The $\not{E}_T$ distribution without cuts.

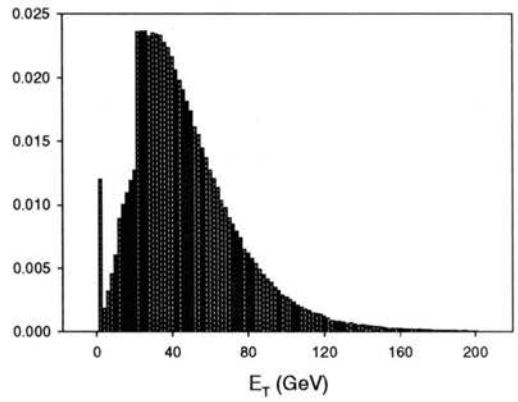

(b) The $\not{E}_T$ distribution with the E_T/p_T and pseudorapidity cuts on the jets and charged leptons.

Figure 24. $\not{E}_T$ distribution for the parameters $n = 3$, $\tan\beta = 15$, $M/\Lambda = 20$ and $\Lambda = 25\,\text{TeV}$.

Table IX. Inclusive tau-jet branching ratios for the dominant production mechanisms for the parameters $n = 3$, $\tan\beta = 15$, $\Lambda = 25\,\text{TeV}$ and $M = 500\,\text{TeV}$.

Production Mode	1 τ-jet	2 τ-jets	3 τ-jets	4 τ-jets	5 τ-jets
$\chi_1^+\chi_1^-$: no cuts	0.3597	0.4040	0.1110	0.0306	0.0033
with cuts	0.2336	0.1138	0.0077	0.0003	*negl.*
$\chi_1^\pm\chi_2^0$: no cuts	0.2110	0.4077	0.2912	0.0443	0.0085
with cuts	0.2452	0.1682	0.0332	0.0010	*negl.*
$\tilde{\tau}_1^+\tilde{\tau}_1^-$: no cuts	0.4555	0.4210	-	-	-
with cuts	0.2258	0.0797	-	-	-
$\tilde{e}_1^+\tilde{e}_1^-$: no cuts	0.1128	0.3121	0.3833	0.1764	-
with cuts	0.1998	0.0779	0.0063	0.0002	-

two τ-jet mode at 40.4%, but the one and three τ-jets modes are also appreciable. After implementing the cuts, the branching ratios are greatly decreased: the two τ-jets branching ratio becomes only 11.4% and the one τ-jet branching ratio becomes 23.4%. The three τ-jet branching ratio becomes essentially negligible. The situation changes as Λ increases. Table X gives the inclusive τ-jet branching ratios for $\Lambda = 40\,\text{TeV}$. The branching ratio for greater numbers of τ-jets are now larger. This is due to the decrease in the branching ratio for $\chi_1^\pm \to \tilde{\tau}_1\nu_\tau$ from which one can get only one τ-jet from the chargino and the increase in $\chi_1^\pm \to \chi_1^0 W$ which can give three τ-jets and $\chi_1^\pm \to \tilde{\nu}_\tau\tau$ which can also give three τ-jets. The two τ-jets mode in $\chi_1^+\chi_1^-$ production is still dominant at 34.8%, but now the three τ-jets mode is appreciable at 28.6%. After cuts, the three τ-jets rate drops to 5% and the one τ-jet mode becomes dominant at 30.1%.

Turning now to $\chi_2^0\chi_1^\pm$ production, we see from Table IX that at low Λ, there is the potential to produce up to five τ-jets (three from $\chi_1^\pm \to \tilde{\nu}_\tau\tau$ with the subsequent decays $\tilde{\nu}_\tau \to \chi_1^0\nu_\tau$ and $\chi_1^0 \to \tilde{\tau}_1\tau$ and two τ-jets from $\chi_2^0 \to \tilde{\nu}_\tau\nu_\tau$), but the branching ratios for more than three τ-jets are rather small. As usual the dominant decay mode is to two τ-jets with a before cuts branching ratio of 40.8%, but the three

Table X. Inclusive tau-jet branching ratios for the dominant production mechanisms for the parameters $n = 3$, $\tan\beta = 15$, $\Lambda = 40\,\text{TeV}$ and $M = 800\,\text{TeV}$.

Production Mode	1 τ-jet	2 τ-jet	3 τ-jets	4 τ-jets	5 τ-jets
$\chi_1^+\chi_1^-$: no cuts	0.1890	0.3484	0.2863	0.1155	0.0223
with cuts	0.3011	0.2123	0.0500	0.0057	0.0003
$\chi_1^\pm\chi_2^0$: no cuts	0.1457	0.3342	0.3301	0.1395	0.0236
with cuts	0.2991	0.2343	0.0672	0.0082	0.0008
$\tilde{\tau}_1^+\tilde{\tau}_1^-$: no cuts	0.4556	0.4208	-	-	-
with cuts	0.3396	0.1395	-	-	-
$\tilde{e}_1^+\tilde{e}_1^-$: no cuts	0.1128	0.3121	0.3833	0.1765	-
with cuts	0.3213	0.1270	0.0048	0.0001	-

τ-jets branching ratio is large at 29.1%. After cuts these fall to 16.8% and 3.3%, respectively. The one τ-jet mode becomes dominant with a branching ratio of 24.5%. Table X gives the results for $\Lambda = 40\,\text{TeV}$. The four τ-jets mode has a substantial decay rate before cuts, but this mode becomes negligible after cuts due to the typical softness of the fourth τ-jet which is produced further down the decay chain. On the other hand, the three τ-jets branching ratio is now higher at 6.7%.

Slepton production for this case is largely the same as in the previous case. With $\tilde{\tau}_1 \to \tau\,\tilde{G}$ being essentially the only decay mode for the lightest stau, the τ-jet branching ratios before cuts are completely dictated by the hadronic branching ratio for the τ lepton. For $\tilde{\mu}_1^+\tilde{\mu}_1^-$ and $\tilde{e}_1^+\tilde{e}_1^-$ production, up to four τ-jets can be produced, but after cuts the rates for three and four τ-jets are greatly reduced.

Putting all the pieces together, we can now answer the question as to the probability of observing these events at Tevatron's Run II and Run III. Fig. 25 shows the branching ratios for the inclusive τ-jet modes before cuts for all the considered SUSY production modes combined. The two τ-jets mode is the mode with the largest $\sigma\cdot\text{BR}$, but the production rates for one and three τ-jets are close to this. After including cuts, the one τ-jet mode is dominant and the two τ-jets mode is respectably high as

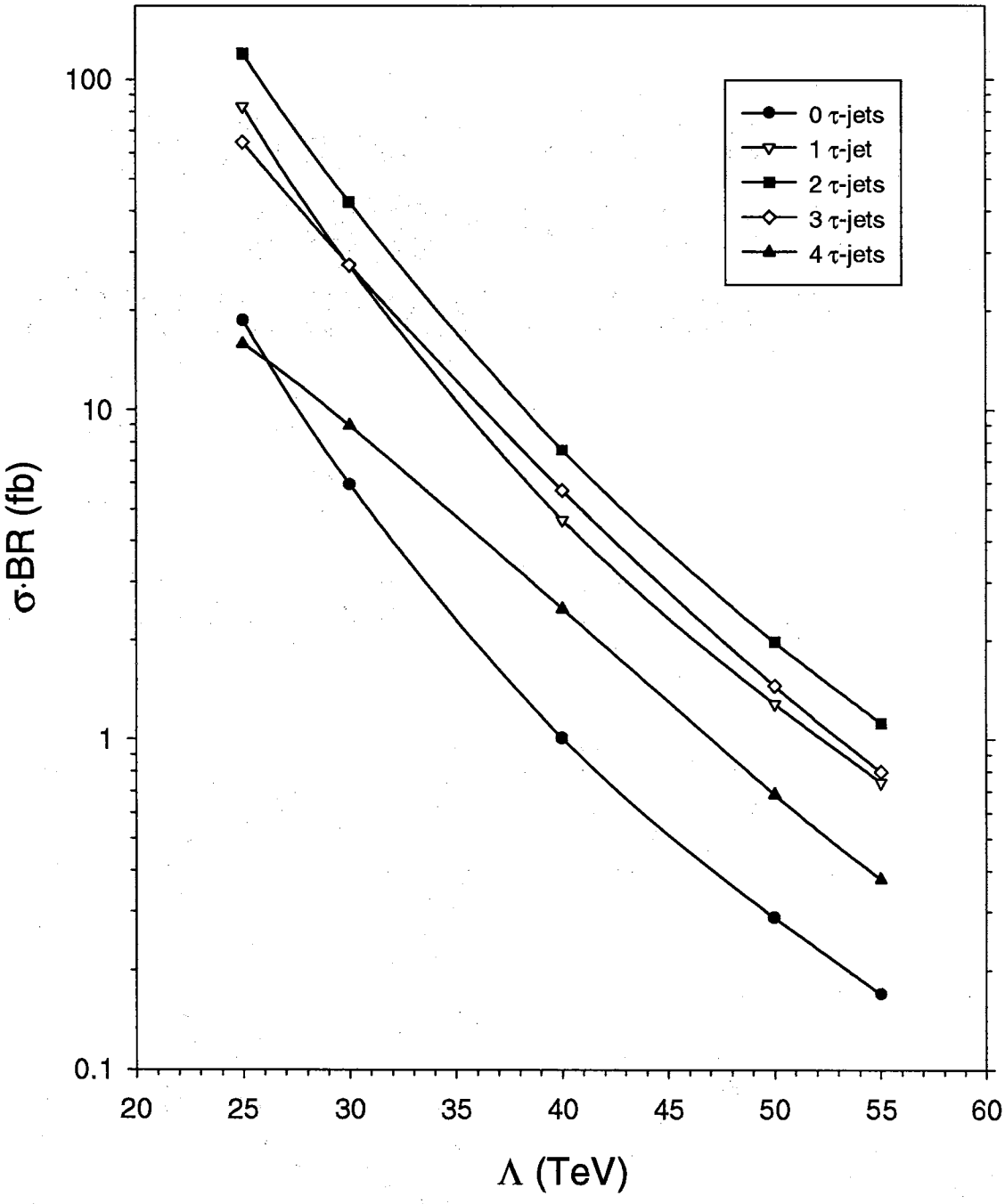

Figure 25. $\sigma \cdot BR$ before cuts for the inclusive τ-jet modes for the parameters $n = 3$, $\tan\beta = 15$ and $M/\Lambda = 20$.

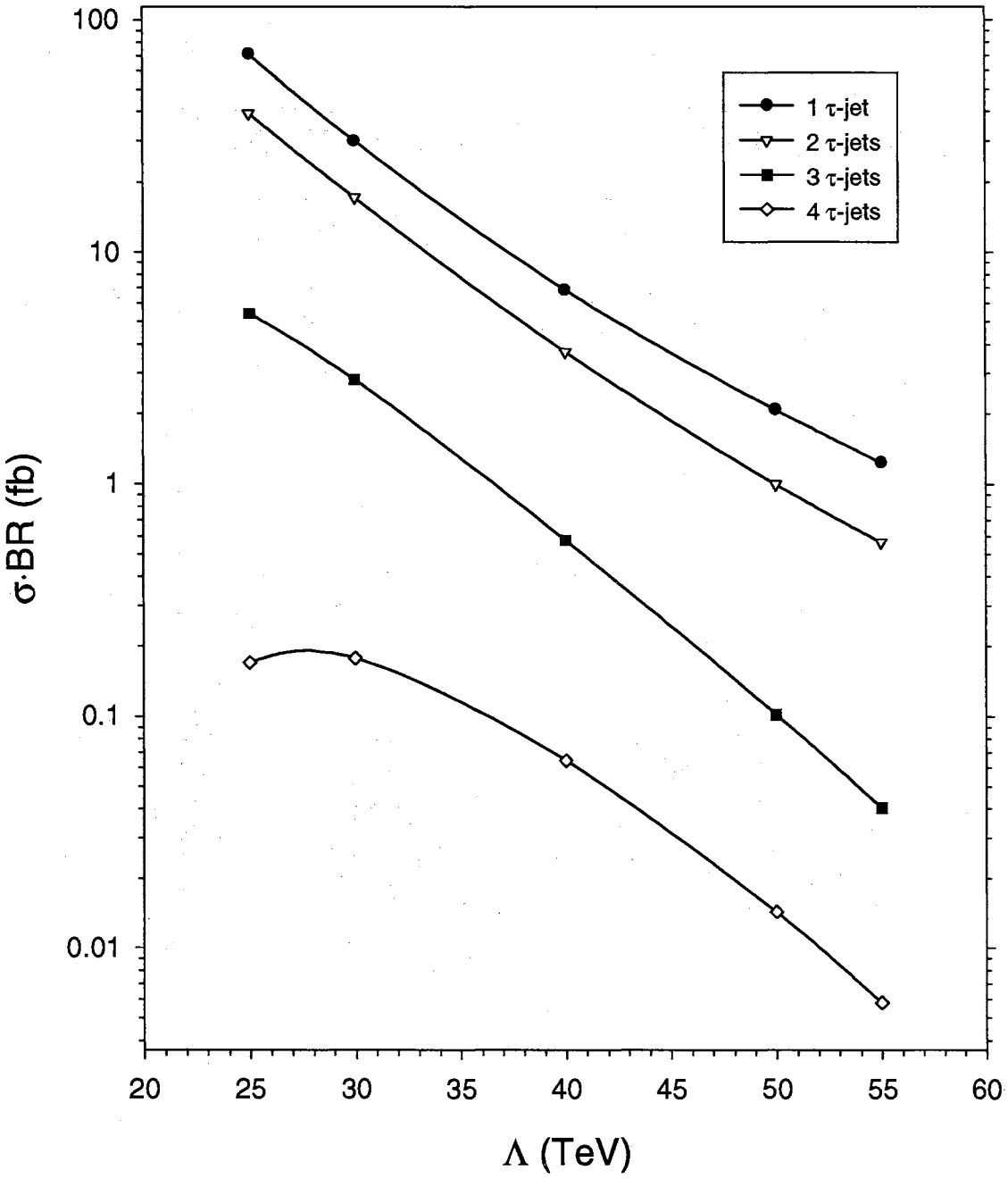

Figure 26. $\sigma \cdot BR$ after cuts for the inclusive τ jets modes for the parameters $n = 3$, $\tan\beta = 15$ and $M/\Lambda = 20$.

seen in Fig. 26. For $\Lambda = 25\,\text{TeV}$, the three τ-jets rate is 5.4 fb giving ~ 11 events for $2\,\text{fb}^{-1}$ of data and ~ 162 events for $30\,\text{fb}^{-1}$ of data. The two τ-jet rate of 39.3 fb gives ~ 79 and ~ 1180 events, respectively. For the higher Λ value of 50 TeV, the rates are cut down significantly. The two τ-jets rate of 1.0 fb gives ~ 2 and ~ 30 events for $2\,\text{fb}^{-1}$ and $30\,\text{fb}^{-1}$ of data, respectively.

A Co-NLSP Case

The co-NLSP case refers to when the mass difference between $\tilde{e}_1$ (and $\tilde{\mu}_1$) and $\tilde{\tau}_1$ is less than the mass of the τ lepton. When this is the case, the three-body decay mode $\tilde{e}_1 \to e\tau\tilde{\tau}_1$ is not kinematically allowed and the main decay mode for the selectron is the two-body mode $\tilde{e}_1 \to e\tilde{G}$. The parameters for the example of this case that is considered here are $n = 3$, $\tan\beta = 3$ and $M/\Lambda = 3$. Λ is varied from 25 to 65 TeV. The masses of the sparticles of interest are given in Fig. 27. We see that the ordering of the masses here is a special case of type 3: $M_{\chi_2^0} \gtrsim M_{\chi_1^\pm} > m_{\tilde{\nu}} > M_{\chi_1^0} > m_{\tilde{e}_1,\tilde{\mu}_1} \approx m_{\tilde{\tau}_1}$. With this ordering of the masses there are typically many decays mode of the sparticles to consider. The cross sections for the major SUSY production modes are given in Fig. 28. Due to the rapid increase in the sparticle masses (especially the gaugino masses) as Λ is increased, the cross sections tend to decrease fairly rapidly.

The branching ratios for the sparticles of interest are given in Table XI. Since the lighter selectron and the lighter smuon have about the same mass as the stau, the branching ratios for $\chi_1^0 \to \tilde{\tau}_1\tau$, $\chi_1^0 \to \tilde{\mu}_1\mu$ and $\chi_1^0 \to \tilde{e}_1 e$ are nearly equal. The decay to the stau is slightly favored.

The chargino's decays strongly depend on the value of Λ. For values of Λ that are 30 TeV and below, the dominant decay mode of the chargino is $\chi_1^\pm \to \tilde{\tau}_1\nu_\tau$. As Λ is increased above this, the chief decay modes are the decays to the sneutrinos and the decay $\chi_1^\pm \to \chi_1^0 W$ which tends to dominate when kinematically allowed. As Λ increases above 30 TeV, the masses of the heavier sleptons ($\tilde{\tau}_2$, $\tilde{\mu}_2$ and $\tilde{e}_2$) fall below the mass of the chargino, and so the decays to these heavier sleptons are allowed as well.

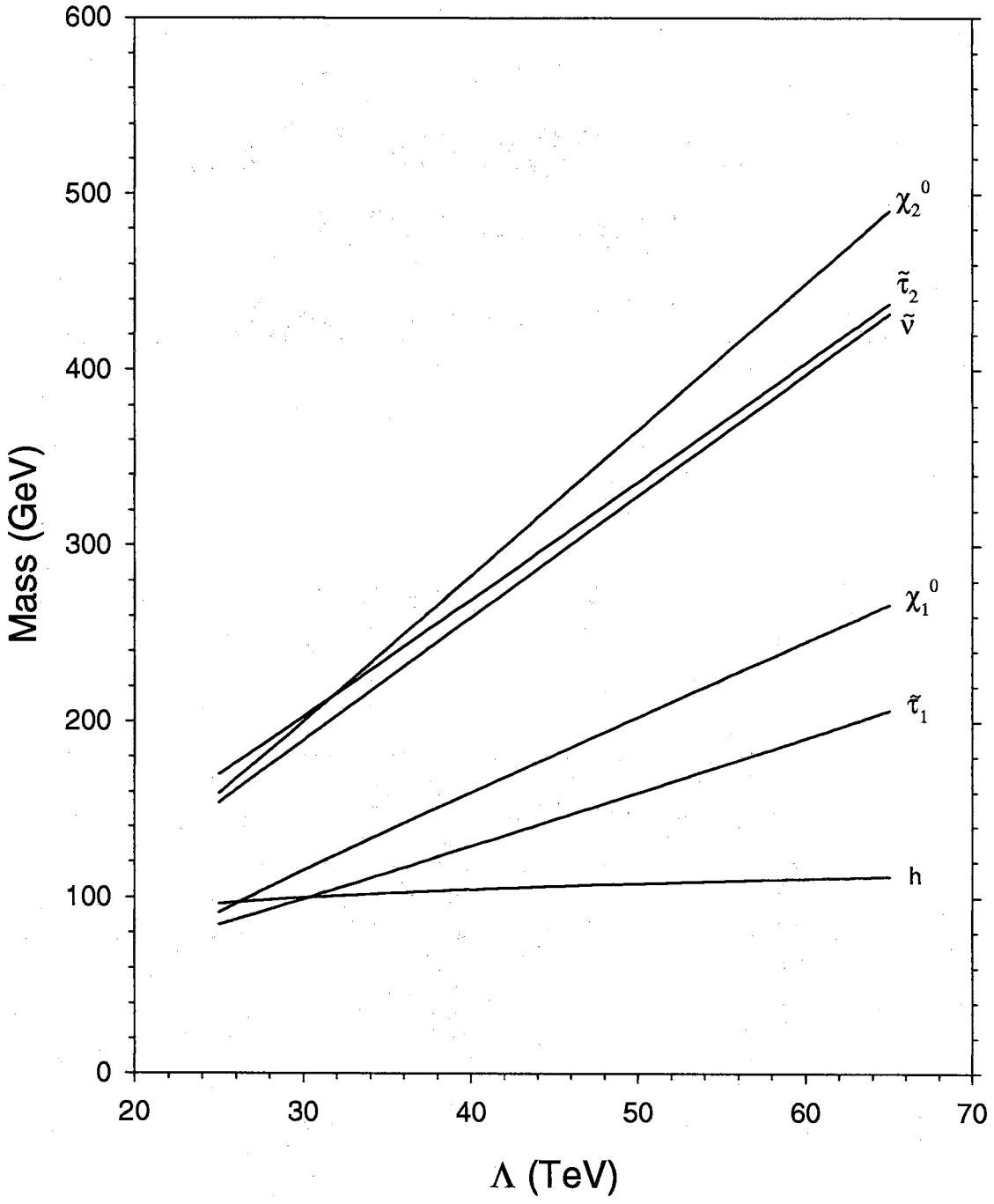

Figure 27. The masses for the sparticles of interest for the co-NLSP example where $n = 3$, $\tan\beta = 3$ and $M/\Lambda = 3$.

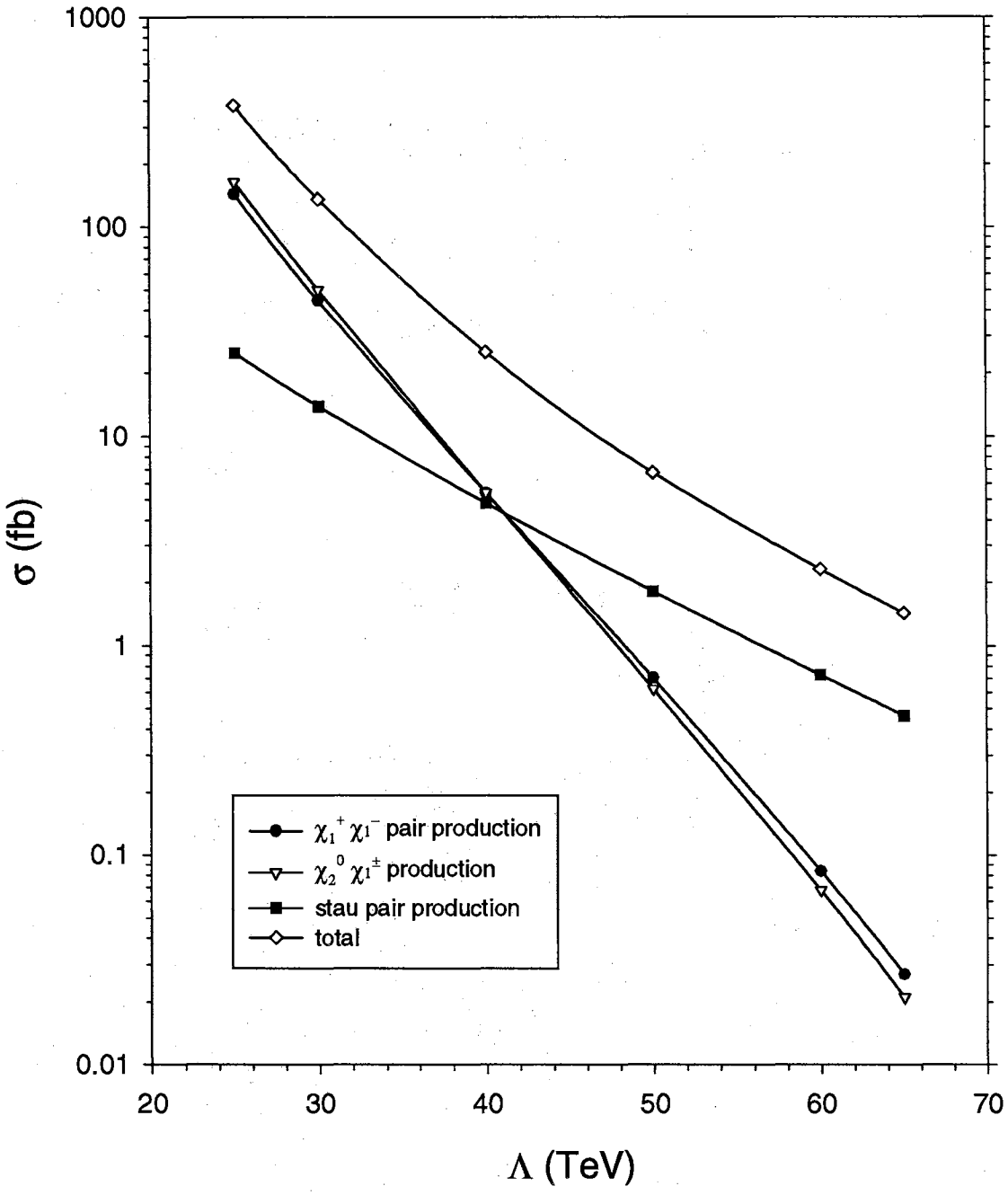

Figure 28. The SUSY production cross sections for the co-NLSP example where $n = 3$, $\tan\beta = 3$ and $M/\Lambda = 3$.

Table XI. Branching ratios of some of the sparticles of interest for the parameter set with $n = 3$, $\tan\beta = 3$ and $M/\Lambda = 3$.

	Λ (TeV)					
Decay Mode	25	30	40	50	60	65
$\chi_1^\pm \to \tilde{\tau}_1 \nu_\tau$	1	0.3416	0.0225	0.0099	0.0063	0.0053
$\chi_1^\pm \to \tilde{\nu}_\tau \tau$	-	0.2147	0.1426	0.1390	0.1402	0.1410
$\chi_1^\pm \to \tilde{\nu}_e e$	-	0.2219	0.1418	0.1383	0.1396	0.1405
$\chi_1^\pm \to \chi_1^0 W$	-	-	0.4514	0.3436	0.2781	0.2552
$\chi_1^\pm \to \tilde{\tau}_2 \nu_\tau$	-	-	0.0326	0.0765	0.0984	0.1055
$\chi_1^\pm \to \tilde{e}_2 \nu_e$	-	-	0.0336	0.0772	0.0989	0.1060
$\chi_2^0 \to \tilde{\tau}_1 \tau$	0.3340	0.3135	0.1384	0.0577	0.0302	0.0232
$\chi_2^0 \to \tilde{e}_1 e$	0.3223	0.2977	0.1265	0.0505	0.0252	0.0190
$\chi_2^0 \to \tilde{\nu}_\tau \nu_\tau$	0.0071	0.0304	0.0820	0.0987	0.1062	0.1086
$\chi_2^0 \to \tilde{\nu}_e \nu_e$	0.0071	0.0303	0.0819	0.0986	0.1061	0.1085
$\chi_2^0 \to \chi_1^0 \mathrm{h}$	-	-	0.2146	0.2763	0.2800	0.2779
$\chi_2^0 \to \tilde{\tau}_2 \tau$	-	-	0.0447	0.0866	0.1049	0.1100
$\chi_2^0 \to \tilde{e}_2 e$	-	-	0.0456	0.0871	0.1051	0.1101
$\chi_1^0 \to \tilde{\tau}_1 \tau$	0.3593	0.3437	0.3378	0.3362	0.3355	0.3353
$\chi_1^0 \to \tilde{e}_1 e$	0.3203	0.3281	0.3311	0.3319	0.3322	0.3323
$\tilde{\nu}_\tau \to \chi_1^\pm \tau$	0.0047	-	-	-	-	-
$\tilde{\nu}_\tau \to \nu_\tau \chi_1^0$	0.9953	0.9940	0.9889	0.9875	0.9870	0.9869
$\tilde{\nu}_\tau \to \tilde{\tau}_1 W$	-	0.0060	0.0111	0.0125	0.0130	0.0131
$\tilde{\nu}_e \to \chi_1^0 \nu_e$	0.9928	1	1	1	1	1
$\tilde{\nu}_e \to \chi_1^\pm e$	0.0072	-	-	-	-	-
$\tilde{\tau}_2 \to \chi_1^0 \tau$	0.4640	0.8960	1	1	1	1
$\tilde{\tau}_2 \to \chi_1^\pm \nu_\tau$	0.4155	0.0983	-	-	-	-
$\tilde{\tau}_2 \to \chi_2^0 \tau$	0.1206	0.0057	-	-	-	-
$\tilde{e}_2 \to, \chi_1^0 e$	1	1	1	1	1	1
$\tilde{e}_1 \to \tilde{G} e$	1	1	1	1	1	1

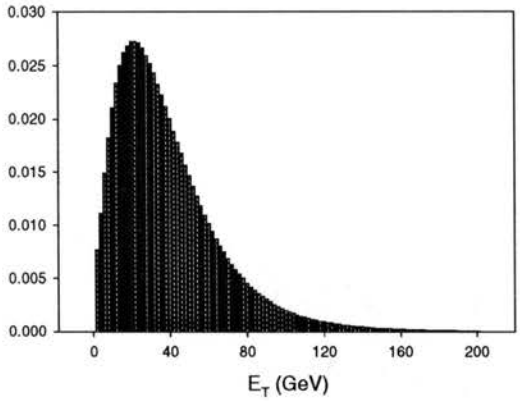

(a) The E_T distribution without cuts.

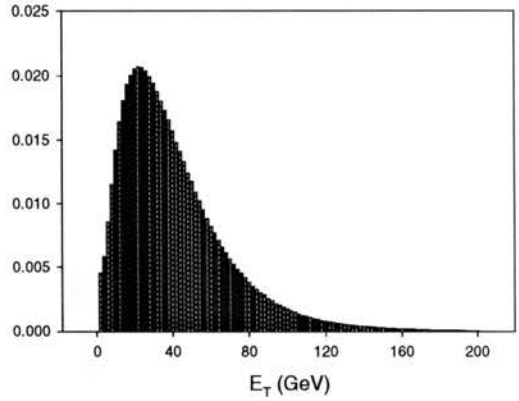

(b) The E_T distribution with the pseudorapidity cut $|\eta| < 1$ on τ-jets.

Figure 29. The E_T distributions of the highest E_T τ-jet for the parameters $n = 3$, $\tan\beta = 3$, $M/\Lambda = 3$ and $\Lambda = 25\,\mathrm{TeV}$.

For the second lightest neutralino, there are again up to 11 main decay modes. At low values of Λ, the decays to the lighter sleptons are dominant with $\chi_2^0 \to \tilde{\tau}_1\tau$ having a slight edge over the other two slepton decays. As Λ increases the decays to the sneutrinos gradually become more important. In addition the decay $\chi_2^0 \to \chi_1^0\,\mathrm{h}$ and the decays to the heavier sleptons become kinematically allowed and dominate over the other decays.

In chargino pair production at low values of Λ, two τ leptons are always produced because essentially the only decay mode for the chargino is $\chi_1^\pm \to \tilde{\tau}_1\nu_\tau$ while the stau decays via $\tilde{\tau}_1 \to \tau\tilde{G}$. On the other hand, the now classic three τ signature for $\chi_2^0\chi_1^\pm$ production will be diminished since $\chi_2^0 \to \tilde{\tau}_1\tau$, $\chi_2^0 \to \tilde{\mu}_1\mu$ and $\chi_2^0 \to \tilde{e}_1 e$ are all roughly equal. Since the subsequent decays of the selectron and smuon to the gravitino produces no τ leptons (unlike the three-body decay modes $\tilde{e}_1 \to e\tau\tilde{\tau}_1$ and $\tilde{\mu}_1 \to \mu\tau\tilde{\tau}_1$ that were dominant in the other two cases), there will tend to be a depletion in τ-jets here relative to the previous type 3 case which didn't satisfy the co-NLSP condition. For larger values of Λ, the situation is more complicated, but the decay chain will frequently involve the lightest neutralino. The lightest neutralino in turn tends to decay to $\tilde{\tau}_1$, $\tilde{\mu}_1$ and $\tilde{e}_1$ roughly equally. Thus there is again a relative depletion in events with τ-jets.

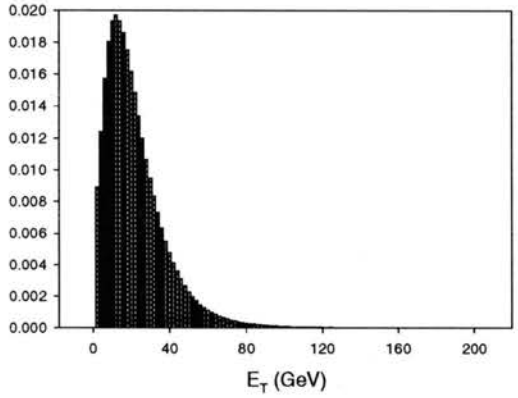

(a) The E_T distribution without cuts.

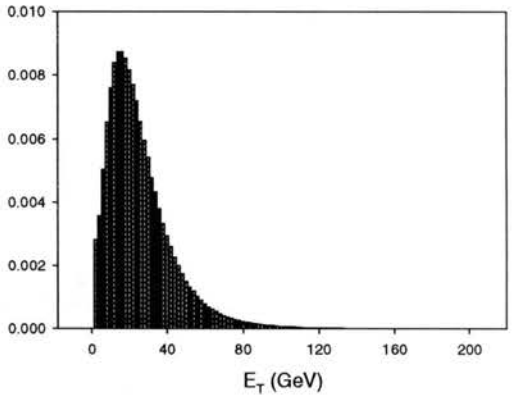

(b) The E_T distribution with the pseudorapidity cut $|\eta| < 1$ on τ-jets.

Figure 30. The E_T distributions of the second highest E_T τ-jet for the parameters $n = 3$, $\tan\beta = 3$, $M/\Lambda = 3$ and $\Lambda = 25\,\text{TeV}$.

The E_T distribution for the leading τ-jet when $\Lambda = 25\,\text{TeV}$ is given in Fig. 29. The E_T distribution of the secondary τ-jet is given in Fig. 30. Qualitatively, these are much the same as in the previous cases. At $\Lambda = 25\,\text{TeV}$, the decay chains are relatively short and the τ-jets tend to be quite hard. The $\not{E}_T$ distribution is given in Fig. 31.

We now consider the details of the various final state possibilities. Table XII gives the inclusive branching ratios for different numbers of τ-jets for $\Lambda = 25\,\text{TeV}$. With $\chi_1^\pm \to \tilde{\tau}_1\nu_\tau$ being the only decay mode here, $\chi_1^+\chi_1^-$ production produces two τ leptons. Thus the probability for τ-jets before cuts is dictated by the hadronic branching ratio of the τ lepton. Including cuts diminishes the number of events with a given number of τ-jets. For example, the branching ratio for 2 τ-jets falls from 42% to 10.5%. When Λ is increased, the situation changes dramatically. Table XIII gives the inclusive branching ratios for $\Lambda = 40\,\text{TeV}$. The possibility exists to create many τ-jets, but the probability for creating more than three is low. In addition, the probability for producing no τ-jets is high at $\sim 35\%$. After cuts, the only appreciable modes are the two τ-jets mode at 10% and the one τ-jet mode at 18%.

Turning now to $\chi_2^0\chi_1^\pm$ production, we see that at low Λ, there is the potential to produce up to three τ-jets. The rates are diminished by the strong presence of

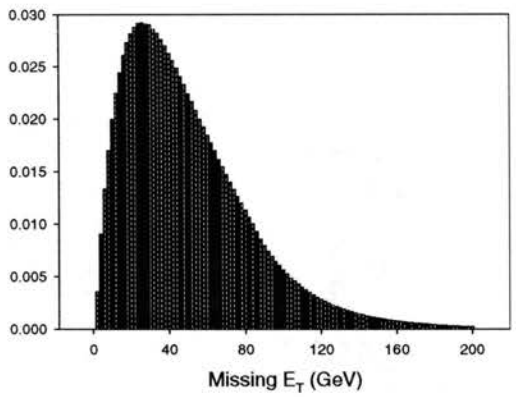

(a) The $\not\!\!E_T$ distribution without cuts.

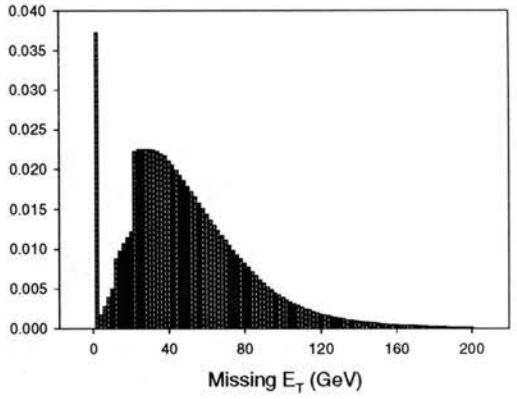

(b) The $\not\!\!E_T$ distribution with the E_T/p_T and pseudorapidity cuts on the jets and charged leptons.

Figure 31. $\not\!\!E_T$ distribution of the secondary τ-jet for the parameters $n = 3$, $\tan\beta = 3$, $M/\Lambda = 3$ and $\Lambda = 25\,\text{TeV}$.

Table XII. Inclusive τ-jet branching ratios for the various production mechanisms for the parameters $n = 3$, $\tan\beta = 3$, $\Lambda = 25\,\text{TeV}$ and $M = 75\,\text{TeV}$.

Production Mode	1 τ-jet	2 τ-jets	3 τ-jets
$\chi_1^+\chi_1^-$: no cuts	0.4562	0.4200	-
with cuts	0.2514	0.1053	-
$\chi_1^\pm\chi_2^0$: no cuts	0.5088	0.1514	0.0935
with cuts	0.2480	0.0666	0.0153
$\tilde{\tau}_1^+\tilde{\tau}_1^-$: no cuts	0.4560	0.4203	-
with cuts	0.2427	0.0891	-

Table XIII. Inclusive τ-jet branching ratios for the various production mechanisms for the parameters $n = 3$, $\tan\beta = 3$, $\Lambda = 40\,\text{TeV}$ and $M = 120\,\text{TeV}$.

Production Mode	1 τ-jet	2 τ-jets	3 τ-jets	4 τ-jets	5 τ-jets
$\chi_1^+\chi_1^-$: no cuts	0.2903	0.2272	0.0937	0.0299	0.0054
with cuts	0.1826	0.0996	0.0227	0.0034	0.0002
$\chi_1^\pm\chi_2^0$: no cuts	0.2613	0.2299	0.0826	0.0298	0.0057
with cuts	0.1903	0.1054	0.0232	0.0038	0.0004
$\tilde{\tau}_1^+\tilde{\tau}_1^-$: no cuts	0.4560	0.4202	-	-	-
with cuts	0.3419	0.1410	-	-	-

$\chi_2^0 \to \tilde{e}_1 e$ and $\chi_2^0 \to \tilde{\mu}_1 \mu$, however, and the rate no for τ-jets is high at $\sim 25\%$. After cuts, the two τ-jets branching ratio is only about 7% and the one τ-jet rate is about 25%. For $\Lambda = 40\,\text{TeV}$, the potential exists to create many more τ-jets, but the one and two τ-jets modes remain dominant with after cuts branching ratios of 19% and 11%, respectively.

For $\tilde{\tau}_1^+\tilde{\tau}_1^-$, the situation is pretty much the same as it is in the previous cases considered. With $\tilde{\tau}_1 \to \tau\,\tilde{G}$ being the only decay mode of the lightest stau, the probability for a given number of τ-jets is completely dictated by the hadronic branching ratio of the τ lepton. The branching ratios after cuts are largely dictated by the mass of the stau. The τ-jets from the stau decays have a greater probability of passing the cuts as the mass of the stau increases.

We now consider the possibility of observing these events at the Tevatron's Run II and TeV33. Fig. 32 shows the combined production rates for the inclusive τ-jet modes before cuts for all the SUSY production modes considered. We do not include the cross sections for more than three τ-jets as these are prohibitively small. In sharp contrast to the previous cases, the most typical situation is that no τ-jets are produced. For low values of Λ ($\Lambda < 40\,\text{TeV}$), however, the production rates for one and two τ-jets are comparable. The results after cuts are shown in Fig. 33. The one τ-jet mode is dominant and the two τ-jet mode is respectably high. For $\Lambda = 25\,\text{TeV}$,

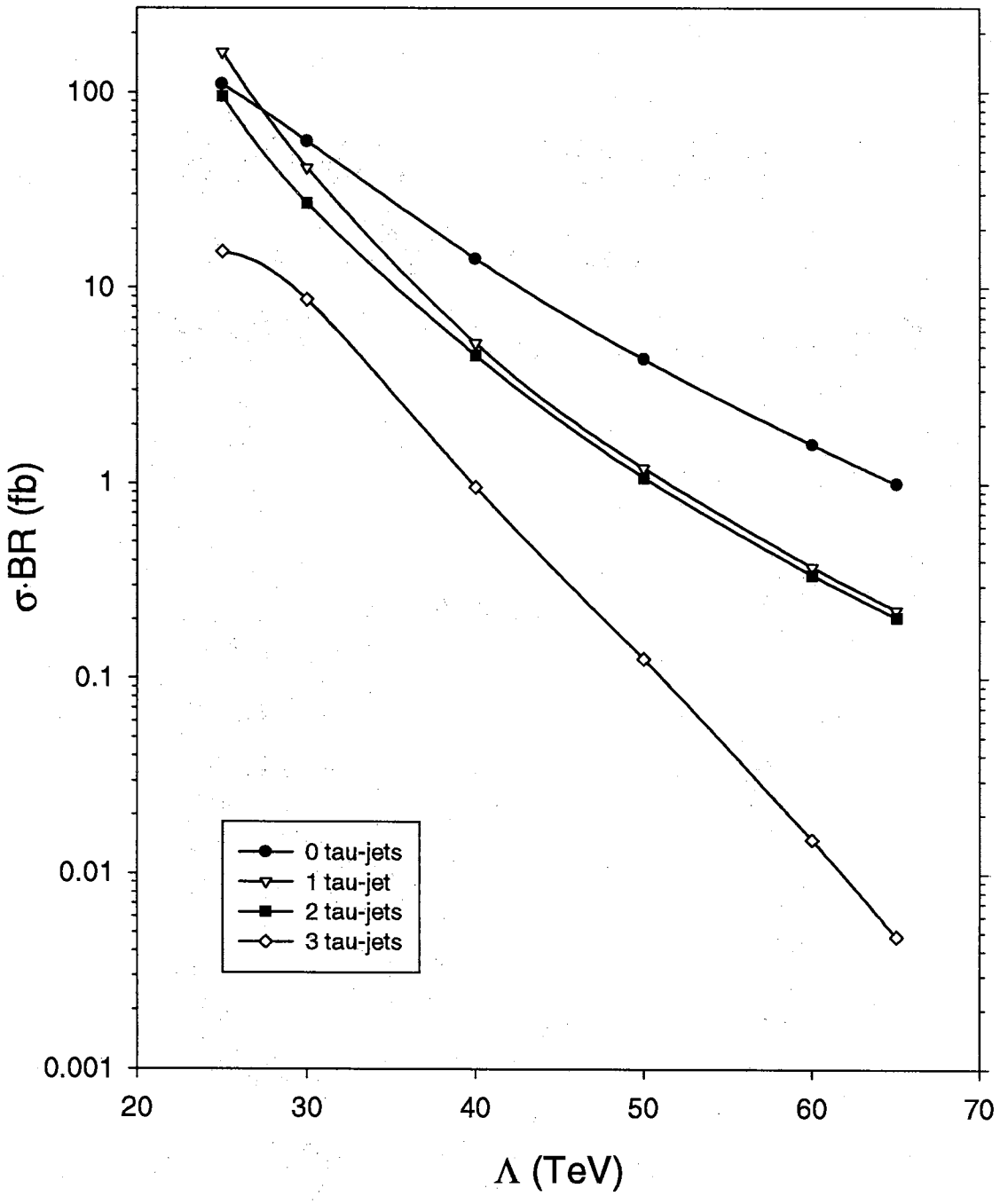

Figure 32. $\sigma \cdot BR$ before cuts for the inclusive τ-jet modes for the parameters $n = 3$, $\tan\beta = 3$ and $M/\Lambda = 3$.

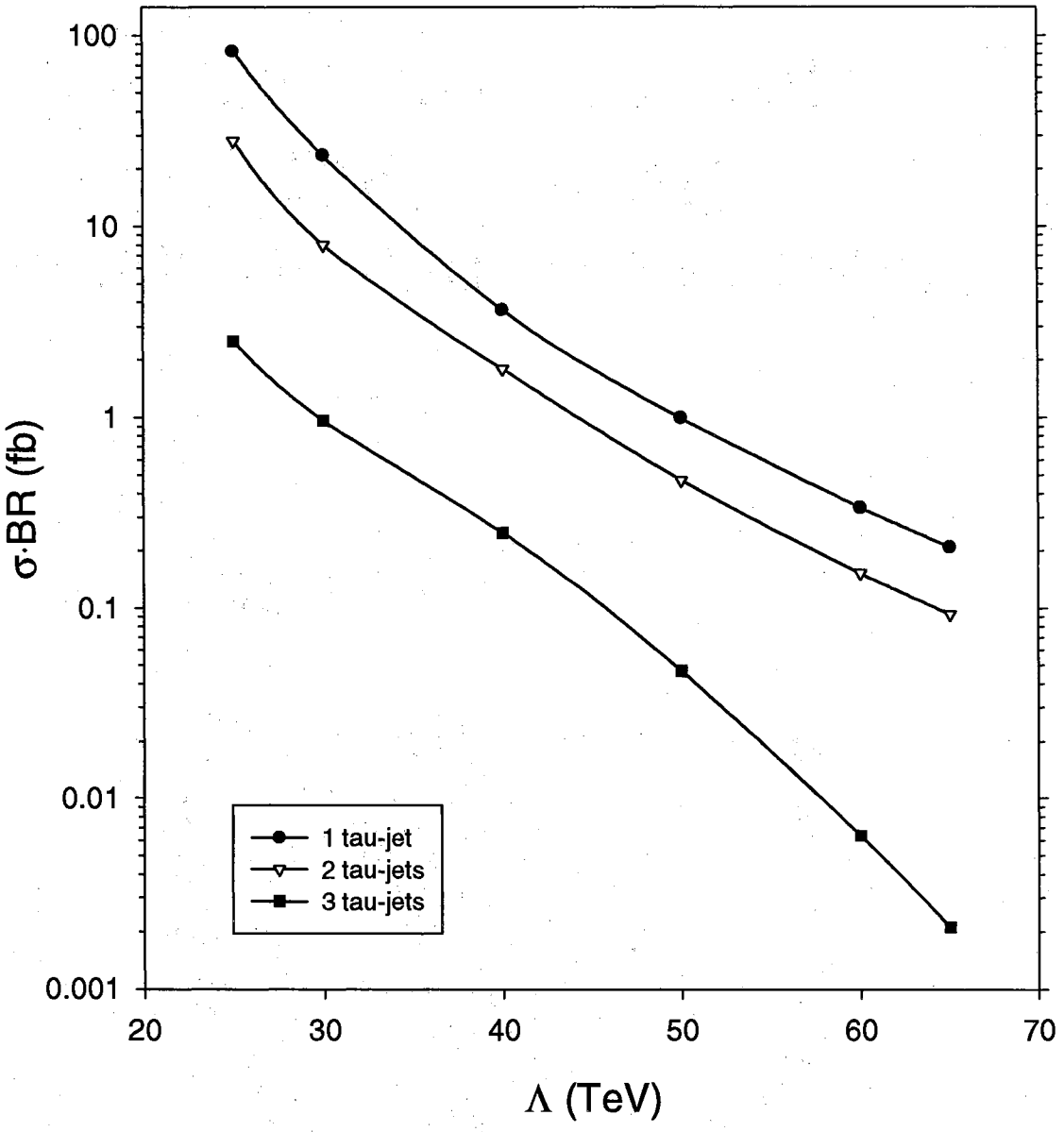

Figure 33. $\sigma \cdot BR$ after cuts for the inclusive τ-jet modes for the parameters $n = 3$, $\tan\beta = 3$ and $M/\Lambda = 3$.

Table XIV. Production rates in fb for some of the more interesting final state configurations with and without cuts for the parameters $n = 3$, $\tan\beta = 3$ and $M/\Lambda = 3$.

	$\Lambda = 25\,\text{TeV}$		$\Lambda = 30\,\text{TeV}$	
	no cuts	cuts	no cuts	cuts
τ-jet	-	28.84	-	5.39
2 τ-jets	70.57	23.11	8.01	4.49
e/μ & τ-jet	38.20	12.71	4.35	3.82
$2e/2\mu$ & τ-jet	-	6.48	3.99	2.75

the two τ-jets rate is about 28 fb which gives 56 events for $2\,\text{fb}^{-1}$ of data and 840 events for $30\,\text{fb}^{-1}$ of data. For $\Lambda = 40\,\text{TeV}$, we have a lower production rate of 1.8 fb. For $2\,\text{fb}^{-1}$ of data this corresponds to ~ 4 events, while $30\,\text{fb}^{-1}$ of data gives about 54 events.

The branching ratios for some of the more important individual modes are given in Table XIV. Unlike the previous cases considered, there is the potential that modes with specific numbers of charged leptons could be important. We see from the table that for $\Lambda = 25\,\text{TeV}$, the rate for an electron and a τ-jet is 12.7 fb after cuts. For electrons and muons combined, this cross section is 25.4 fb. For an integrated luminosity of $2\,\text{fb}^{-1}$, this corresponds to about 50 events, while for an integrated luminosity of $30\,\text{fb}^{-1}$, this corresponds to about 762 events. A better signal is the 2 e + τ-jet and 2 μ + τ-jet signals. The combined cross section for this is 13 fb. For $2\,\text{fb}^{-1}$ of data, this corresponds to 26 events. For $30\,\text{fb}^{-1}$ of data, this corresponds to about 390 events.

Conclusion

We have considered the phenomenology of GMSB models where the lighter stau is the NLSP and decays promptly within the detector. For this situation, the dominant SUSY production processes at the Tevatron are $\chi_1^+\chi_1^-$ and $\chi_1^\pm\chi_2^0$. Their decay

chains lead to events typically containing two or three high p_T τ leptons plus large missing transverse energy. These signals are different from the photonic signals that have been previously investigated in GMSB models and the dilepton and trilepton signals in supergravity models. Searching for the τ lepton signals by the hadronic decays of the τ leptons to thin jets is complicated by the fact that, while primary τ-jets can have quite high E_T, the secondary τ-jets tend to be rather soft. As a result, many of the τ-jets tend to be eliminated by the cuts. Our detailed calculations show that the most promising channel is the inclusive two τ-jets channel, although the production of three τ-jets can be important at the higher integrated luminosity expected at Run III. The missing transverse energy associated with the events is quite large providing a good trigger for these events. Good τ identification will be extremely important to detect the signal as well as a detailed understanding of the associated background.

CHAPTER IV

SUPERSYMMETRIC LEFT-RIGHT MODEL

Introduction

One of the questions left unanswered by the SM and the MSSM concerns the origin of parity violation in low energy electroweak interactions. A possibility is that the $SU(2)_L \times U(1)_Y$ theory is the effective low energy form of a theory based on the gauge group $SU(2)_L \times SU(2)_R \times U(1)_{B-L}$. A Lagrangian based on this gauge group is invariant under parity transformations if the gauge couplings for $SU(2)_L$ and $SU(2)_R$ are equal (and the matter content is left-right symmetric). Parity violation at low energies is then attributed to noninvariance of the vacuum under parity.

This model has a number of other attractive features:

1. They imply automatic conservation of baryon number and lepton number which is achieved in the MSSM through the ad-hoc introduction of R-parity [36] .

2. They provide a natural solution to the strong and weak CP problems of the MSSM [37] .

3. They provide a natural embedding of the see-saw mechanism for small neutrino masses [38].

We consider a supersymmetric left-right (SUSYLR) model with gauge mediated SUSY breaking. As in the last chapter, the lighter stau can be lighter than the lightest neutralino. In fact, this occurs in the SUSYLR model for a much wider region of the GMSB parameter space. Thus τ-jets here are an important part of the signature for SUSY production.

Another important aspect of this model is that there are doubly charged scalars and fermions that are relatively light. If they are light enough, then they can be produced at Run II of the Tevatron providing new SUSY production modes. We will find that the doubly charged nature of these fields potentially provides a way of distinguishing this model from GMSB models with minimal particle content.

The Model

We now give a detailed account of this supersymmetric left-right model. The $SU(2)_L \times SU(2)_R \times U(1)_{B-L}$ symmetry is broken down to $U(1)_{EM}$ in two stages: $SU(2)_L \times SU(2)_R \times U(1)_{B-L} \rightarrow SU(2)_L \times U(1)_Y \rightarrow U(1)_{EM}$. This is accomplished through the introduction of a number of triplet and bidoublet Higgs fields.

The particle content of the theory is given by Table XV. The first stage of the symmetry breaking is largely controlled by the $SU(2)_R$ triplets Δ^c and $\bar{\Delta}^c$, while the second stage of symmetry breaking is largely controlled by the $SU(2)_L$ triplets Δ and $\bar{\Delta}$ and the bidoublet Higgs fields $\Phi_{1,2}$. In a nonsupersymmetric model, we would only require the Δ, Δ^c and Φ_1, but here we have to double the Higgs content for the same reasons that we had to have at least two Higgs doublets in the MSSM.

The LR symmetric superpotential for this theory is given by (generation indices have been suppressed)

$$\begin{aligned} W &= h_q^{(i)} Q^T \tau_2 \Phi_i \tau_2 Q^c + h_l^{(i)} L^T \tau_2 \Phi_i \tau_2 L^c + i(f L^T \tau_2 \Delta L + f_c L^{cT} \tau_2 \Delta^c L^c) \\ &+ M_\Delta [\mathrm{Tr}(\Delta\bar{\Delta}) + \mathrm{Tr}(\Delta^c \bar{\Delta}^c)] + \lambda S(\Delta\bar{\Delta} - \Delta^c\bar{\Delta}^c) + \mu_S S^2 \\ &+ \mu_{ij} \mathrm{Tr}(\tau_2 \Phi_i^T \tau_2 \Phi_j) + W_{NR} \end{aligned} \tag{23}$$

where W_{NR} denotes non-renormalizable terms arising from higher scale physics such as grand unified theories or Planck scale effects. It is taken to have the form

$$W_{NR} = A[\mathrm{Tr}(\Delta^c\bar{\Delta}^c)]^2/2 + B\mathrm{Tr}(\Delta^c\Delta^c)\mathrm{Tr}(\bar{\Delta}^c\bar{\Delta}^c)/2 \tag{24}$$

where A and B are of order $1/M_{\mathrm{Planck}}$. We will see below that we need to introduce these terms in order to give mass to certain doubly charged fermions.

Table XV. The field content of the left-right model used in this chapter. Q refers to a given generation of quarks and L refers to a given generation of leptons. S is assumed to be odd under parity. U and V denote the $SU(2)_L$ and $SU(2)_R$ transformations respectively.

Field	$SU(2)_L \times SU(2)_R \times U(1)_{B-L}$	Group Transformation
Q	$(2, 1, +\frac{1}{3})$	UQ
Q^c	$(1, 2, -\frac{1}{3})$	VQ^c
L	(2, 1, -1)	UL
L^c	(1, 2, +1)	VL^c
$\Phi_{1,2}$	(2, 2, 0)	$U\Phi V^\dagger$
Δ	(3, 1, +2)	$U\Delta U^\dagger$
$\bar{\Delta}$	(3, 1, -2)	$U\bar{\Delta}U^\dagger$
Δ^c	(1, 3, +2)	$V\Delta^c V^\dagger$
$\bar{\Delta}^c$	(1, 3, -2)	$V\bar{\Delta}^c V^\dagger$
S	(1, 1, 0)	S

We have that in the SUSY limit, the doubly charged fields from the Δ^c and $\bar{\Delta}^c$ are massless [39–44]. This can be seen as follows: begin by writing down the F-terms for the S, Δ^c and $\bar{\Delta}^c$ terms:

$$F_S = 2\mu_S S + \lambda(\Delta\bar{\Delta} - \Delta^c\bar{\Delta}^c) \quad (25)$$

$$F_\Delta = (\lambda S + M_\Delta)\bar{\Delta} \quad (26)$$

$$F_{\Delta^c} = (-\lambda S + M_\Delta)\bar{\Delta}^c \quad (27)$$

With the effective SUSY breaking scale below the LR scale, these F-terms must vanish. If we then choose the Δ^c and $\bar{\Delta}^c$ VEVs (denoted by v_R and $\bar{v}_R$ respectively) to be nonvanishing (so that $SU(2)_R \times U(1)_{B-L} \to U(1)_Y$ can occur), then we must have $\langle S \rangle = M_\Delta/\lambda$. This implies that the Δ and $\bar{\Delta}$ VEVs vanish and the masses of the fields are of order $2M_\Delta$. Thus the left-handed triplet fields decouple from the low energy spectrum. As for the Δ^c and $\bar{\Delta}^c$, one neutral and two singly charged degrees of freedom are absorbed to give masses to the right-handed gauge bosons. The

remaining neutral and singly charged fields pick up mass of order v_R and disappear from the low energy spectrum. The doubly charged fields, however, are massless in the SUSY limit in the absence of the nonrenormalizable terms.

The doubly charged fields must obtain masses as it is not phenomenologically allowed for them to be massless. The doubly charged scalar fields obtain part of their mass at two loops from the messenger fields. In addition, they receive a mass of $\mathcal{O}(\frac{M_R^2}{M_{\rm Planck}})$ from the higher dimensional operators if they are present. For the doubly charged Higgsinos, however, there are no SUSY breaking contributions. Thus we need to introduce the nonrenormalizable operators to give mass to these fermions, and then their masses are of order $\mathcal{O}(\frac{M_R^2}{M_{\rm Planck}})$.

We now consider the question of what the low energy theory looks like. After integrating out the heavy fields at the left-right scale, we are left with the following additional part to the MSSM superpotential:

$$W = M_\Delta \hat{\Delta}^{c--}\hat{\Delta}^{c++} + f_{ij}\hat{l}_i^c\hat{l}_j^c\hat{\Delta}^{c\pm\pm} \ . \tag{28}$$

We will assume that f is diagonal (so that $f_{ij} = 0$ when $i \neq j$), then we have three separate couplings f_1, f_2 and f_3 which correspond to the first, second and third generations, respectively. This interaction gives rise to the processes $\mu^+e^- \to \mu^-e^+$ with a strength $G_{M\bar{M}} \simeq \frac{f_1 f_2}{4\sqrt{2}M_\Delta^2}$ where $G_{M\bar{M}}$ is the strength of the effective four-fermion interaction. A recent PSI experiment [45] has yielded a 90% C.L. upper limit on $G_{M\bar{M}}$ of $3 \times 10^{-3}\, G_F$. For $M_\Delta = 100\,\text{GeV}$, this implies that $f_1 f_2 \leq 1.2 \times 10^{-3}$. Thus we expect each of the couplings to be less than 0.1 assuming that f_1 and f_2 are not too different. There is no such constraint on f_3 from experiments. In the analysis we take it to be around 0.5.

To summarize, our low energy theory contains "right-handed" doubly charged bosons and fermions. These doubly charged particles couple to leptons, but not to quarks. In addition, the coupling to the third generation of leptons could be much larger than the couplings to the first and second generation of leptons and we assume that this is the case.

These facts have a number of consequences for phenomenology. First, the doubly charged particles could have masses low enough that they could be produced at the Tevatron. This is especially so for the Higgsinos since they obtain mass solely from the nonrenormalizable terms. Thus we have potential new SUSY production mechanisms here. Second, if $f_3 \gg f_1, f_2$, then the decays of the doubly charged Higgs bosons and Higgsinos typically lead to τ leptons. Since our model is in the context of GMSB, the lighter stau can be lighter than the lightest neutralino. As we will see in the next section, this can be greatly enhanced here due to the coupling f_3. Thus τ-jets will always be an important part of the signature for this model just as it can be in the GMSB model with minimal particle content considered in chapter III.

Sparticle Masses and Production

In the GMSB model, the sparticle spectrum depends on the following parameters: M, Λ, n, $\tan\beta$, f_3, $M_{\tilde{\Delta}}(M)$ and the sign of μ. M is the messenger scale. The parameter n is dictated by the choice of the vector-like messenger sector. In this calculation we will assume that each flavor in the messenger sector consists of a vector like isosinglet pair of fields $(Q + \bar{Q})$ and a vector like weak isodoublet pair $L + \bar{L}$. $M_{\tilde{\Delta}}(M)$ is the messenger scale value for the deltino mass. As mentioned previously, constraints coming from $b \to s\gamma$ strongly favor negative values for μ [31], and μ is taken to be negative in the cases considered in this chapter. Demanding that the EW symmetry be broken radiatively fixes the magnitude of μ and the parameter B (from the $B\mu H_u H_d$ term in the scalar potential) in terms of the other parameters of the theory. The soft gaugino and scalar masses at the messenger scale are given by Eqs. 21 and 22 from chapter III.

We calculate the SUSY mass spectrum by using the appropriate renormalization group equations [33]. We first run the Yukawa couplings (including the three new couplings $f_{1,2,3}$) and the gauge couplings from the weak scale up to the messenger scale. At the messenger scale, we apply the boundary conditions given by Eqs. 21 and 22 and then use the RGEs for the soft SUSY couplings and masses in order to run down to the weak scale.

The mass spectrum here is much like that expected in minimal GMSB models. The gravitino is always the LSP. Since SUSY breaking is communicated to the visible sector by gauge interactions, the mass differences between the superparticles depend on their gauge interactions. This creates a hierarchy in mass between electroweak and strongly interacting sparticles. Eq. 21 shows that the gluino is more massive than the charginos and neutralinos, while Eq. 22 shows that the squarks are considerably more massive than the sleptons. Thus in minimal GMSB models, the lightest neutralino and the lighter stau fight for the NLSP spot [46]. In this model, the deltino also joins the race to become the NLSP.

We will concentrate the analysis on those regions of the parameter space where either the lighter stau or the deltino is the NLSP. Whether or not the deltino is the NLSP depends on the mass it gets from the higher dimensional terms. If this mass is too high, then either the $\tilde{\tau}_1$ or χ_1^0 is the NLSP. The lighter stau can be much lighter in our SUSYLR model than in conventional GMSB models due to the presence of the additional coupling f_3. Thus the lighter stau will be lighter than the χ_1^0 for a larger region of the parameter space and the $\tilde{\tau}_1$ has a greater potential to be the NLSP in this SUSYLR model.

There are a number of potential SUSY production mechanisms here. Given the current lower bounds on the various sparticle masses and the hierarchy of sparticle masses in GMSB models, the important SUSY production mechanisms will typically include EW gaugino production. At the Tevatron, chargino pair ($\chi_1^+\chi_1^-$) production takes place through s-channel Z and γ exchange, while $\chi_2^0\chi_1^\pm$ production is through s-channel W exchange. Squark exchange via the t-channel also contributes to both processes, but the contributions are expected to be negligible since the squark masses are large in GMSB models. The production of $\chi_1^0\chi_1^\pm$ is suppressed due to the smallness of the coupling involved.

In addition to these usual SUSY production mechanisms of the MSSM, we also have deltino pair ($\tilde{\Delta}^{c++}\tilde{\Delta}^{c--}$) production. This proceeds through s-channel Z and γ exchange. Given that the $\tilde{\Delta}^{c\pm\pm}$ can be relatively light, deltino pair production can

be a very important SUSY production mode. In fact, it frequently is the dominant mode.

The possible final state configurations at the Tevatron depend on the sparticle spectrum and on which SUSY production mode is dominant, but they will have certain aspects in common. When the $\tilde{\tau}_1$ is the NLSP, the various possible decay modes will (usually) produce at least two τ leptons arising from the decays of the lighter staus. In addition, there can also be large $\not\!\!E_T$ due to the stable gravitinos and neutrinos escaping detection. When the deltino is the NLSP, the standard SUSY production modes involving EW gauginos can still produce large numbers of τ-jets if the $\tilde{\tau}_1$ is the next to next to lightest SUSY particle (in which case the $\tilde{\tau}_1$ is lighter than the χ_1^0) so that the decay chains of the sparticles will still lead to the $\tilde{\tau}_1$.

Pair production of the deltino leads to copious quantities of τ leptons irrespective of what the NLSP is. This is because the deltino couples to leptons/sleptons but not to quarks/squarks. In addition, the coupling to the third generation can be much greater than the small coupling to the 1st and 2nd generations. Thus, when the $\tilde{\tau}_1$ is the NLSP, the deltino decays via $\tilde{\Delta}^{c\pm\pm} \to \tilde{\tau}_1^{\pm}\tau^{\pm}$ with the stau decaying via $\tilde{\tau}_1 \to \tau\tilde{G}$. On the other hand, when the deltino is the NLSP, it decays via the $\tilde{\tau}$ mediated three-body decay mode $\tilde{\Delta}^{c\pm\pm} \to \tau^{\pm}\tau^{\pm}\tilde{G}$. Thus $\tilde{\Delta}^{c\pm\pm}$ pair production generally results in the production of four τ leptons (two from each deltino).

Tau Jet Analysis

As mentioned above, SUSY production for this SUSYLR model leads to the production of copious quantities of τ leptons. τ leptons are typically identified at colliders by their hadronic decays to thin jets. We now give a detailed account of the possible τ-jet signatures for SUSY production at the Tevatron in the context of the left-right GMSB model.

This analysis is performed in the context of the Main Injector (MI) and TeV33 upgrades of the Tevatron collider. The center of mass energy is taken to be $\sqrt{s} = 2\,\text{TeV}$ and the integrated luminosity is taken to be $2\,\text{fb}^{-1}$ for the MI upgrade and $30\,\text{fb}^{-1}$ for the TeV33 upgrade.

In performing this analysis, the cuts employed are that final state charged leptons must have $p_T > 10\,\text{GeV}$ and $|\eta| < 1$. Jets must have $E_T > 10\,\text{GeV}$ and $|\eta| < 2$. In addition, hadronic final states within a cone size of $\Delta R \equiv \sqrt{(\Delta\phi)^2 + (\Delta\eta)^2} = 0.4$ are merged to a single jet. Leptons within this cone radius of a jet are discounted. For a τ-jet to be counted as such, it must have $|\eta| < 1$. The most energetic τ-jet is required to have $E_T > 20\,\text{GeV}$. In addition, a missing transverse energy cut of $\not\!\!E_T > 30\,\text{GeV}$ is imposed.

The signatures for SUSY production depend on the hierarchy of sparticle masses. This, in turn, depends on the values the parameters of the theory take. The parameters considered in this analysis are $\tan\beta = 15$, $n = 2$, $M/\Lambda = 3$, $f_3 = 0.5$, $f_2 = 0.05$ and $f_1 = 0.05$. We vary Λ from 35 to 85 TeV. For the messenger scale deltino mass, we use the values 90, 120 and 150 GeV. The masses of some of the particles of interest are given in Figs. 34 and 35. In Fig. 34 we take $M_{\tilde{\Delta}}(M) = 90\,\text{GeV}$, but the masses of the gauginos and sleptons (with the exception of the stau) do not vary much with the messenger scale deltino mass. Fig. 35 gives the masses of the delta boson and the deltino. The deltino mass is not very sensitive to the value of Λ, while the delta boson mass is highly dependent on Λ due to the contributions from the messenger scale loops (which contribute to its mass along with the nonrenormalizable terms). Given the substantially higher Δ^c boson mass, Δ^c production is not very important at the Tevatron.

There are several potential SUSY production modes here. The cross sections for the more traditional SUSY production modes are given in Fig. 36. We also have deltino pair production; the cross sections for which are tabulated in Table XVI. Since the deltino mass does not vary much over the values of Λ considered, the cross section for deltino pair production does not vary much either. This cross section is high enough for all the deltino masses considered that deltino pair production is always an important SUSY production mode. For low values of Λ, the EW gaugino production cross section is large with values in the hundreds of fb at $\Lambda = 35\,\text{TeV}$, but the cross section falls off substantially as Λ increases. As Λ increases above about 55 TeV, the cross section for EW gaugino production starts to fall below that of

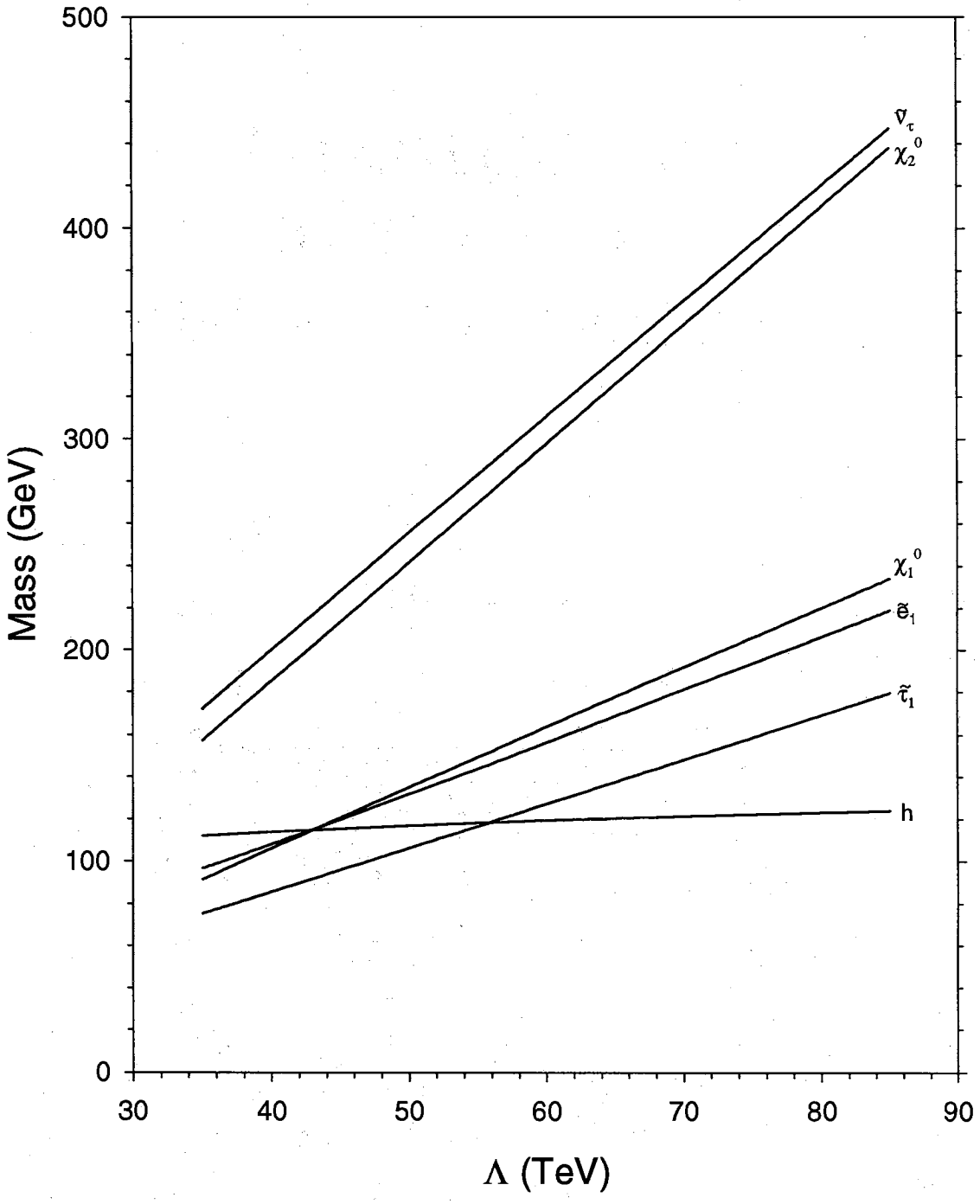

Figure 34. Masses of the particles of interest for the input parameters $\tan\beta = 15$, $M/\Lambda = 3$, $n = 2$, $f_3 = 0.5$, $f_2 = 0.05$, $f_1 = 0.05$ and $M_{\tilde{\Delta}}(M) = 90\,\mathrm{GeV}$.

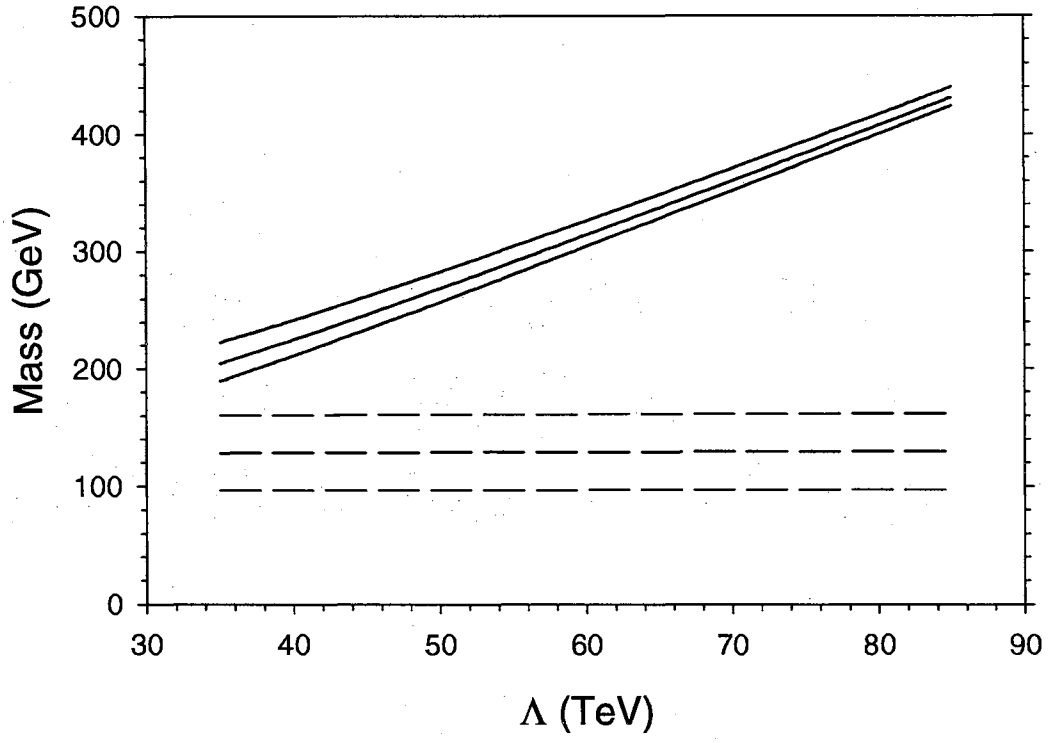

Figure 35. Masses of the delta boson and the deltino. The dashed lines represent the deltino, while the solid lines represent the delta boson. The parameters used are $\tan\beta = 15$, $n = 2$ and $M/\Lambda = 3$. From bottom to top, the lines in each set are for a messenger scale deltino mass of 90, 120 and 150 GeV.

slepton production (in particular $\tilde{\tau}_1^+\tilde{\tau}_1^-$). In a minimal model, these sleptons modes would become the dominant SUSY production modes, but here the cross sections for slepton production fall far below that of deltino pair production. Thus the dominant SUSY production modes here are deltino pair production and, at values of Λ below 45 TeV or so, $\chi_1^+\chi_1^-$ and $\chi_2^0\chi_1^\pm$ production.

The decay chains depend on which sparticle is the NLSP. For the values of the parameters that are considered here, either the lighter stau or the deltino is the NLSP. Since the mass of the lighter stau increases with increasing Λ, the lighter stau is the NLSP for lower values of Λ, while the deltino is the NLSP for higher values of Λ. For a messenger scale deltino mass of 90 GeV, the lighter stau is the NLSP for Λ below about 43 TeV. For $M_{\tilde{\Delta}}(M) = 120$ and 150 GeV, the boundaries are given by about 58 and 73 TeV, respectively. When the lighter stau is the NLSP, it decays via

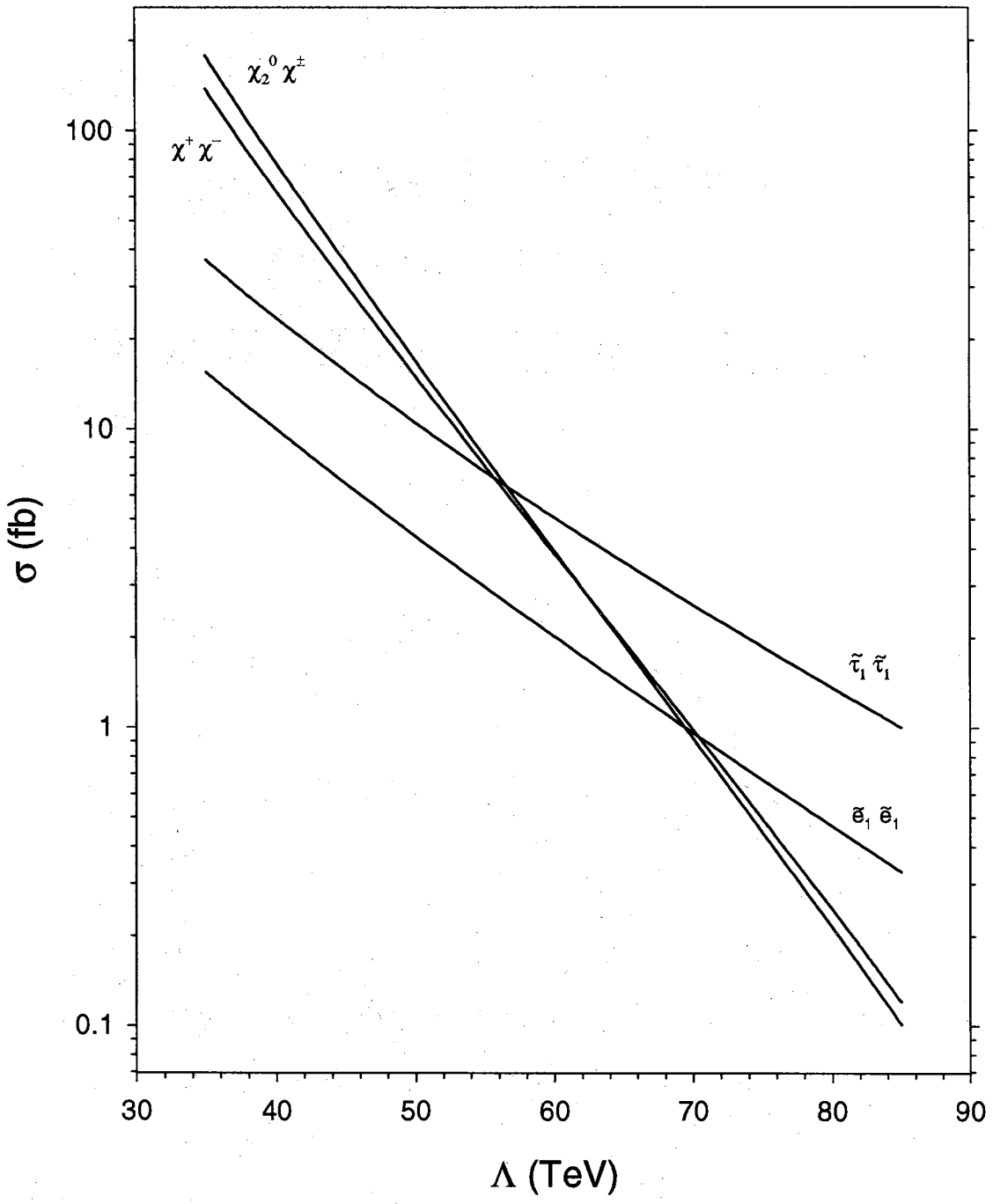

Figure 36. Cross sections for the standard SUSY production modes for the parameters $\tan\beta = 15$, $M/\Lambda = 3$, $n = 2$, $f_3 = 0.5$, $f_2 = 0.05$, $f_1 = 0.05$ and $M_{\vec{\Delta}}(M) = 90\,\mathrm{GeV}$.

Table XVI. Cross sections (in fb) for deltino pair production for various values of Λ. The other parameters used are $\tan\beta = 15$, $n = 2$ and $M/\Lambda = 3$.

$M_{\tilde{\Delta}}(M)$	$\Lambda = 35\,\mathrm{TeV}$	$\Lambda = 60\,\mathrm{TeV}$	$\Lambda = 85\,\mathrm{TeV}$
90 GeV	643.0	629.9	621.5
120 GeV	228.2	222.9	219.6
150 GeV	91.6	89.2	87.7

$\tilde{\tau}_1 \to \tau\,\tilde{G}$, and the deltino decays via the two-body mode $\tilde{\Delta}^c \to \tilde{\tau}_1\tau$. Then deltino pair production leads to four τ leptons. On the other hand, if the deltino is the NLSP, it decays via the stau mediated three-body mode $\tilde{\Delta}^c \to \tau\tau\tilde{G}$. So, once again, deltino pair production again leads to the production of four τ leptons.

The decays of the lighter selectron and smuon are given in Table XVII. At values of Λ around 35 to 40 TeV, the neutralino is lower in mass than the $\tilde{e}_1$ and $\tilde{\mu}_1$. When this is the case, the main decay mode of the selectron is $\tilde{e}_1 \to \chi_1^0 e$ and the smuon decay is correspondingly $\tilde{\mu}_1 \to \chi_1^0 \mu$. When this decay is not kinematically allowed, the decay $\tilde{e}_1 \to \tilde{\Delta}^c e$ is typically dominant if kinematically allowed. If it isn't, then the selectron decays via the three-body decays $\tilde{e}_1^+ \to e^+\tau^+\tilde{\tau}_1^-$ and $\tilde{e}_1^+ \to e^+\tau^-\tilde{\tau}_1^+$ and/or the two-body mode $\tilde{e}_1 \to e\,\tilde{G}$.

The branching ratios for the neutralinos and lighter chargino are given in Table XVIII. The lighter neutralino has only the three decay modes $\chi_1^0 \to \tilde{\tau}_1\tau$, $\chi_1^0 \to \tilde{\mu}_1\mu$ and $\chi_1^0 \to \tilde{e}_1 e$ over the parameter space considered. Since the lighter neutralino is lighter than $\tilde{\mu}_1$ and $\tilde{e}_1$ for $\Lambda < 43\,\mathrm{TeV}$, the only decay mode for χ_1^0 is $\chi_1^0 \to \tilde{\tau}_1\tau$. As Λ increases beyond the point where the decays to the selectron and smuon become kinematically available, the branching ratios for $\chi_1^0 \to \tilde{\mu}_1\mu$ and $\chi_1^0 \to \tilde{e}_1 e$ increase, but the $\chi_1^0 \to \tilde{\tau}_1\tau$ decay remains dominant due in large part to the fact that the mass of the $\tilde{\tau}_1$ is much lower than that of the selectron and smuon.

The chargino has only two decay modes over the allowed parameter space: $\chi_1^\pm \to \tilde{\tau}_1\nu_\tau$ and $\chi_1^\pm \to \chi_1^0 W$. At the lower values of Λ considered, the decay to the lighter stau is either the only decay mode available or is the dominant decay

Table XVII. Branching ratios of the sleptons. The values of the parameters are $\tan\beta = 15$, $n = 2$ and $M/\Lambda = 3$.

	Λ (TeV)						
	35	40	50	60	70	80	85
			$M_{\tilde{\Delta}}(M) = 90\,\mathrm{GeV}$				
$\tilde{e}_1 \to e\,\chi_1^0$	1	0.9252	-	-	-	-	-
$\tilde{e}_1 \to e\,\tilde{\Delta}$	-	0.0748	1	1	1	1	1
$\tilde{\tau}_1 \to \tau\,\tilde{G}$	1	1	-	-	-	-	-
$\tilde{\tau}_1 \to \tau\,\tilde{\Delta}$	-	-	1	1	1	1	1
			$M_{\tilde{\Delta}}(M) = 120\,\mathrm{GeV}$				
$\tilde{e}_1 \to e\,\chi_1^0$	1	1	-	-	-	-	-
$\tilde{e}_1^+ \to e^+\tau^+\tilde{\tau}_1^-$	-	-	0.2065	-	-	-	-
$\tilde{e}_1^+ \to e^+\tau^-\tilde{\tau}_1^+$	-	-	0.1684	-	-	-	-
$\tilde{e}_1 \to e\,\tilde{\Delta}$	-	-	0.6251	1	1	1	1
$\tilde{\tau}_1 \to \tau\,\tilde{G}$	1	1	1	1	-	-	-
$\tilde{\tau}_1 \to \tau\,\tilde{\Delta}$	-	-	-	-	1	1	1
			$M_{\tilde{\Delta}}(M) = 150\,\mathrm{GeV}$				
$\tilde{e}_1 \to e\,\chi_1^0$	1	1	-	-	-	-	-
$\tilde{e}_1^+ \to e^+\tau^+\tilde{\tau}_1^-$	-	-	0.5532	0.5643	-	-	-
$\tilde{e}_1^+ \to e^+\tau^-\tilde{\tau}_1^+$	-	-	0.4468	0.4357	-	-	-
$\tilde{e}_1 \to e\,\tilde{\Delta}$	-	-	-	-	1	1	1
$\tilde{\tau}_1 \to \tau\,\tilde{G}$	1	1	1	1	1	-	-
$\tilde{\tau}_1 \to \tau\,\tilde{\Delta}$	-	-	-	-	-	1	1

Table XVIII. Branching ratios of some of the sparticles of interest. The values of the parameters are $\tan\beta = 15$, $n = 2$ and $M/\Lambda = 3$. The messenger scale deltino mass is 90 GeV, but the branching ratios of these sparticles have little dependence on the deltino mass.

Λ (TeV)	35	40	50	60	70	80	85
$\chi_1^\pm \to \tilde{\tau}_1 \nu_\tau$	1	1	0.7153	0.5807	0.5166	0.4796	0.4663
$\chi_1^\pm \to \chi_1^0 W$	-	-	0.2847	0.4193	0.4834	0.5204	0.5337
$\chi_2^0 \to \tilde{\tau}_1 \tau$	0.6312	0.6587	0.6860	0.4034	0.3133	0.2706	0.2560
$\chi_2^0 \to \tilde{e}_1 e$	0.1844	0.1707	0.1366	0.0625	0.0386	0.0270	0.0232
$\chi_2^0 \to \tilde{\mu}_1 \mu$	0.1844	0.1707	0.1366	0.0625	0.0386	0.0270	0.0232
$\chi_2^0 \to \chi_1^0 Z$	-	-	0.0408	0.0325	0.0277	0.0252	0.0243
$\chi_2^0 \to \chi_1^0 \mathrm{h}$	-	-	-	0.4392	0.5818	0.6501	0.6733
$\chi_1^0 \to \tilde{\tau}_1 \tau$	1	1	0.9692	0.9099	0.8723	0.8506	0.8436
$\chi_1^0 \to \tilde{e}_1 e$	-	-	0.0154	0.0451	0.0638	0.0747	0.0782
$\chi_1^0 \to \tilde{\mu}_1 \mu$	-	-	0.0154	0.0451	0.0638	0.0747	0.0782

mode. For Λ around 40 TeV and below, the only decay mode for the lighter chargino is $\chi_1^\pm \to \tilde{\tau}_1 \nu_\tau$. For these values of Λ, the lighter stau decays via $\tilde{\tau}_1 \to \tau \tilde{G}$ as discussed above. Thus in chargino pair production, two τ leptons are produced. As Λ increases, the decay mode $\chi_1^\pm \to \chi_1^0 W$ appears. With the subsequent decays of the lighter neutralino to the sleptons and with the deltino as the NLSP, the number of τ leptons produced is typically four or six (in principle eight τ leptons can be produced although this requires the rather rare three-body decays of the selectron and smuon).

The branching ratios of the second lightest neutralino are particularly sensitive to the value of Λ. At lower values of Λ, the decays to the sleptons are dominant. In particular, the decay $\chi_2^0 \to \tilde{\tau}_1 \tau$ is dominant due to the lower mass of the $\tilde{\tau}_1$ and the fact that the χ_2^0 is mostly wino. When the $\tilde{\tau}_1$ is the NLSP, $\chi_2^0 \chi_1^\pm$ production typically produces three τ-jets. When the lighter stau isn't the NLSP and decays via $\tilde{\tau}_1 \to \tau \tilde{\Delta}^c$, then seven τ leptons are usually produced, although five is also common due to the decays of the χ_2^0 to the $\tilde{\mu}_1$ and $\tilde{e}_1$ followed by their decays to the deltino. As Λ

Table XIX. Inclusive τ-jet production cross sections for a messenger scale deltino mass of 90 GeV. The other parameters are $\tan\beta = 15$, $n = 2$ and $M/\Lambda = 3$.

Λ (TeV)	35	40	50	60	70	80	85
	$\sigma \cdot$ BR (fb)						
1 τ-jet: before cuts	198.6	132.9	73.11	71.64	70.86	70.34	70.14
after cuts	168.7	156.2	97.49	91.90	90.15	89.33	89.05
2 τ-jets: before cuts	362.6	277.3	203.6	196.7	196.3	194.8	194.2
after cuts	124.6	93.11	89.59	82.91	80.59	79.63	79.33
3 τ-jets: before cuts	306.0	273.5	253.6	244.7	240.9	238.8	238.0
after cuts	32.31	17.75	32.45	29.02	27.53	26.88	26.73
4 τ-jets: before cuts	119.4	116.9	126.42	116.5	113.1	111.6	111.1
after cuts	3.21	1.18	5.26	4.28	3.67	3.45	3.39

increases, the decay $\chi_2^0 \to \chi_1^0 \mathrm{h}$ becomes dominant, but at these values of Λ, the cross section for EW gaugino production falls far below that of deltino pair production.

In summary, the dominant SUSY production modes at low values of Λ are deltino pair production and EW gaugino production. We expect four τ leptons to be produced in deltino pair production, while EW gaugino production is typically expected to produce two or three τ leptons. For larger values of Λ, the possibility exists to produce many τ leptons in EW gaugino production, but the cross sections for such production modes are much smaller than that for deltino pair production. Thus four τ leptons are generally produced at larger values of Λ.

We now consider the observability of these modes at Tevatron's Run II. Tables XIX, XX and XXI give the inclusive τ-jet production cross sections for a messenger scale deltino mass of 90, 120 and 150 GeV, respectively. We include in the figures only up to four τ-jets as the cross sections for more than four τ-jets are small. Considering Table XIX, we see that before cuts the production of two and three τ-jets are dominant, but the four τ-jet cross section is also significant at slightly over 100 fb. After the cuts are applied, however, the situation changes substantially. The

Table XX. Inclusive τ-jet production cross sections for a messenger scale deltino mass of 120 GeV. The other parameters are $\tan\beta = 15$, $n = 2$ and $M/\Lambda = 3$.

Λ (TeV)	35	40	50	60	70	80	85
	$\sigma \cdot$ BR (fb)						
1 τ-jet: before cuts	151.5	86.21	39.60	29.72	25.30	25.00	24.90
after cuts	125.3	85.20	53.68	75.87	42.16	41.38	41.16
2 τ-jets: before cuts	232.8	148.0	90.27	75.93	70.06	69.15	68.83
after cuts	93.94	71.59	49.79	28.57	43.81	42.83	42.55
3 τ-jets: before cuts	147.6	115.9	96.70	88.92	86.55	85.16	84.71
after cuts	25.99	23.22	17.33	0.55	17.37	16.80	16.64
4 τ-jets: before cuts	46.22	44.03	42.59	40.70	40.72	39.55	39.22
after cuts	3.05	3.09	2.29	0.06	2.70	2.50	2.44

one τ-jet mode is now dominant, but the cross section for two τ-jets is not far below and the three τ-jets cross section is not insignificant.

We first consider the $M_{\tilde{\Delta}}(M) = 90\,\text{GeV}$ case. We see from Table XIX that for $\Lambda = 35\,\text{TeV}$ the cross section for inclusive production of three τ-jets is 32.3 fb. For an integrated luminosity of $2\,\text{fb}^{-1}$ (the approximate initial value at Run II), this corresponds to about 65 events. For $30\,\text{fb}^{-1}$, the number of observable events is $\sim$ 970. For $\Lambda = 85\,\text{TeV}$, the production cross section for three τ-jets has gone down slightly due to the decrease in production of charginos and neutralinos. With a value of 26.7 fb, the number of expected events is about 53 and 800 for $2\,\text{fb}^{-1}$ and $30\,\text{fb}^{-1}$ of data, respectively. The cross section for two τ-jets is considerably higher. For $\Lambda = 35\,\text{TeV}$, the $\sigma \cdot$ BR for two τ-jets is 125 fb which corresponds to 250 events for $2\,\text{fb}^{-1}$ of data and 3750 events for $30\,\text{fb}^{-1}$ of data. For $\Lambda = 85\,\text{TeV}$, $\sigma \cdot$ BR has decreased to 79 fb. This gives about 160 and 2370 events for $2\,\text{fb}^{-1}$ and $30\,\text{fb}^{-1}$ of data, respectively. In comparison to the GMSB model considered in chapter III, the two τ-jets and the three τ-jets cross sections are considerably higher in this model.

Table XXI. Inclusive τ-jet production cross sections for a messenger scale deltino mass of 150 GeV. The other parameters are $\tan\beta = 15$, $n = 2$ and $M/\Lambda = 3$.

Λ (TeV)	35	40	50	60	70	80	85
	$\sigma \cdot$ BR (fb)						
1 τ-jet: before cuts	136.2	70.92	24.42	14.61	11.80	10.07	10.00
after cuts	105.3	65.54	32.12	22.59	23.50	19.28	18.97
2 τ-jets: before cuts	190.3	105.7	48.32	34.22	30.01	27.89	27.67
after cuts	72.17	50.55	31.35	24.29	18.99	21.75	21.46
3 τ-jets: before cuts	95.31	63.85	45.21	37.72	35.14	34.47	34.14
after cuts	17.23	14.64	12.24	10.14	5.53	9.32	9.24
4 τ-jets: before cuts	21.81	19.75	18.58	17.00	16.16	16.23	15.96
after cuts	1.73	1.81	1.89	1.67	0.59	1.46	1.47

As the mass of the deltino increases, the production rates go down and more variation appears. The inclusive τ-jet cross sections for $M_{\tilde{\Delta}}(M) = 120$ GeV are shown in Table XX. Considering the inclusive three τ-jets mode, the production cross section at $\Lambda = 35$ TeV is 26 fb. This corresponds to 52 events for $2\,\text{fb}^{-1}$ of data and 780 events for $30\,\text{fb}^{-1}$ of data. This goes down to about 17 fb at $\Lambda = 85$ TeV. This gives about 34 and 510 events for $2\,\text{fb}^{-1}$ and $30\,\text{fb}^{-1}$ of data, respectively. The production rate for two τ-jets is higher. At $\Lambda = 35$ TeV, $\sigma \cdot \text{BR} = 94$ fb which gives 190 and 2820 events for $2\,\text{fb}^{-1}$ and $30\,\text{fb}^{-1}$ of data, respectively.

Angular Distributions

The excess of τ-jets expected in this model does not constitute an unequivocal signal for this model. τ-jets are part of the signatures for other models including the minimal GMSB model with the lighter stau as the NLSP. The question then arises as to whether there is any way to distinguish this model from the minimal GMSB

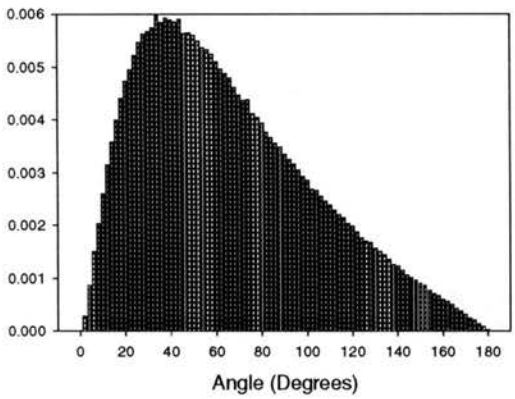

(a) Distribution when the τ-jets come from same sign τ leptons.

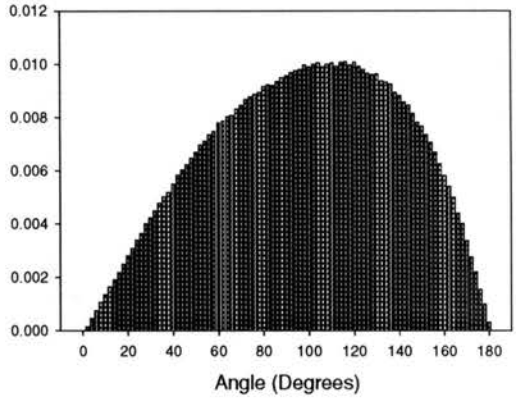

(b) Distribution when the τ-jets come from opposite sign τ leptons.

Figure 37. Angular distribution between the two most energetic τ-jets for deltino pair production at the Tevatron. The deltino mass is about 97 GeV.

model. A possible distinguishing characteristic is the distribution in angle between the two highest E_T τ-jets when they come from same sign τ-jets.

Consider deltino pair production. The deltino tends to decay to like sign τ leptons. This occurs directly when the deltino is the NLSP and so decays via the three-body decay $\tilde{\Delta}^{\pm\pm} \to \tau^{\pm}\tau^{\pm}\tilde{G}$. When the two-body decay of the deltino $\tilde{\Delta}^{\pm\pm} \to \tilde{\tau}_1^{\pm}\tau^{\pm}$ occurs, then the second like sign τ lepton comes from the subsequent decay of the stau. In the rest frame of the deltino, the τ leptons are widely distributed. In the lab frame, however, the deltinos are quite energetic and have a large velocity, especially if their masses are small. As a consequence of this, the decay products of the deltino tend to be collimated in the direction in which the deltino was moving. Thus when the two most energetic τ-jets have the same sign in deltino pair production, the angle between them tends to be smaller than when the two most energetic τ-jets have opposite sign charges.

Fig. 37 gives the distribution in angle between the two most energetic τ-jets for deltino pair production. This example is for a weak scale deltino mass of about 97 GeV. We can see that the distribution in angle for like sign τ-jets, which is given in Fig. 37(a), peaks at about 40°. Fig. 37(b) gives the distribution in angle between

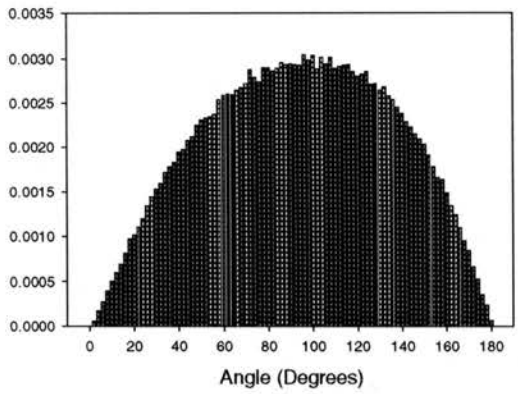

(a) The distribution when the τ-jets come from same sign τ leptons.

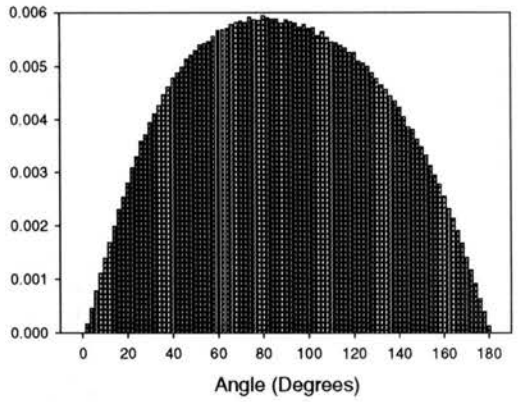

(b) The distribution when the τ-jets come from opposite sign τ leptons.

Figure 38. Angular distribution between the two most energetic τ-jets for EW gaugino production at the Tevatron where the mass of χ_2^0 is 100 GeV.

the two most energetic τ-jets when they come from opposite sign τ leptons. In stark contrast to the previous case, here the peak occurs at 110°.

The question then arises as to how these distributions look in the usual SUSY production modes. Fig. 38 shows the angular distributions for combined $\chi_2^0\chi_1^\pm$ and $\chi_1^+\chi_1^-$ production for the input parameters $M = 100\,\text{TeV}$, $\Lambda = 45\,\text{TeV}$, $n = 1$ and $\tan\beta = 10$. For these values of the parameters, the weak scale χ_2^0 mass is $\sim 100\,\text{GeV}$. The distribution for same sign τ-jets is given in Fig 38(a). We see that the peak occurs at about 110°. In this situation, same-sign τ-jets do not come from $\chi_1^+\chi_1^-$ production. In $\chi_2^0\chi_1^\pm$ production, one of the same sign τ-jets generally comes from the chargino and the other from the neutralino. We now consider the angular distribution for opposite sign τ-jets which are given in Fig. 38(b). In $\chi_2^0\chi_1^\pm$ production, opposite sign τ-jets frequently come from the neutralino, while in $\chi_1^+\chi_1^-$ production one of the τ-jets comes from one of the charginos and the other τ-jet comes from the other chargino. Since there is a strong possibility that the opposite sign τ-jets come from the same particle (χ_2^0), the distribution should peak at a lower angle than for same sign τ-jets. We see from the figure that the peak occurs at about 85°.

These distributions change somewhat as the gaugino masses are increased. Fig. 39 gives the angular distribution for a χ_2^0 mass of 150 GeV. We see that the

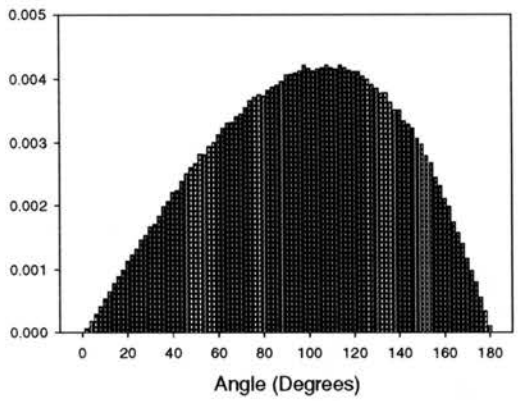

(a) The distribution when the τ-jets come from same sign τ leptons.

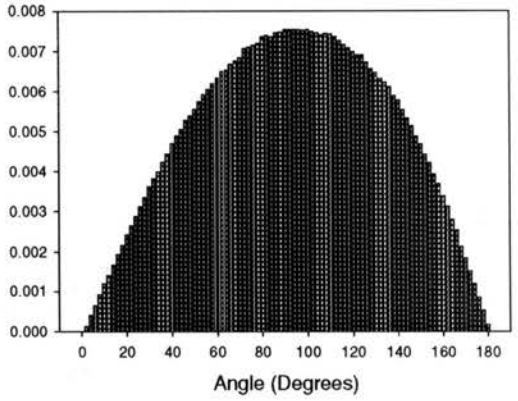

(b) The distribution when the τ-jets come from opposite sign τ leptons.

Figure 39. Angular distribution between the two most energetic τ-jets for EW gaugino production at the Tevatron. The mass of χ_2^0 is about 150 GeV.

same sign distribution still peaks at about 110°, while the opposite sign distribution has now shifted to a slightly higher value of about 95°.

The actual angular distribution between the two highest E_T τ-jets depends on which SUSY production modes are important. For certain regions of the parameter space (depending, in particular, on the values of Λ and the messenger scale deltino mass), deltino pair production is the only important SUSY production mode. When this is the case, the angular distributions are simply given by those for deltino pair production. The signal should be particularly striking in these regions as Fig. refd90 suggests. In other regions of the parameter space, EW gaugino production can significantly affect the angular distributions.

We consider the angular distributions for some examples with the input parameters $\tan\beta = 15$, $n = 2$ and $M/\Lambda = 3$. Three values of the messenger scale deltino mass are considered: 90, 120 and 150 GeV. The angular distributions for $M_{\tilde{\Delta}}(M) = 90\,\text{GeV}$ are given in Fig. 40. Since the deltino is especially light with a mass of 96 GeV, deltino pair production is the dominant SUSY production mode. Thus deltino pair production largely dictates the form of the angular distributions.

Fig. 40(a) gives the angular distribution between the two highest E_T τ-jets when they come from same sign τ leptons. In the figure we can see the rather striking peak

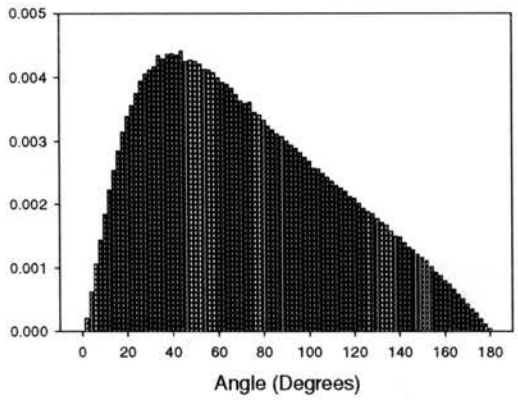

(a) The distribution when the τ-jets come from same sign τ leptons.

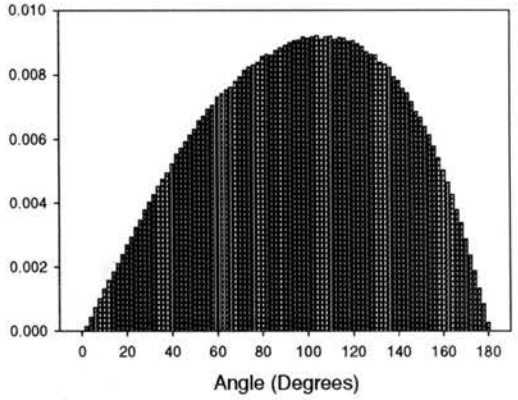

(b) The distribution when the τ-jets come from opposite sign τ leptons.

Figure 40. Angular distribution between the two most energetic τ-jets for combined SUSY pair production at the Tevatron. The messenger scale deltino mass is 90 GeV. The other parameters are $\tan\beta = 15$, $n = 2$ and $M/\Lambda = 3$.

at around 40°. This is due to the same sign τ-jets coming mostly from the decay of the same deltino. Since the deltino mass is especially light compared to the beam energy, they typically move rapidly in the lab frame. Thus their decay products tend to be more tightly collimated than in the production of the heavier particles.

Fig. 40(b) gives the angular distribution between the two highest E_T τ-jets when they come from opposite sign τ leptons. We see from this figure that the peak occurs at about 110°. Here the τ-jets typically come from the decay chains of different particles and so the angle between the τ-jets is typically quite large.

The situation changes as the deltino mass gets larger. This is due in part to the fact that the deltino pair production cross section gets smaller and so the production of charginos and neutralinos can have a larger impact on the distributions. In addition, a larger deltino mass means the deltinos will typically be moving slower. Thus the boost effect won't have as dramatic an effect on the deltino's decay products. The example with $M_{\tilde{\Delta}}(M) = 120\,\text{GeV}$ is given in Fig. 41. We can see that the distribution for same sign τ-jets peaks at about 70°. On the other hand, the opposite sign τ-jet angular distribution still peaks at around 110°. Thus the angle between the τ-jets is less striking a signature than it was before, but it is still distinctive.

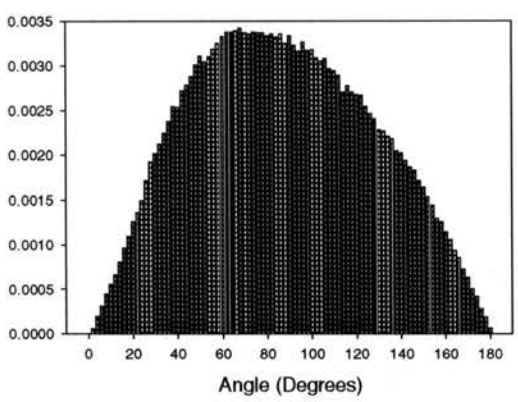

(a) The distribution when the τ-jets come from same sign τ leptons.

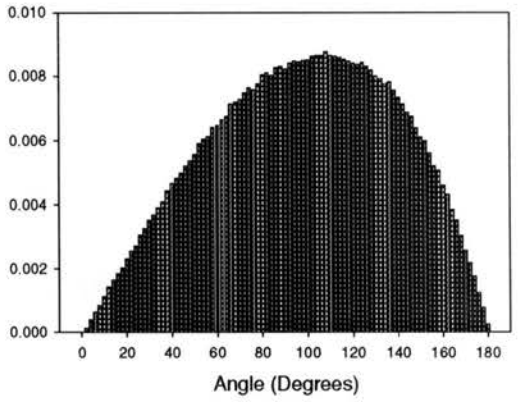

(b) The distribution when the τ-jets come from opposite sign τ leptons.

Figure 41. Angular distribution between the two most energetic τ-jets for combined SUSY production at the Tevatron. The messenger scale deltino mass is 120 GeV. The other parameters are $\tan\beta = 15$, $n = 2$ and $M/\Lambda = 3$.

The results for a messenger scale deltino mass of 150 GeV are given in Fig. 42. The peak in the distribution in angle between the two highest E_T τ-jets when they have the same sign peaks at a rather high 95°. As before, the peak in the distribution for the two highest E_T τ-jets when they have opposite sign is at 110°. Thus the distinctiveness due to the angle between the two highest E_T τ-jets is nearly lost for such a large value of the deltino mass. This is partially due to the deltino pair cross section of 92 fb being quite a bit lower than the cross section for $\chi_1^\pm \chi_2^0$ production and $\chi_1^+\chi_1^-$ production. In addition, as discussed above, there is also the reduction in the boost effect as the mass of the decaying deltino increases.

Conclusion

In conclusion, we have found that the doubly charged Higgs bosons of LR models can be potentially observable at Run II of the Tevatron through the production of τ-jets. In a GMSB type theory, SUSYLR models typically produce large numbers of two and three τ-jet final states. This large τ-jet signal is due in large part to pair production of the doubly charged Higgsino. It is also due to the relatively low mass of

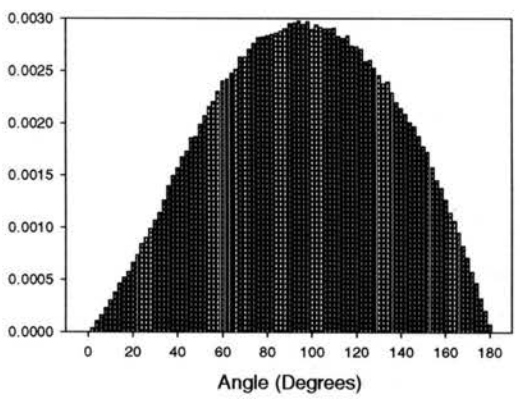

(a) The distribution when the τ-jets come from same sign τ-jets.

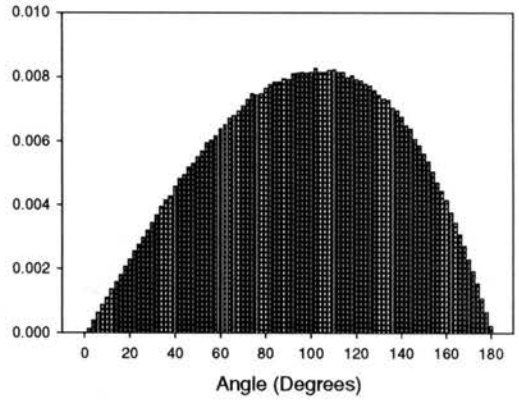

(b) The distribution when the τ-jets come from opposite sign τ-jets.

Figure 42. Angular distribution between the two most energetic τ-jets for combined SUSY production at the Tevatron. The messenger scale deltino mass is 150 GeV. The other parameters are $\tan\beta = 15$, $n = 2$ and $M/\Lambda = 3$.

the lighter stau (which is frequently the NLSP) in these models, which is due to the additional coupling f. We have also shown that the distribution in angle between the two highest E_T τ-jets is different from other models which do not have this doubly charged Higgsino and could help to distinguish this model.

CHAPTER V

CONCLUSION

In this work we have investigated the phenomenology of various supersymmetric models. First we have considered the Higgs sector of the Minimal Supersymmetric Standard Model. We found that if the charged Higgs boson is light enough, the decays of the top quark to the charged Higgs boson greatly modify the expected signatures for top quark production. This is particularly true for the dilepton with dijets mode and the four jets with a lepton mode; both of which are important low background channels for investigating top quark production at the Tevatron. In addition, for $\tan\beta$ below about one, there are modes available that are not present in the Standard Model due to the three-body decay $H^+ \to \bar{b}bW$. This includes the very low background five jets with one charged lepton mode and the six jets with one charged lepton mode.

We then investigated the phenomenology of gauge mediated supersymmetry breaking models. We found that for a wide range of the parameter space, the lighter stau is the NLSP. When this is the case, the signature for SUSY production involves substantial production of τ leptons. We find that searching for events that have two or three τ-jets at Run II and Run III of the Tevatron could be a feasible means of testing this theory.

We then considered a GMSB model based on a left-right symmetric theory with the gauge group $\mathrm{SU}(2)_L \times \mathrm{SU}(2)_R \times \mathrm{U}(1)_{B-L}$. The light doubly charged particles in this theory could be light enough to be produced at the current and next generation of colliders. This is especially true for the light doubly charged Higgsino which receives no mass contributions from messenger loops. For a wide range of the parameter space, the lighter stau is lighter than the lightest neutralino. When this occurs, τ-jets will be an important part of the signature just as it is for GMSB models with MSSM

particle content in the visible sector. Two facts distinguish this left-right model, however. First, deltino pair production can greatly enhance the signal. Second, the distribution in angle between the two highest E_T τ-jets can peak at low values when they come from same-sign τ-jets. This is due to many of the τ-jets coming from the decay of a doubly charged particle and is not expected in models with minimal particle content.

BIBLIOGRAPHY

1. J. Wess and B. Zumino, Nucl. Phys. **B70**, 34 (1974); J. Wess and J. Bagger, *Supersymmetry and Supergravity*, Princeton University Press, Princeton, N. J. (1983); P. Fayet and S. Ferrara, Phys. Rep. **32**, 249 (1977).

2. S. Coleman and J. Mandula, Phys. Rev. **159**, 1251 (1967); R. Haag, J. Lopuszanski and M. Sohnius, Nucl. Phys. **B88**, 257 (1975).

3. H. Haber and G. Kane, Phys. Rep. **117C**, 75 (1985).

4. J. Schwinger, Annals Phys. **2**, 407 (1957); S. Adler, Phys. Rev. **177**, 2426 (1969); J. Bell and R. Jackiw, Nuovo Cim. **60A**, 47 (1969); W. Bardeen, Phys. Rev. **184**, 1848 (1969); D. Gross and R. Jackiw, Phys. Rev. **D6**, 477 (1972); C. Bouchait, J. Iliopoulos and P. Meyer, Phys. Lett. **38B**, 519 (1972); H. Georgi and S. Glashow, Phys. Rev. **D6**, 429 (1972); L. Alvarez-Gaume and E. Witten, Nucl. Phys. **B234**, 269 (1983).

5. S. Weinberg, Phys. Rev. **D26**, 287 (1982); N. Sakai and T. Yanagida, Nucl. Phys. **B197**, 533 (1982); S. Dimopolous, S. Raby and F. Wilczek, Phys. Lett. **112B**, 133 (1982); J. Ellis, D. Nanopolous and S. Rudaz, Nucl. Phys. **B202**, 43 (1982).

6. C. Carlson, P. Roy and M. Sher, Phys. Lett. **357B**, 99 (1995); G. Bhattacharyya, hep-ph/9709395; J. Goity and M. Sher, Phys. Lett. **346B**, 69 (1995); H. Dreiner, to be published in *Perspectives in Supersymmetry*, ed. G. Kane, World Scientific, Singapore (1998), hep-ph/9707435; G. Altarelli, *et. al.*, Nucl. Phys. **B506**, 3 (1997).

7. G. Ferrar and P. Fayet, Phys. Lett. **76B**, 575 (1978); F. Zwirner, Phys. Lett. **132B**, 103 (1983); L. Hall and M. Suzuki, Nucl. Phys. **B231**, 419 (1984); J. Ellis, G. Gelmini, C. Jarlskog, G. Ross and J. Valle, Phys. Lett. **150B**, 142 (1985); G. Ross and J. Valle, Phys. Lett. **151B**, 375 (1985); S. Dawson, Nucl. Phys. **B261**, 297 (1985); S. Dimopolous and L. Hall, Phys. Lett. **207B**, 210 (1988); T.Banks, Y. Grossman, E. Nardi and Y. Nir, Phys. Rev. **D**, 5319 (1995); B. de Carlos and P. White, Phys. Rev. **D54**, 3427 (1996); E. Nardi, Phys. Rev. **D55**, 5772 (1997).

8. S. Dimopoulos and H. Georgi, Nucl. Phys. **B193**, 150 (1981); N. Sakai, Z. Phys. **C11**, 153 (1981); L. Giradello and M. Grisaru, Nucl. Phys. **B194**, 65 (1982); K. Harada and N. Sakai, Prog. Theor. Phys. **67**, 67 (1982); P. Fayet, Phys. Lett. **69B**, 489 (1977); *ibid.*, **84B**, 416 (1979).

9. S. Ferrara, L. Girardello and F. Palumbo, Phys. Rev. **D20**, 403 (1979).

10. H. L. Lai, J. Botts, J. Huston, J. G. Morfin, J. F. Owens, J. Qui, W. K. Tung and H. Weerts, Phys. Rev. **D51**, 4763 (1995). Code available at http://www.phys.psu.edu/~cteq/.

11. J. F. Gunion and H. E. Haber, Nucl. Phys. **B272**, 1 (1986); *ibid.* **B278**, 449 (1986); J. F. Gunion *et al.*, *The Higgs Hunter's Guide*, Addison-Wesley Publishing Company (1990).

12. E. Ma, D. P. Roy, and J. Wudka, Phys. Rev. Lett. **80**, 1162 (1998).

13. Opal Collaboration, OPAL PN-366, paper submitted to the ICHEP'98 conference, Vancouver, July 1998.

14. M. Diaz and H. Haber, Phys. Rev. **D45**, 4246 (1992).

15. M. Battaglia *et al.* of the Delphi Collaboration, DELPHI 98-96 CONF 164, paper submitted to the ICHEP'98 conference, Vancouver, July 1998; R. Barate *et al.*, ALEPH Collaboration, CERN-PPE/97-129, submitted to Phys. Lett. B; K. Ackerstaff *et al.*, OPAL Collaboration, CERN-PPE/97-168, submitted to Phys. Lett. B; M. Acciarri *et al.*, L3 Collaboration, CERN-EP/98-149, submitted to Phys. Lett. B.

16. Y. Grossman, H. E. Haber, and Y. Nir, Phys. Lett. **357B**, 630 (1995).

17. J. A. Coarasa, R. A. Jiménez, and J. Solà, Phys. Lett. **406B**, 337 (1997).

18. F. Abe *et al.*, Phys. Rev. Lett. **79**, 357 (1997); *ibid.*, Phys. Rev. **D54**, 735 (1996); *ibid.* Phys. Rev. Lett. **73**, 2667 (1994).

19. M. Guchait and D. P. Roy, Phys. Rev. **D55**, 7263 (1997); D. P. Roy, talk presented at the *32nd Recontres de Moriond: QCD and High-Energy Interactions*, Les Arcs, France, March, 1997, TIFR-TH-97-18.

20. Juame Guasch and Joan Solà, Phys. Lett. **416B**, 353 (1998).

21. G. Velev for the CDF Collaboration, FERMILAB-Conf-98/192-E, published in the proceedings of the *12th Rencontres de Physique de la Vallee D'Aosta: Results and Perspectives in Particle Physics*, La Thuile, Italy, March 1998.

22. F. Abe *et al.*, Phys. Rev. Lett. **79**, 3819 (1997).

23. M. Chertok for the CDF and D0 Collaborations, talk presented at the *33rd Recontres de Moriond: QCD and High Energy Hadronic Interactions*, Les Arcs, France, March 21-28, 1998, FERMILAB-Conf-98/156-E; S. Abachi *et al.*, D0 Collaboration, Phys. Rev. Lett. **80**, 442 (1998).

24. R. Barate *et al.*, ALEPH Collaboration, Phys. Lett. **420B**, 127 (1998); M. Acciarri *et al.*, L3 Collaboration, CERN-PPE/97-130; K. Ackerstaff *et al.*, OPAL Collaboration, Eur. Phys. J. **C1**, 21 (1998); P. Abreu *et al.*, DELPHI Collaboration, Eur. Phys. J. **C1**, 1 (1998).

25. S. Park, representing the CDF collaboration, "Search for New Phenomena in CDF" in *10th Topical Workshop on Proton-Antiproton Collider Physics*, edited by R. Raja and J. Yoh (AIP Press, New York, 1995), report FERMILAB-CONFE-95/155-E; R. Culbertson for the CDF and D0 collaborations, talk presented at the *5th International Conference on Supersymmetries in Physics* (SUSY 97), Philepdelphia, PA, May 27-31, 1997, FERMILAB-Conf-97/227/E.

26. M. Dine and A. Nelson, Phy. Rev. **D47**, 1277 (1993); M. Dine, A. Nelson and Y. Shirman, Phys. Rev. **D51**, 1362 (1995); M. Dine, A. Nelson, Y. Nir and Y. Shirman, Phys. Rev. **D53**, 2658 (1996); M. Dine, Y. Nir and Y. Shirman, Phys. Rev. **D55**, 1501 (1997).

27. I. Affleck, M. Dine and N. Seiberg, Nucl. Phys. **B256**, 557 (1997); R. N. Mohapatra and S. Nandi, Phys. Rev. Lett. **79**, 181 (1997); B. Dobrescu, Phys. Lett. **403B**, 285, (1997); Z. Chacko, B. Dutta, R. N. Mohapatra and S. Nandi, Phys. Rev. **D56**, 5466 (1997).

28. G.F. Guidice and R. Rattazzi, hep-ph/9801271; S. Dimopoulos, S. Thomas and J. D. Wells, Nucl. Phys. **B488**, 39 (1997); J. Bagger, D. Pierce, K. Matchev and R.-J. Zhang, Phys. Rev. **D55**, 3188 (1997); K. S. Babu, C. Kolda and F. Wilczek, Phys. Rev. Lett. **77**, 3070 (1996); S. Ambrosanio, G. L. Kane, G. D. Kribs, S. P. Martin and S. Mrenna, Phys. Rev. **D54**, 5395 (1996); *ibid.*, Phys. Rev. **D55**, 1372 (1997); H. Baer, M. Brhlik, C.-H. Chen and X. Tata, Phys. Rev. **D56**, 4463 (1997); D. A. Dicus, B. Dutta and S. Nandi, Phys. Rev. Lett. **78**, 3055 (1997); *ibid.*, Phys. Rev. **D56**, 5748, (1997); K. Cheung, D. A. Dicus, B. Dutta and S. Nandi, hep-ph/9711216; A. Riotto, O. Tornkvist and R. N. Mohapatra, Phys. Lett. **388B**, 599 (1996); G. Bhattacharyya, A. Romanino; Phys. Rev. **D55**, 7015 (1997); A. Datta, A. Kundu, B. Mukhopadhyaya and S. Roy, Phys. Lett. **416B**, 117 (1998); Y. Nomura and K. Tobe, Phys. Rev. **D58**, 5500 (1998); S. Raby and K. Tobe, Phys. Lett. **437B**, 337 (1998); S. Raby, Phys. Lett. **422B**, 158 (1998); S. P. Martin and J. D. Wells, hep-ph/9805289.

29. S. Dimopoulos, M. Dine, S. Raby and S. Thomas, Phys. Rev. Lett. **76**, 3494 (1996); S. Ambrosanio, G. L. Kane, G. D. Kribs, S. P. Martin and S. Mrenna, Phys. Rev. Lett. **76**, 3498 (1996); D. R. Stump, M. Wiest and C.P. Yuan, Phys. Rev. **D54**, 1936 (1996).

30. B. Dutta and S. Nandi, hep-ph/9709511; J. L. Feng and T. Moroi, Phys. Rev. **D58**, 3501 (1998).

31. S. Dimopoulos, S. Thomas and J.D. Wells, Nucl. Phys. **B488**, 39 (1997) ; H. Baer, M. Brhlik, C.-H. Chen and X. Tata, Phys. Rev. **D55**, 4463 (1997); N. G. Deshpande, B. Dutta and S. Oh, Phys. Rev. **D56**, 519 (1997); R. Rattazzi and Uri Sarid, Nucl. Phys. **B501**, 297 (1997).

32. S. Dimopoulos, G. F. Giudice and A. Pomarol, Phys. Lett. **389B**, 37 (1996); S. P. Martin, Phys. Rev. **D55**, 3177 (1997); S. P. Martin, hep-ph/9709356, to appear in *Perspectives in Supersymmetry*, ed. G. Kane (World Scientific, 1998).

33. V. Barger, M. A. Berger and P. Ohmann, Phys. Rev. **D47**, 1093 (1993); *ibid.* **D49**, 4908 (1994).

34. P. P. Bagley *et al.*, in *Proceedings of the 1996 DPF/DPB Summer Study on New Directions for High Energy Physics (Snowmass '96)*, Snowmass, CO, June 25-July 12, 1996; D. Amidei it et al., unpublished TeV33 Committee report, available at http://www-theory.fnal.gov/tev33.ps.

35. A. Galloni, DELPHI Collaboration, Talk at "The pheno-CTEQ Symposium 98-Frontiers of Phenomenology", Madison, Wisconsin March 23-26, 1998; V. Büscher, ALEPH Collaboration, Talk at Fermilab, July 10, 1998, http://alephwww.cern.ch/~buescher/w_c/talk.ps.

36. R. N. Mohapatra, Phys. Rev. **D34**, 3457 (1986); A. Font, L. Ibanez and F. Quevedo, Phys. Lett. **228B**, 79 (1989); S. Martin, Phys. Rev. **D46**, 2769 (1992).

37. R. N. Mohapatra and A. Rasin, Phys. Rev. Lett. **76**, 3490 (1996); R. Kuchimanchi, Phys. Rev. Lett. **76**, 3486 (1996); R. N. Mohapatra, A. Rasin and G. Senjanović, Phys. Rev. Lett. **79**, 4744 (1997).

38. M. Gell-Mann, P. Ramond and R. Slansky, in *Supergravity*, ed. D. Freedman et al. (North Holland, 1979); T. Yanagida, KEK Lectures (1979); R. N. Mohapatra and G. Senjanović, Phys. Rev. Lett. **44**, 912 (1980).

39. R. Kuchimanchi and R. N. Mohapatra, Phys. Rev. **D48**, 4352 (1993); *ibid.* Phys. Rev. lett. **75**, 3989 (1995).

40. C. S. Aulakh, A. Melfo and G. Senjanović, Phys. Rev. **D57**, 4174 (1998); C. S. Aulakh, A. Melfo, A. Rasin and G. Senjanović, Phys. Rev. **D58**, 1150 (1998).

41. Z. Chacko and R. N. Mohapatra, Phys. Rev. **D58**, 150 (1998).

42. C. S. Aulakh, K. Benakli and G. Senjanović, Phys. Rev. Lett. **79**, 2188 (1997).

43. R. N. Mohapatra and S. Nandi, Phys. Rev. Lett. **79**, 181 (1997); Z. Chacko, B. Dutta, R. N. Mohapatra and S. Nandi, Phys. Rev. **D56**, 5466 (1997).

44. B. Dutta and R. N. Mohapatra, hep-ph/9804277 (to appear in PRD).

45. L. Willmann *et al.*, hep-ex/9807011; K. Jungman, invited talk at PASCOS98 (1998).

46. J. A. Bagger, K. Matchev, D. M. Pierce, R-J. Zhang, Phys. Rev. **D55**, 3188 (1997).

VITA

David J. Muller

Candidate for the Degree of

Doctor of Philosophy

Thesis: COLLIDER PHENOMENOLOGY OF SUPERSYMMETRIC MODELS

Major Field: Physics

Biographical:

Education: Graduated from Oak Park and River Forest High School, Oak Park, Illinois in June 1988; received Bachelor of Science degree in Physics from the University of Illinois, Urbana, Illinois in May 1992. Completed the requirements for the Doctor of Philosophy degree with a major in Physics at Oklahoma State University in December, 1998.

Experience: Graduate teaching assistant, Department of Physics, Oklahoma State University, August 1992 to December 1998; graduate research assistant, Department of Physics, Oklahoma State University, May 1994 to December 1998.

Professional Memberships: The Divison of Particles and Fields of the American Physical Society.